MAGIS-100: Current Status and Outlook

Dylan J Temples *on behalf of the MAGIS-100 Collaboration*

Fermilab Users Meeting

11 July 2024

FERMILAB-SLIDES-24-0140-ETD

Outline

- Project & collaboration overview
- Atom interferometry* & gradiometry basics
- Science with MAGIS-100
- Current project status
- Conclusions

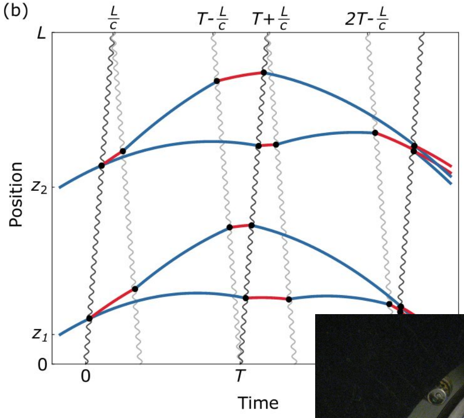

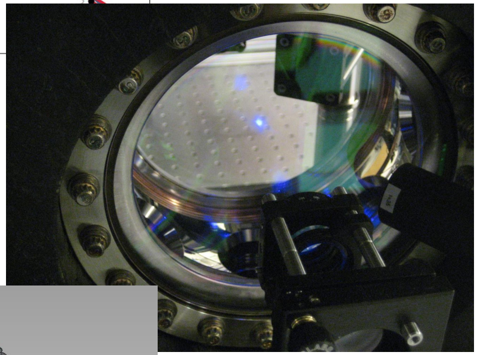

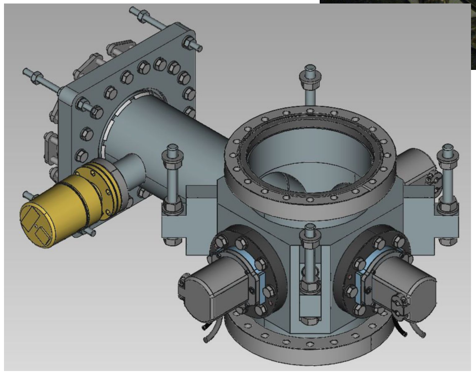

** In this talk, “AI” == Atom Interferometry, not artificial intelligence*

Matter-wave Atomic Gradiometer Interferometric Sensor

MAGIS-100: Atom interferometry over ~100-meter vertical baseline

- Three strontium atom sources + imaging system
- Atoms: freely-falling clocks & inertial reference
- Common interferometry laser beam

Searching for dark matter, new forces, gravitational waves, and more!

To be installed in the existing MINOS access shaft at Fermilab

Leverage precision AMO techniques for HEP+ science goals

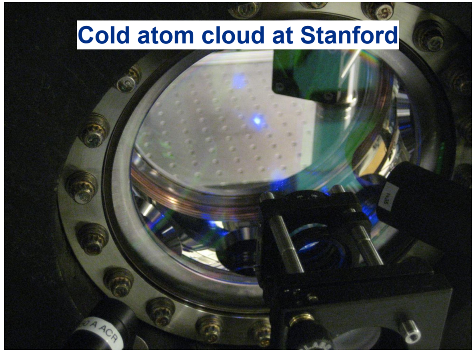

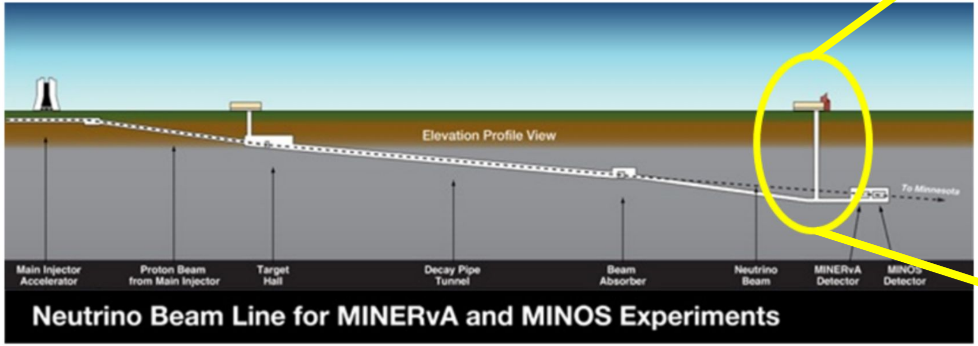

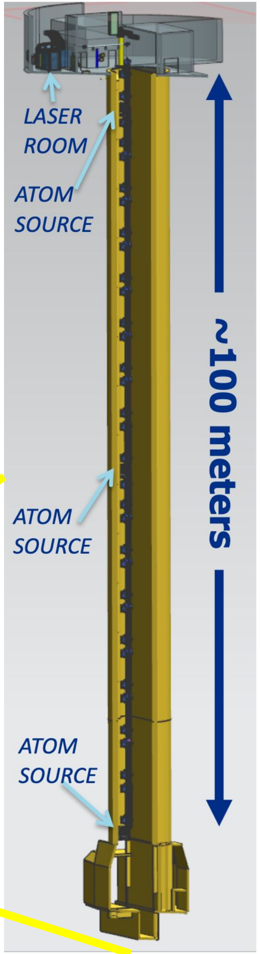

Collaboration

MAGIS-100

Cross-disciplinary collaboration:

- 10 institutions across US & UK
- 70+ scientists & engineers (incl. students)

AMO: atom preparation & manipulation, laser control & delivery, AI operation & optimization

HEP: mechanical & vacuum engineering (now), operations at scale (soon), computing & data infrastructure, analysis & statistical inference, bias mitigation

<u>Unique challenges & opportunities!</u>

Stanford | Johns Hopkins University | Northwestern University | Fermilab | SLAC | Old Dominion University | University of Cambridge | University of Liverpool | University of Oxford | Northern Illinois University

Funding Structure

U.S. DEPARTMENT OF ENERGY | Office of Science

DOE OHEP Project fully funded at $20M through 2027

Additional in-kind contributions total $9.7M

- Stanford: strontium atom sources
- Northwestern: laser system
- Oxford: scientific imaging system
- Liverpool: retro-reflection chamber
- SLAC: distributed imaging system
- Cambridge: environmental monitoring

Project status granted in Oct 2023: moved from QuantISED grant to project funds

Pursuing supplemental funding for collaboration support (software, hardware R&D)

Collaborator's Funding Partners:

UKRI Science and Technology Facilities Council

Gordon and Betty MOORE FOUNDATION

GBMF7945

Light-Pulse Atom Interferometry

Mach-Zehnder Optical Interferometer

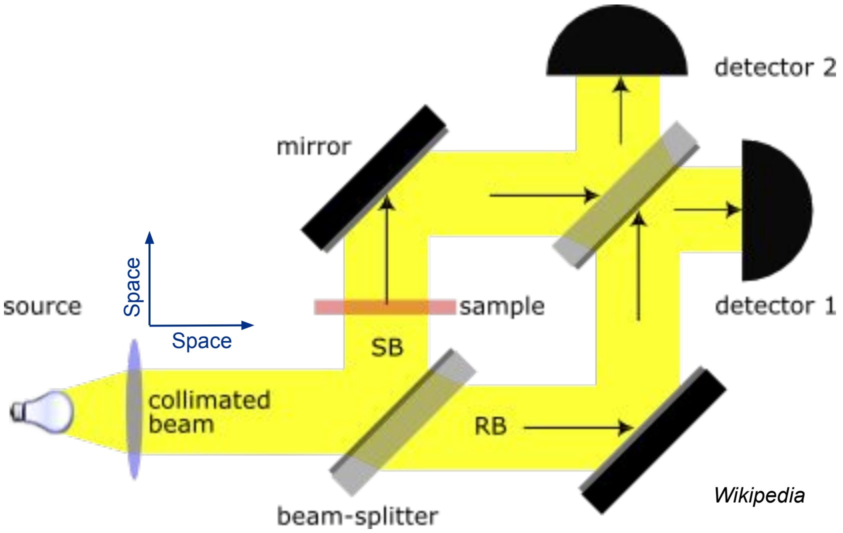

Mach-Zehnder Matter-Wave Interferometer

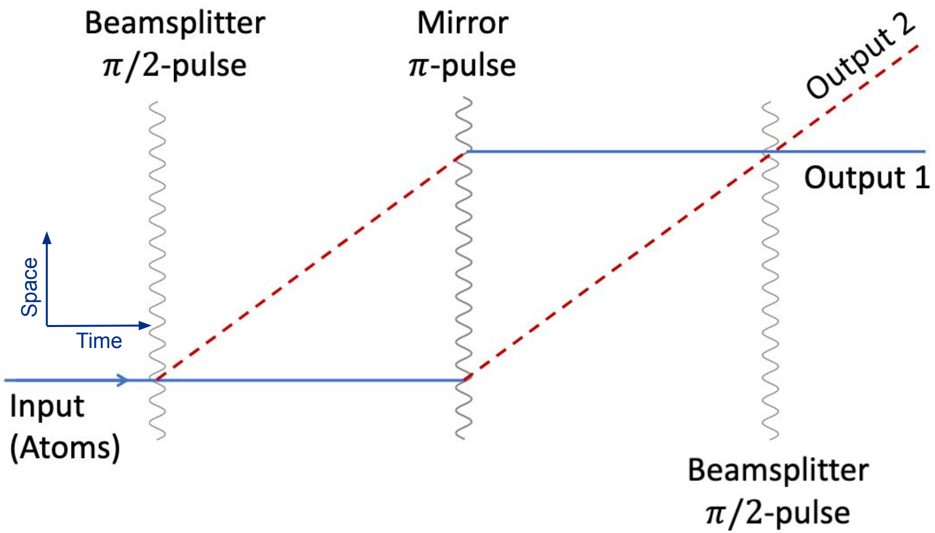

Effects scale with area. For best sensitivity:

- Long time between first BS and mirror pulses
- Large separation (momentum)

Light-Pulse Atom Interferometry

Mach-Zehnder Optical Interferometer

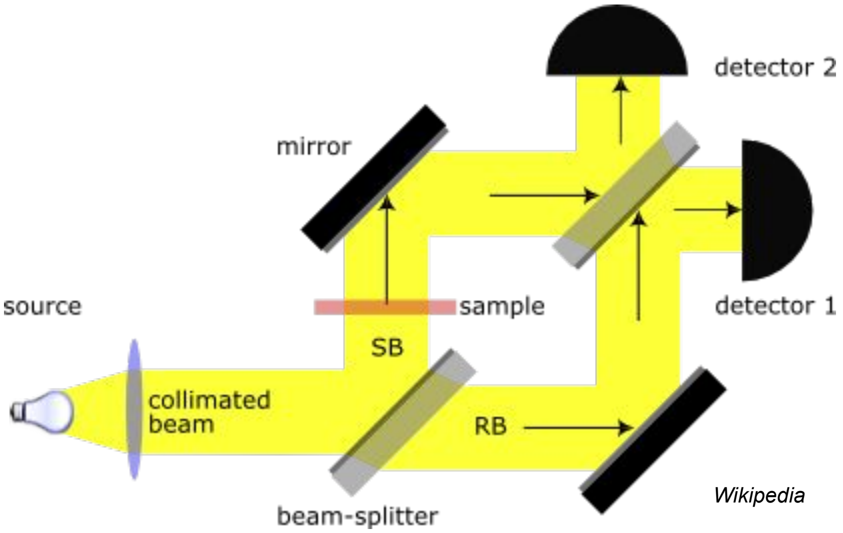

Mach-Zehnder Matter-Wave Interferometer

Abe et al, Quantum Sci. Technol. 6, 044003 (2021) [arxiv:2104.02835]

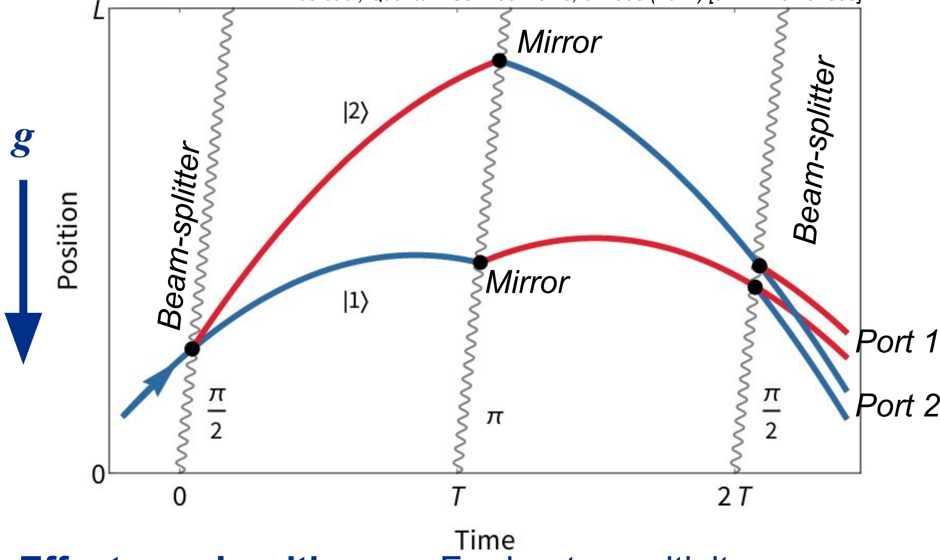

Effects scale with area. For best sensitivity:

- Long time between first BS and mirror pulses
- Large separation (momentum)

Fermilab
MAGIS-100

Light-Pulse Atom Interferometry

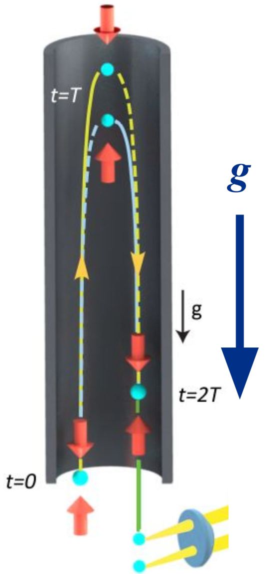

Mach-Zehnder Matter-Wave Interferometer

Abe et al, Quantum Sci. Technol. 6, 044003 (2021) [arxiv:2104.02835]

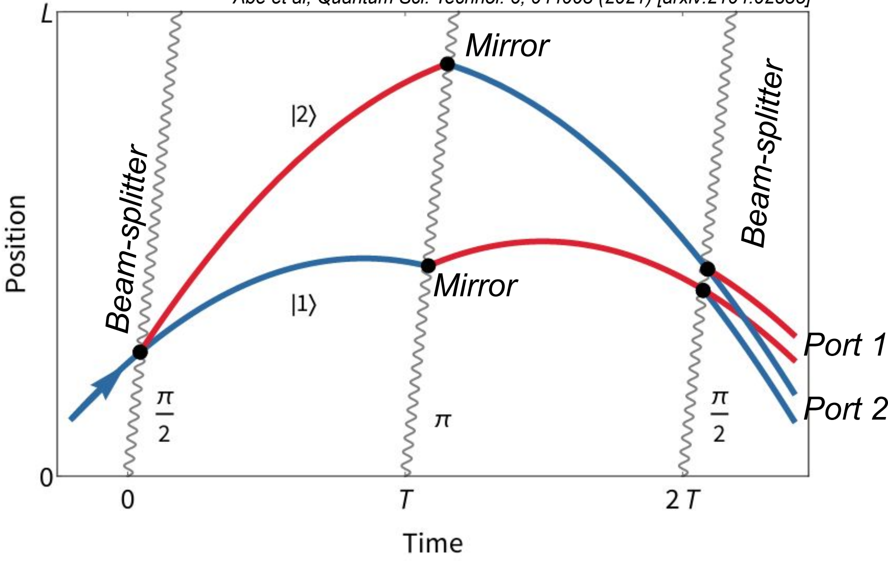

Light-Pulse Atom Interferometry

Probability of observing in port 1 vs port 2 depends on relative accumulated phase

Do this for an ensemble of 10^6 atoms

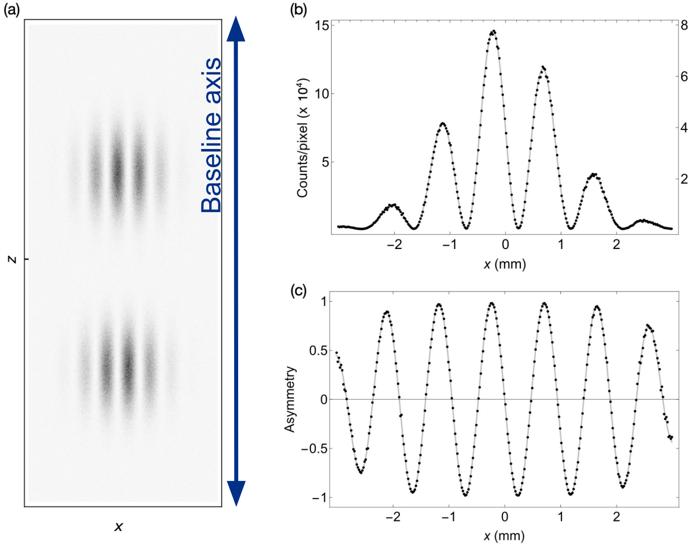

Fit fringe pattern to extract interferometer phase $\delta\varphi$

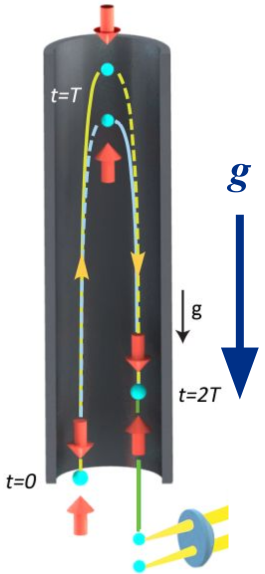

Mach-Zehnder Matter-Wave Interferometer

Abe et al, Quantum Sci. Technol. 6, 044003 (2021) [arxiv:2104.02835]

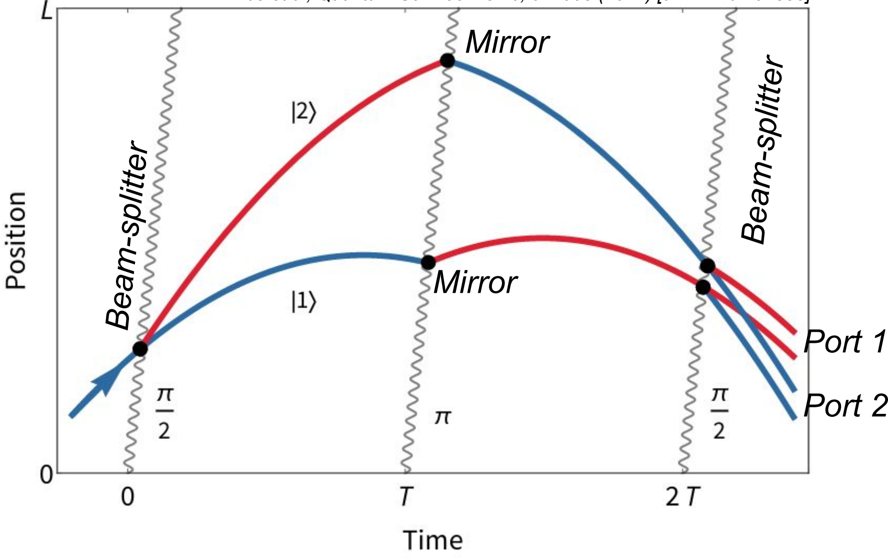

Fermilab MAGIS-100

Gradiometer Configuration

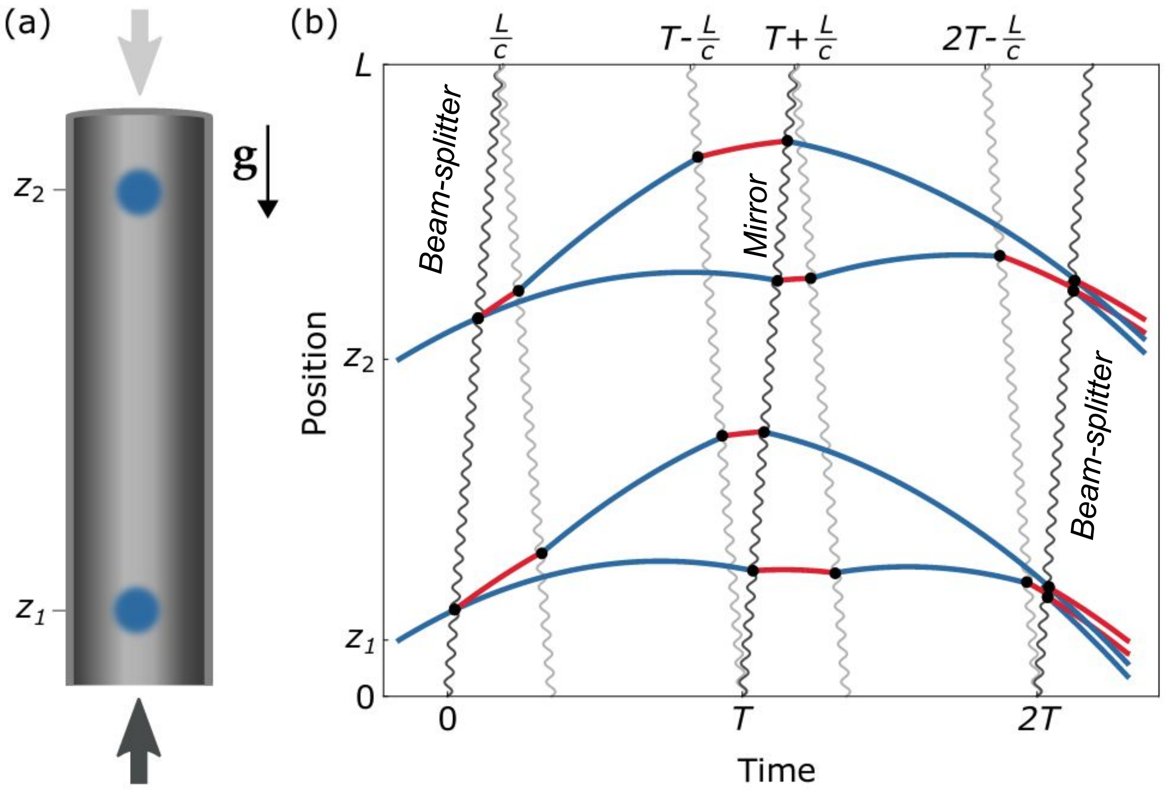

Abe et al, Quantum Sci. Technol. 6, 044003 (2021) [arxiv:2104.02835]

Same laser drives 2+ interferometers

- Laser phase noise imprinted on both clouds
- Differential measurement: common noise & systematics cancel

Fermilab
MAGIS-100

Gradiometer Configuration

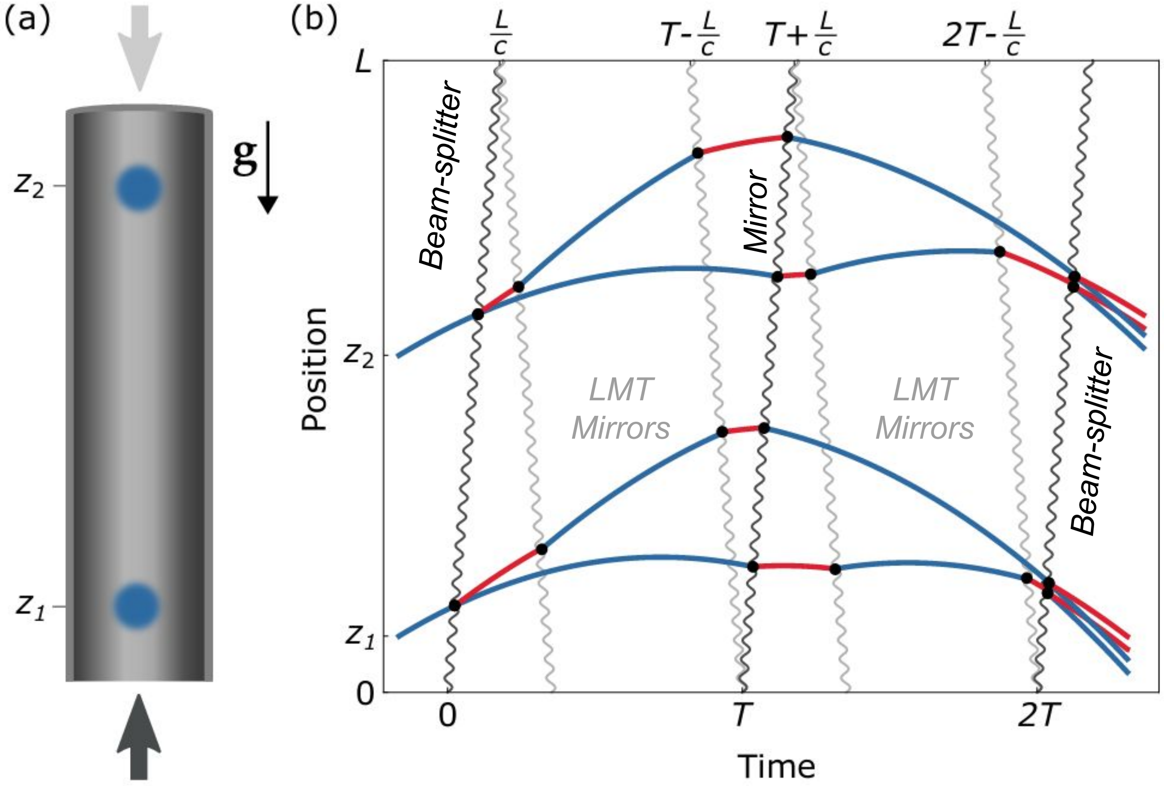

Abe et al, Quantum Sci. Technol. 6, 044003 (2021) [arxiv:2104.02835]

Same laser drives 2+ interferometers

- Laser phase noise imprinted on both clouds
- Differential measurement: common noise & systematics cancel

Large Momentum Transfer (LMT)

- LMT atom optics using π pulses from alternating directions
- Increases arm separation
- Increases signal sensitivity

Phase Evolution

After the interferometer spends time T in the excited state:

$$\frac{1}{\sqrt{2}}|1\rangle + \frac{1}{\sqrt{2}}|2\rangle e^{-i\omega_A T}$$

- ω_A: energy difference between $|1\rangle$, $|2\rangle$
- T: time between laser pulses

Excited state phase difference between interferometer arms:

$$\Delta\phi = \omega_A(2L/c)$$

Phase Evolution

After the interferometer spends time T in the excited state:

$$\frac{1}{\sqrt{2}}|1\rangle + \frac{1}{\sqrt{2}}|2\rangle e^{-i\omega_A T}$$

- ω_A: energy difference between $|1\rangle$, $|2\rangle$
- T: time between laser pulses

Interferometers along baseline L are coupled via light travel time of laser

- First pulse starts clock ticking
  - Two interferometers start at different times due to light travel time
- Something changes number of clock ticks
- Second pulse stops clock ticking

Excited state phase difference between interferometer arms:

$$\Delta\phi = \omega_A(2L/c)$$

Fermilab MAGIS-100

Phase Evolution

After the interferometer spends time T in the excited state:

$$\frac{1}{\sqrt{2}}|1\rangle + \frac{1}{\sqrt{2}}|2\rangle e^{-i\omega_A T}$$

- ω_A: energy difference between $|1\rangle$, $|2\rangle$
- T: time between laser pulses

Interferometers along baseline L are coupled via light travel time of laser

- First pulse starts clock ticking
  - Two interferometers start at different times due to light travel time
- Something changes number of clock ticks
- Second pulse stops clock ticking

Excited state phase difference between interferometer arms:

$$\Delta\phi = \omega_A(2L/c)$$

1. Modulation in atomic energy levels

$$\omega_A \to \omega_A + \delta\omega_A(t)$$

   a. e.g., ultralight scalar

Fermilab MAGIS-100

Phase Evolution

After the interferometer spends time T in the excited state:

$$\frac{1}{\sqrt{2}}|1\rangle + \frac{1}{\sqrt{2}}|2\rangle e^{-i\omega_A T}$$

- ω_A: energy difference between $|1\rangle$, $|2\rangle$
- T: time between laser pulses

Interferometers along baseline L are coupled via light travel time of laser

- First pulse starts clock ticking
  - Two interferometers start at different times due to light travel time
- Something changes number of clock ticks
- Second pulse stops clock ticking

Excited state phase difference between interferometer arms:

$$\Delta\phi = \omega_A(2L/c)$$

1. Modulation in atomic energy levels

$$\omega_A \rightarrow \omega_A + \delta\omega_A(t)$$

   a. e.g., ultralight scalar

2. Modulation in light travel time

$$L \rightarrow L + \delta L(t) = L(1 + h(t))$$

   a. e.g., gravitational wave with strain $h(t)$

Atom Interferometry with MAGIS-100

Single photon clock transitions

- Requires long-lived excited state
- Possibility to support $>10^4$ LMT pulses

3x $^{87/88}$Sr AIs vertically separated by ~50 m

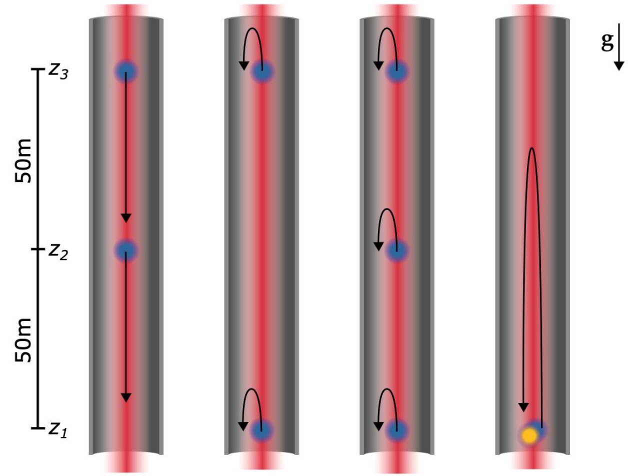

Strontium 87 clock states

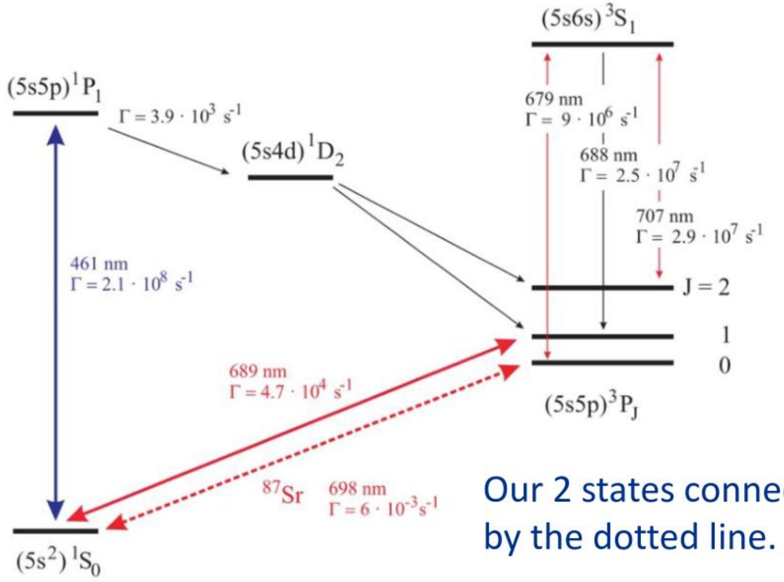

Our 2 states connected by the dotted line.

Fermilab
MAGIS-100

Signals in MAGIS-100

MAGIS-100 will be sensitive to the following effects, in the ~0.1-10 Hz band:

- Modulation of light travel time (via differing path lengths in interferometer)
- Fluctuating fundamental constants: α, m_e (via shifts in atomic energy levels)
- *Acceleration of test masses (via differential response for two isotopes)
- *Precession of spins (via comparison of states with differing nuclear spin)

** non-standard operation modes*

Signals in MAGIS-100

MAGIS-100 will be sensitive to the following effects, in the ~0.1-10 Hz band:

- Modulation of light travel time (via differing path lengths in interferometer)
- Fluctuating fundamental constants: α, m_e (via shifts in atomic energy levels)
- *Acceleration of test masses (via differential response for two isotopes)
- *Precession of spins (via comparison of states with differing nuclear spin)

All result in a time-dependent phase shift

	Initial	Final (goal)
Phase resolution (rad/Hz$^{1/2}$)	10^{-3}	10^{-5}
Strain sensitivity (Hz$^{-1/2}$)	10^{-14}	10^{-19}

* *non-standard operation modes*

Physics Capabilities with MAGIS-100

Dark Matter & New Forces

- Ultralight scalar DM
- Ultralight vector DM
- Ultralight axions
- B-L dark forces

$$\phi(t) \approx \phi_0 \cos(m_\phi t)$$

where $$\phi_0 = \sqrt{2\rho_{\rm DM}}/m_\phi$$

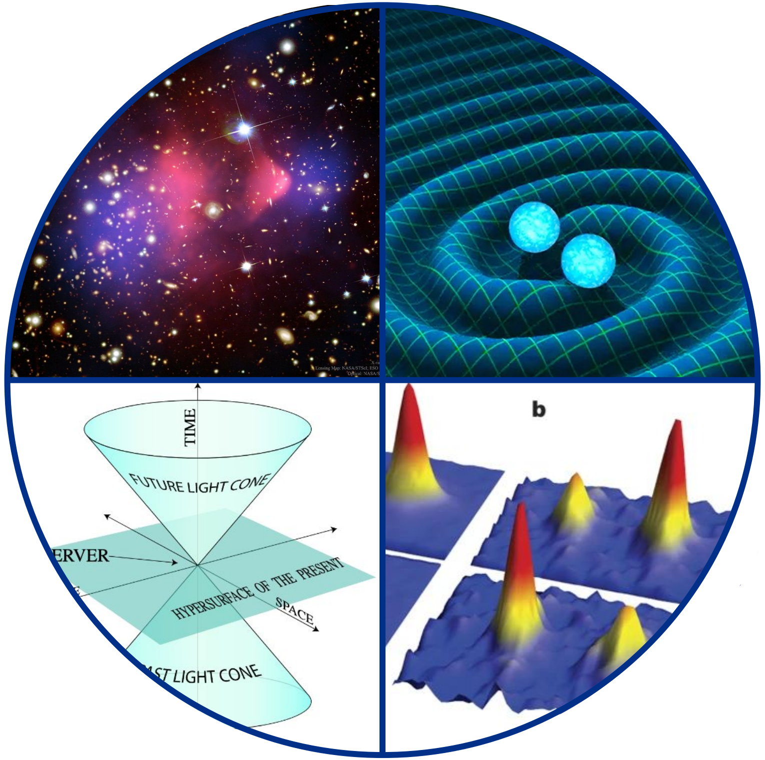

Image Credits (CCW from top left):
NASA/CXC/M. Weiss - Chandra X-Ray Observatory: 1E 0657-56
R. Hurt/Caltech-JPL
T. Kovachy et al. Nature 528, 530–533 (2015)
K. Aainsqatsi at en.wikipedia

Physics Capabilities with MAGIS-100

Dark Matter & New Forces

- Ultralight scalar DM
- Ultralight vector DM
- Ultralight axions
- B-L dark forces

$$\phi(t) \approx \phi_0 \cos(m_\phi t)$$

where $\phi_0 = \sqrt{2\rho_{\rm DM}}/m_\phi$

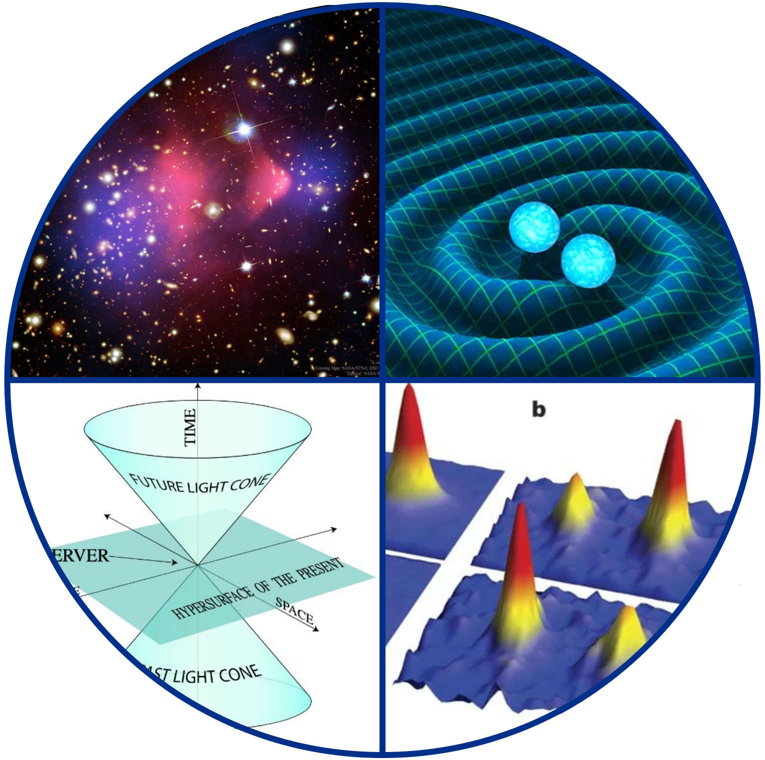

Gravitational Waves

- "Mid-band" frequencies
- Cosmological sources
- Sky localization (~1°)

The mid-band is promising for detecting gravitational waves sources by the very **high energy scales of the early universe**, potentially providing unique insights into HEP.

Image Credits (CCW from top left):
NASA/CXC/M. Weiss - Chandra X-Ray Observatory: 1E 0657-56
R. Hurt/Caltech-JPL
T. Kovachy et al. Nature 528, 530–533 (2015)
K. Aainsqatsi at en.wikipedia

Physics Capabilities with MAGIS-100

Dark Matter & New Forces

- Ultralight scalar DM
- Ultralight vector DM
- Ultralight axions
- B-L dark forces

$$\phi(t) \approx \phi_0 \cos(m_\phi t)$$

where $\quad \phi_0 = \sqrt{2\rho_{\mathrm{DM}}}/m_\phi$

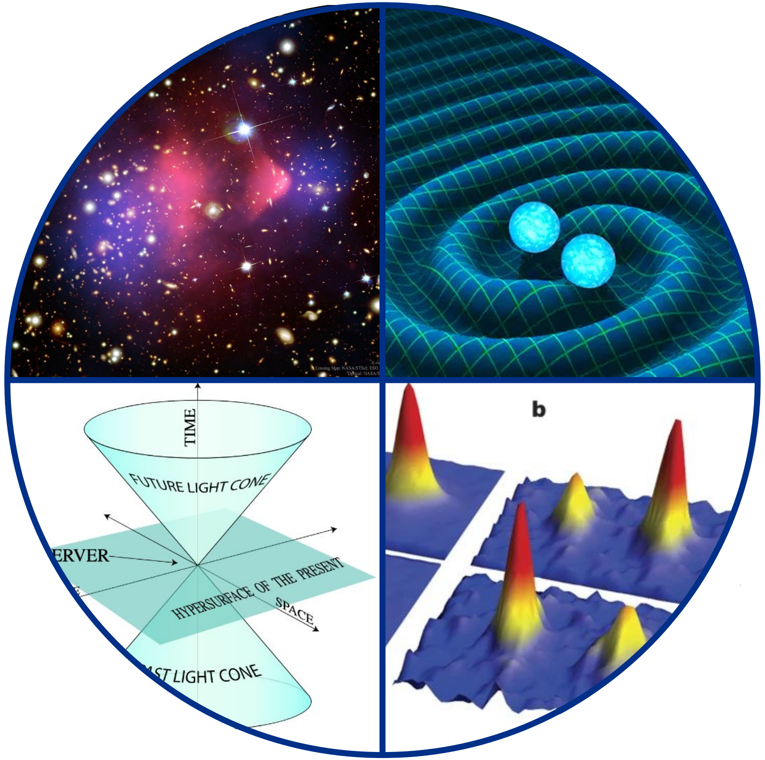

Gravitational Waves

- “Mid-band” frequencies
- Cosmological sources
- Sky localization (~1°)

The mid-band is promising for detecting gravitational waves sources by the very **high energy scales of the early universe**, potentially providing unique insights into HEP.

Quantum Mechanics

- Quantum superposition up to 10m
- Corrections to Schrödinger’s Eq
- Optimal quantum control (QIS)
- Precision measurements of fundamental constants
- Squeezed states

Image Credits (CCW from top left):
NASA/CXC/M. Weiss - Chandra X-Ray Observatory: 1E 0657-56
R. Hurt/Caltech-JPL
T. Kovachy et al. Nature 528, 530–533 (2015)
K. Aainsqatsi at en.wikipedia

Physics Capabilities with MAGIS-100

Dark Matter & New Forces

- Ultralight scalar DM
- Ultralight vector DM
- Ultralight axions
- B-L dark forces

$$\phi(t) \approx \phi_0 \cos(m_\phi t)$$

where $$\phi_0 = \sqrt{2\rho_{\rm DM}}/m_\phi$$

Tests of Relativity

- Equivalence-Principle violation
- Measurements of time dilation

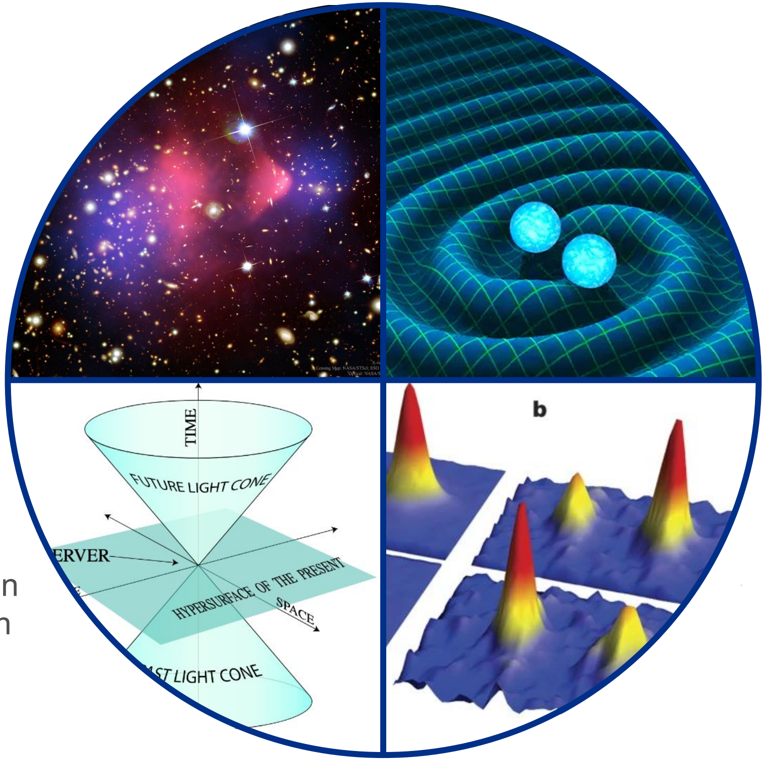

Gravitational Waves

- “Mid-band” frequencies
- Cosmological sources
- Sky localization (~1°)

The mid-band is promising for detecting gravitational waves sources by the very **high energy scales of the early universe**, potentially providing unique insights into HEP.

Quantum Mechanics

- Quantum superposition up to 10m
- Corrections to Schrödinger’s Eq
- Optimal quantum control (QIS)
- Precision measurements of fundamental constants
- Squeezed states

Image Credits (CCW from top left):
NASA/CXC/M. Weiss - Chandra X-Ray Observatory: 1E 0657-56
R. Hurt/Caltech-JPL
T. Kovachy et al. Nature 528, 530–533 (2015)
K. Aainsqatsi at en.wikipedia

Physics Capabilities with MAGIS-100

Dark Matter & New Forces

- Ultralight scalar DM
- Ultralight vector DM
- Ultralight axions
- B-L dark forces

$$\phi(t) \approx \phi_0 \cos(m_\phi t)$$

where $\phi_0 = \sqrt{2\rho_{\mathrm{DM}}}/m_\phi$

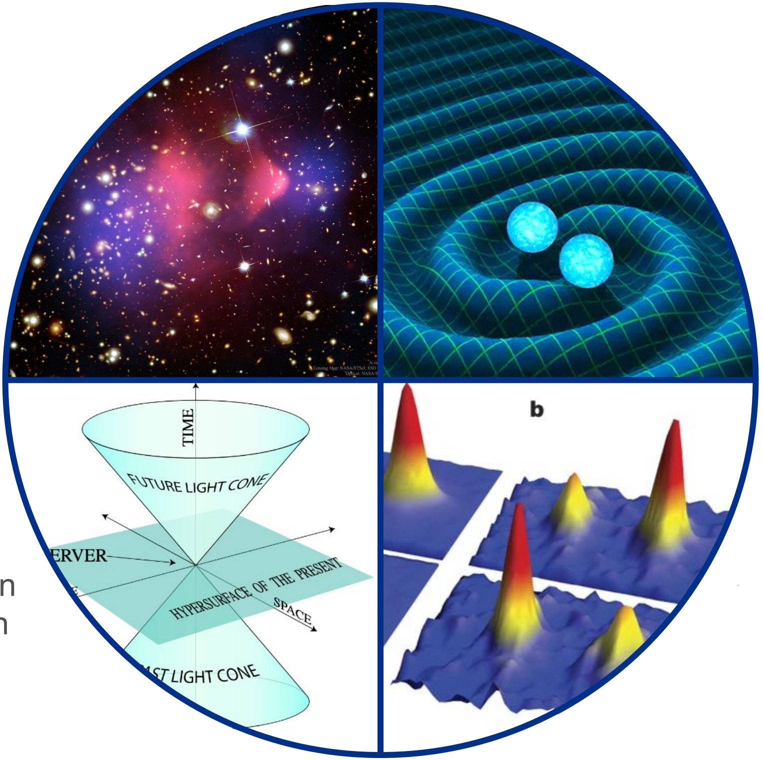

Gravitational Waves

- “Mid-band” frequencies
- Cosmological sources
- Sky localization (~1°)

The mid-band is promising for detecting gravitational waves sources by the very **high energy scales of the early universe**, potentially providing unique insights into HEP.

Quantum Mechanics

- Quantum superposition up to 10m
- Corrections to Schrödinger’s Eq
- Optimal quantum control (QIS)
- Precision measurements of fundamental constants
- Squeezed states

Tests of Relativity

- Equivalence-Principle violation
- Measurements of time dilation

Long-baseline AI technology demonstrator

Image Credits (CCW from top left):
NASA/CXC/M. Weiss - Chandra X-Ray Observatory: 1E 0657-56
R. Hurt/Caltech-JPL
T. Kovachy et al. Nature 528, 530–533 (2015)
K. Aainsqatsi at en.wikipedia

Ultralight Dark Matter Properties

arxiv:2203.14915

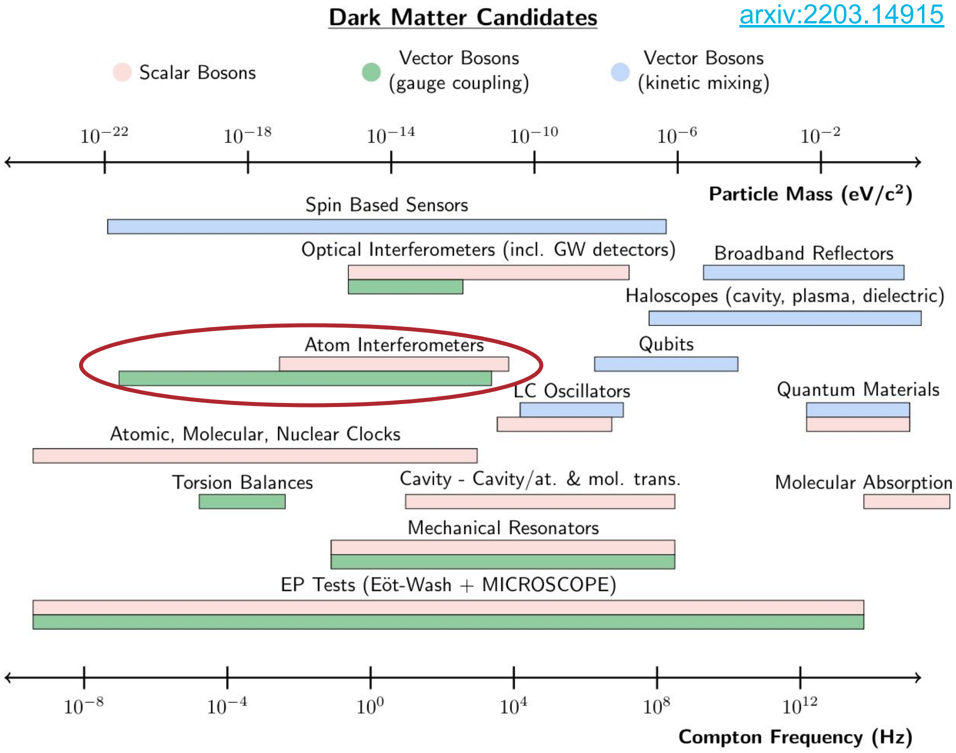

Ultralight Dark Matter Properties

- Required to be bosonic (exclusion)
- m_ϕ << eV → large number density
- Classical oscillating field:

$$\phi\,(t,\mathbf{x}) = \phi_0 \cos\left[m_\phi(t - \mathbf{v}\cdot\mathbf{x}) + \beta\right] + \mathcal{O}\left(|\mathbf{v}|^2\right)$$

$$\text{where} \qquad \phi_0 = \sqrt{2\rho_{\mathrm{DM}}}/m_\phi$$

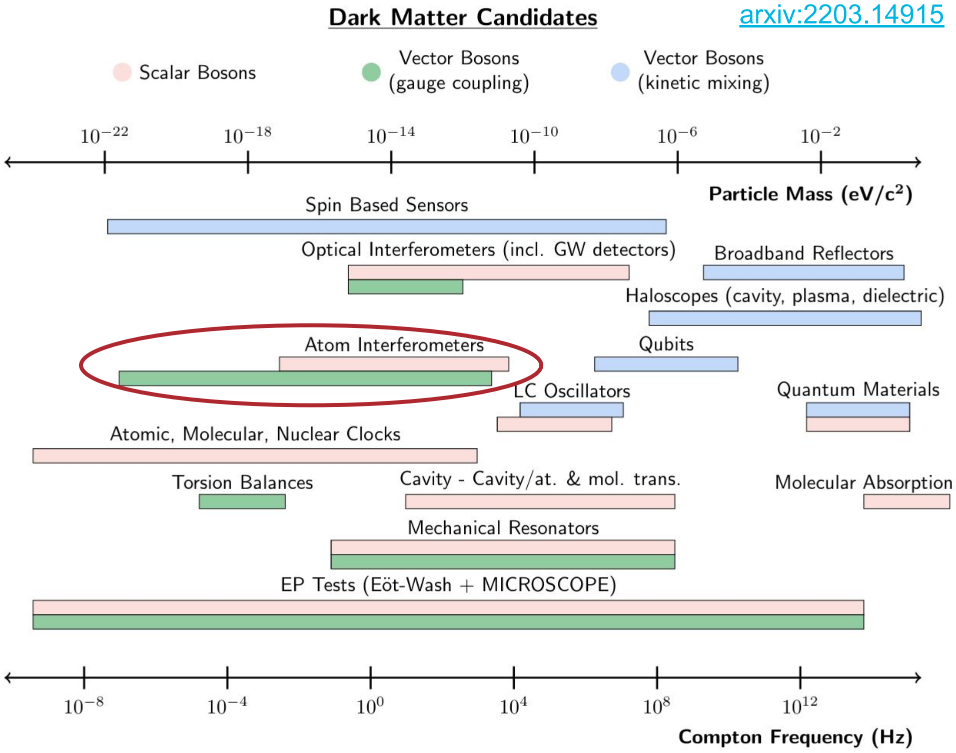

Fermilab MAGIS-100

Ultralight Dark Matter Properties

- Required to be bosonic (exclusion)
- m_ϕ << eV → large number density
- Classical oscillating field:

$$\phi\,(t, \mathbf{x}) = \phi_0 \cos\left[m_\phi(t - \mathbf{v}\cdot\mathbf{x}) + \beta\right] + \mathcal{O}\left(|\mathbf{v}|^2\right)$$

$$\text{where} \qquad \phi_0 = \sqrt{2\rho_{\text{DM}}}/m_\phi$$

Scalar (e.g. dilaton): Time-varying fundamental constants if coupled to electron or photon

$$m_e(t, x) = m_{e0}\left(1 + d_{m_e}\sqrt{4\pi G_N}\phi(t, x)\right)$$

$$\alpha(t, x) = \alpha_0\left(1 + d_e\sqrt{4\pi G_N}\phi(t, x)\right)$$

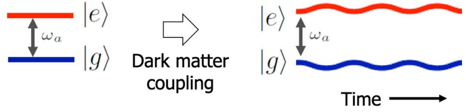

arxiv:2203.14915

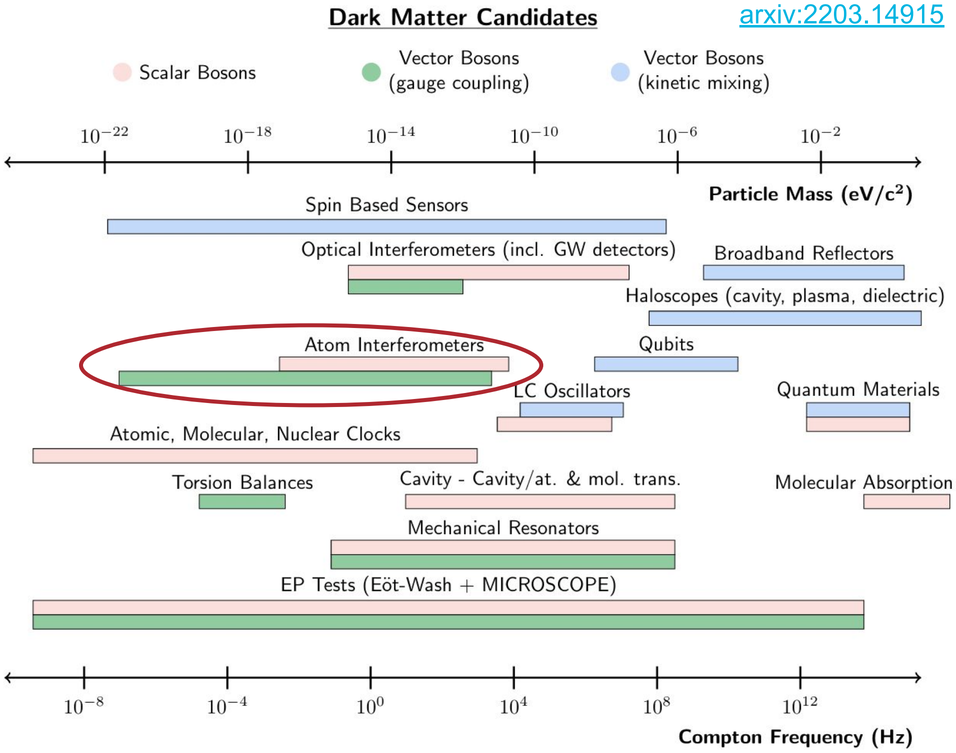

Fermilab MAGIS-100

Ultralight Dark Matter Properties

- Required to be bosonic (exclusion)
- m_ϕ << eV → large number density
- Classical oscillating field:

$$\phi\,(t,\mathbf{x}) = \phi_0 \cos\left[m_\phi(t - \mathbf{v}\cdot\mathbf{x}) + \beta\right] + \mathcal{O}\left(|\mathbf{v}|^2\right)$$

$$\text{where} \qquad \phi_0 = \sqrt{2\rho_{\mathrm{DM}}}/m_\phi$$

Scalar (e.g. dilaton): Time-varying fundamental constants if coupled to electron or photon

$$m_e(t,x) = m_{e0}\left(1 + d_{m_e}\sqrt{4\pi G_N}\phi(t,x)\right)$$

$$\alpha(t,x) = \alpha_0\left(1 + d_e\sqrt{4\pi G_N}\phi(t,x)\right)$$

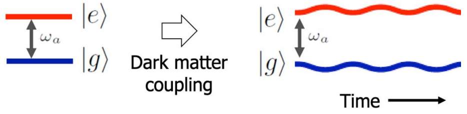

***B-L* Vector**: Differential acceleration of bodies with differing neutron content

arxiv:2203.14915

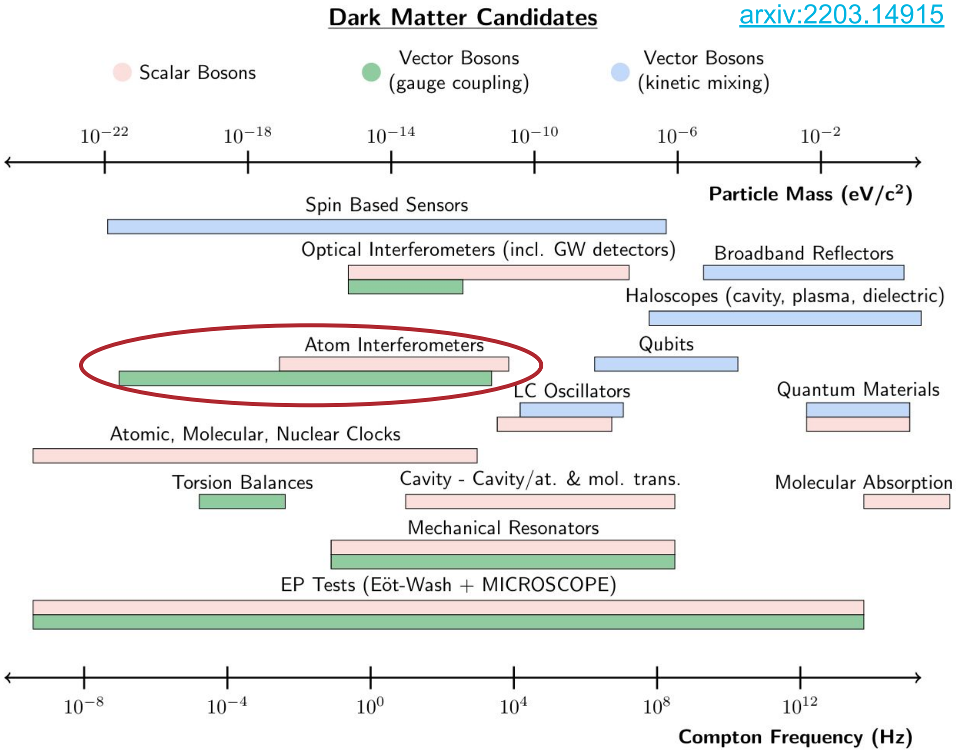

Fermilab
MAGIS-100

MAGIS-100 Projections: Dark Matter & Gravitational Waves

Ultralight Scalar DM
Photon coupling

Atomic energy levels oscillate at DM frequency (mass)

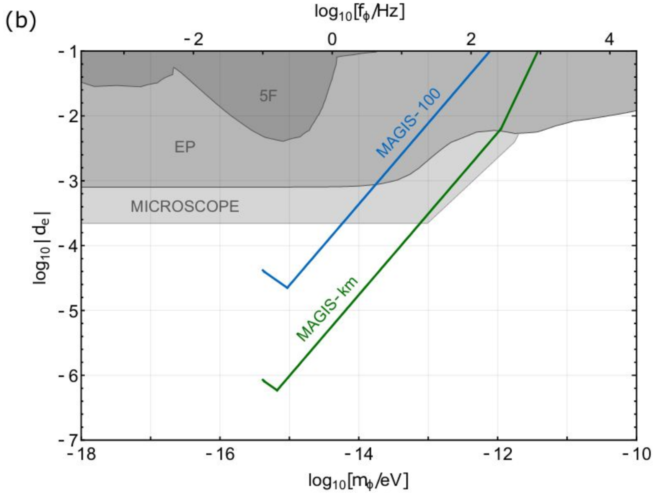

B-L Coupled Vector Boson

Different isotopes ($^{87}Sr/^{88}Sr$) experience different acceleration due to differing neutron content

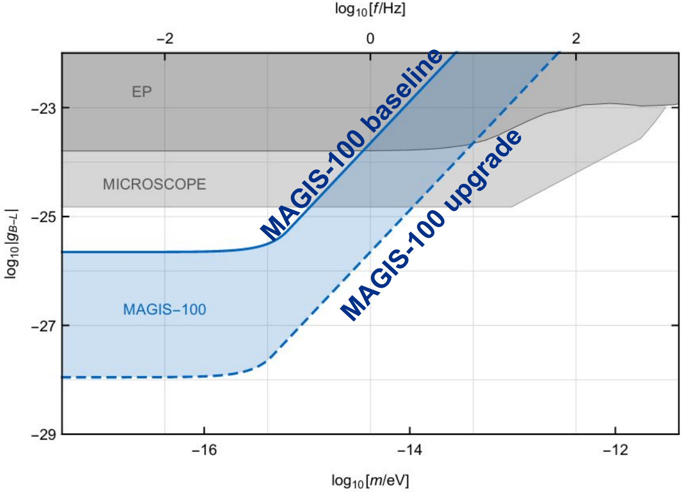

Gravitational Waves
Strain sensitivity

GW-induced strain modulates light travel time across baseline

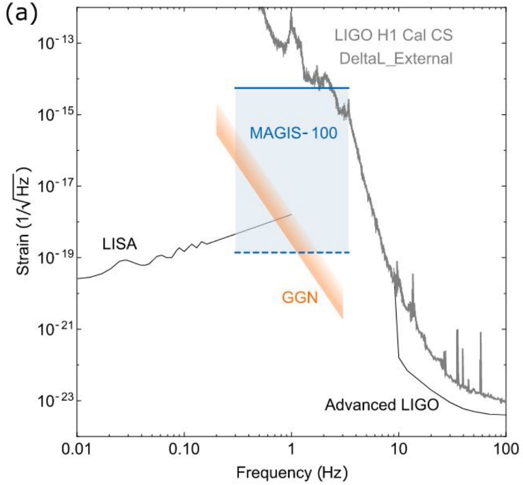

Abe et al, Quantum Sci. Technol. 6, 044003 (2021) [arxiv:2104.02835]

The MAGIS-100 Apparatus & Systems

Laser Delivery

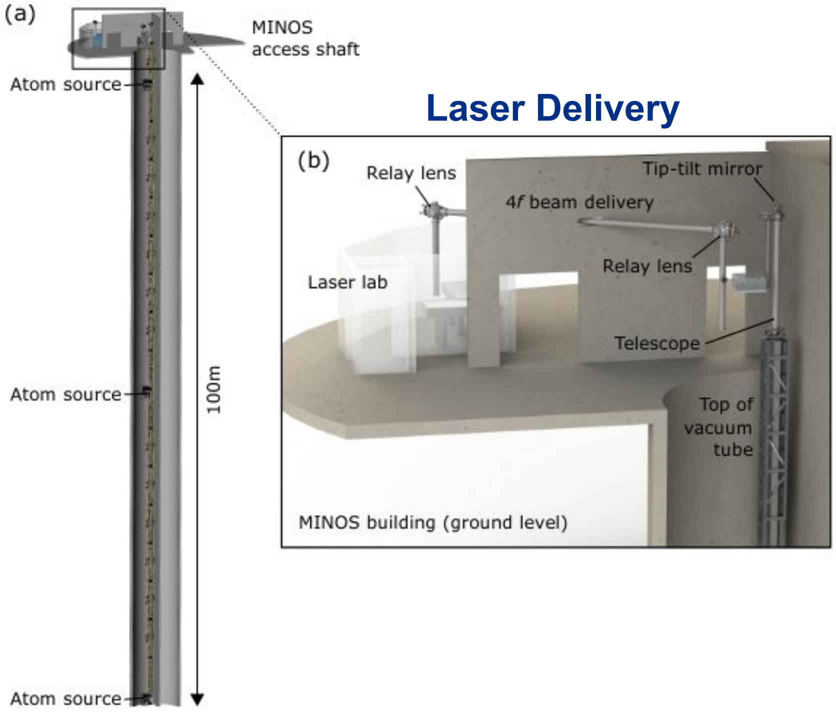

Fermilab
MAGIS-100

The MAGIS-100 Apparatus & Systems

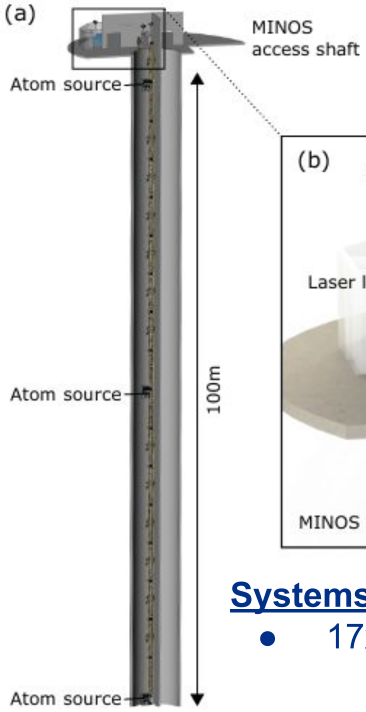

Laser Delivery

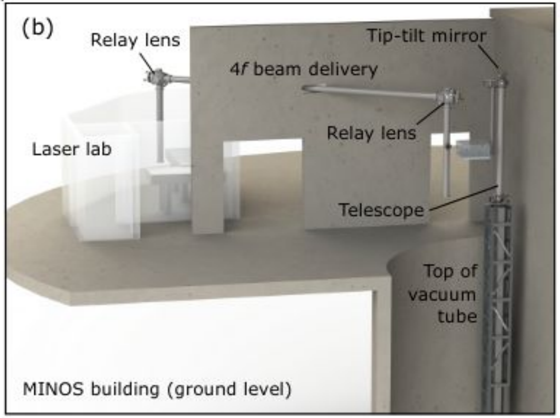

Modular Section

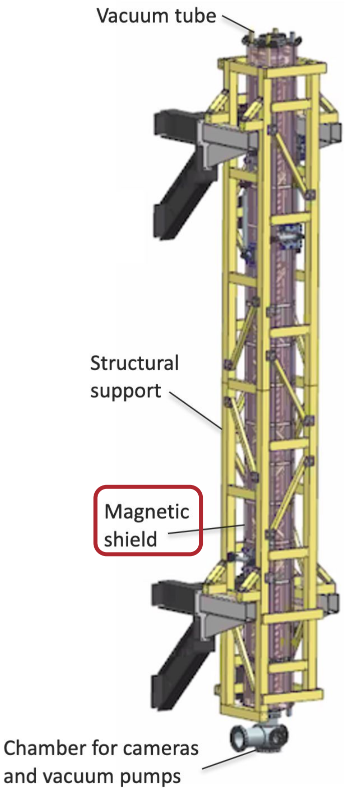

Systems in shaft:

- 17x modular sections

Fermilab MAGIS-100

The MAGIS-100 Apparatus & Systems

Strontium 87 Atom Source

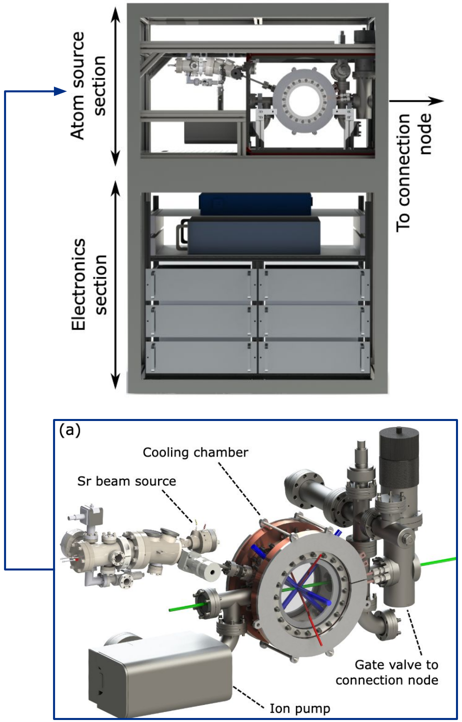

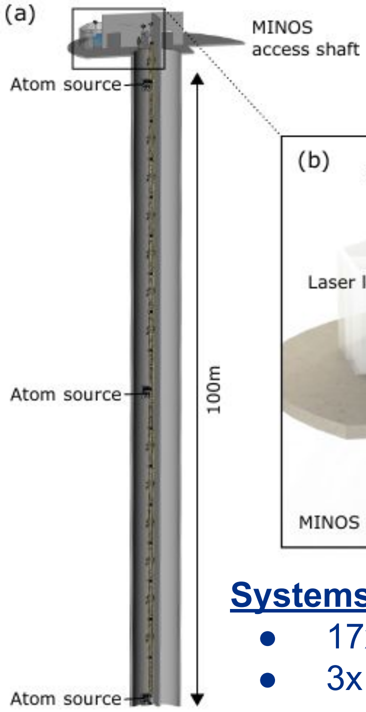

Laser Delivery

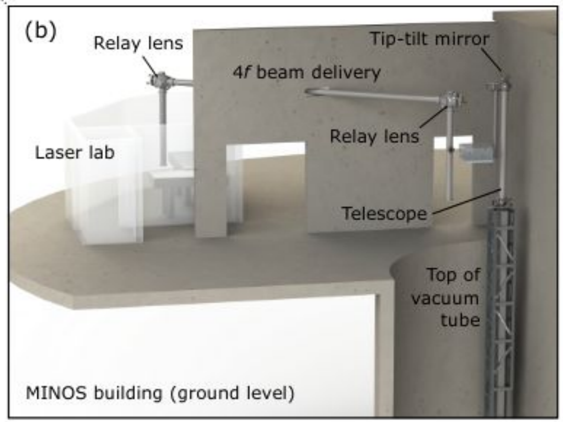

Systems in shaft:

- 17x modular sections
- 3x atom sources

Modular Section

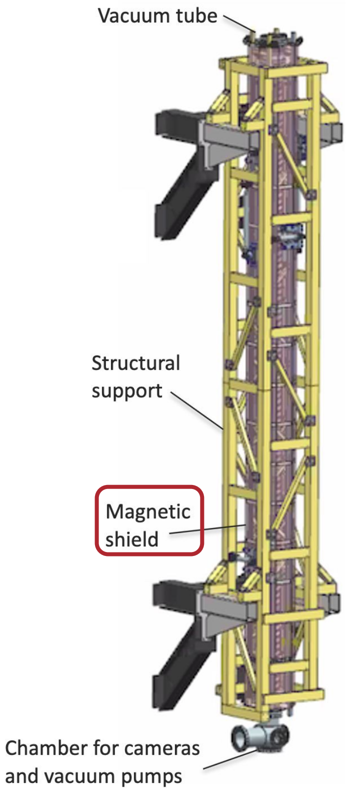

Fermilab
MAGIS-100

The MAGIS-100 Apparatus & Systems

Strontium 87 Atom Source

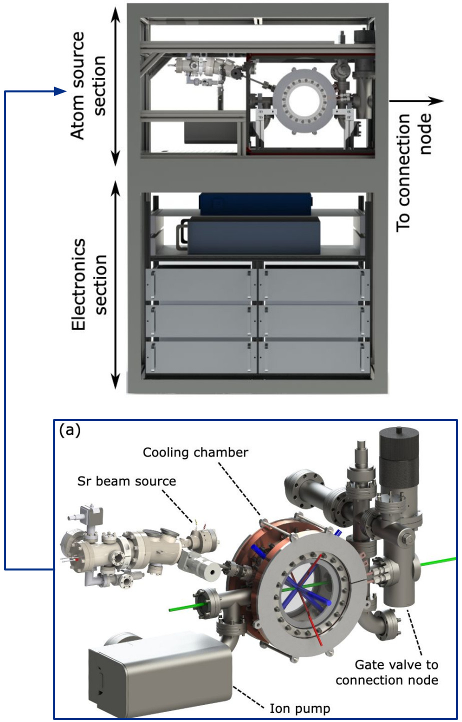

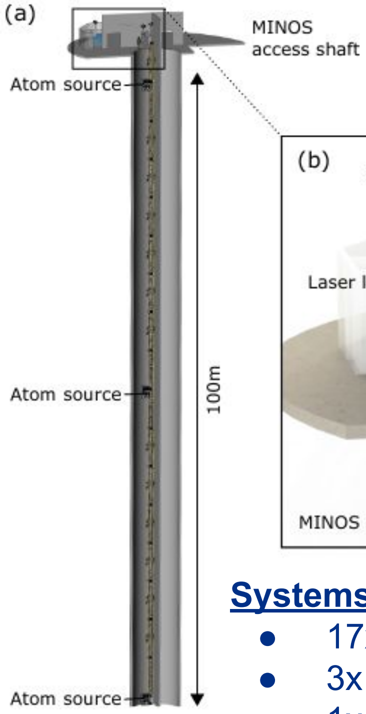

Laser Delivery

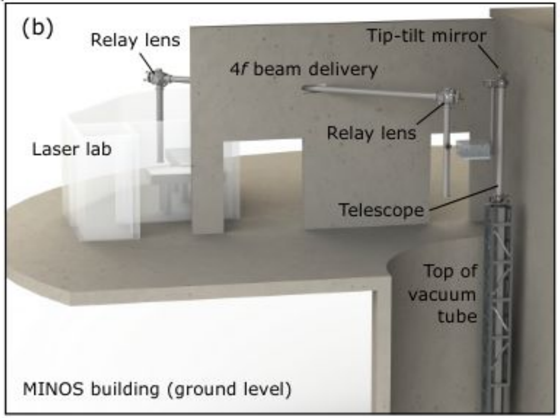

Systems in shaft:

- 17x modular sections
- 3x atom sources
- 1x retroreflection chamber (bottom)
- 2x vacuum roughing stations
- Environmental monitoring

Modular Section

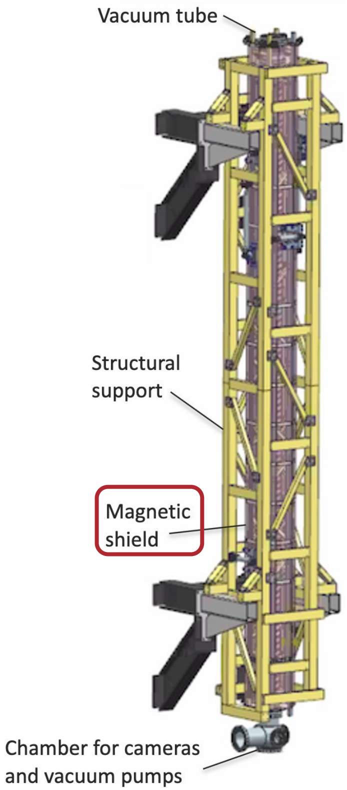

Fermilab MAGIS-100

The MAGIS-100 Apparatus & Systems

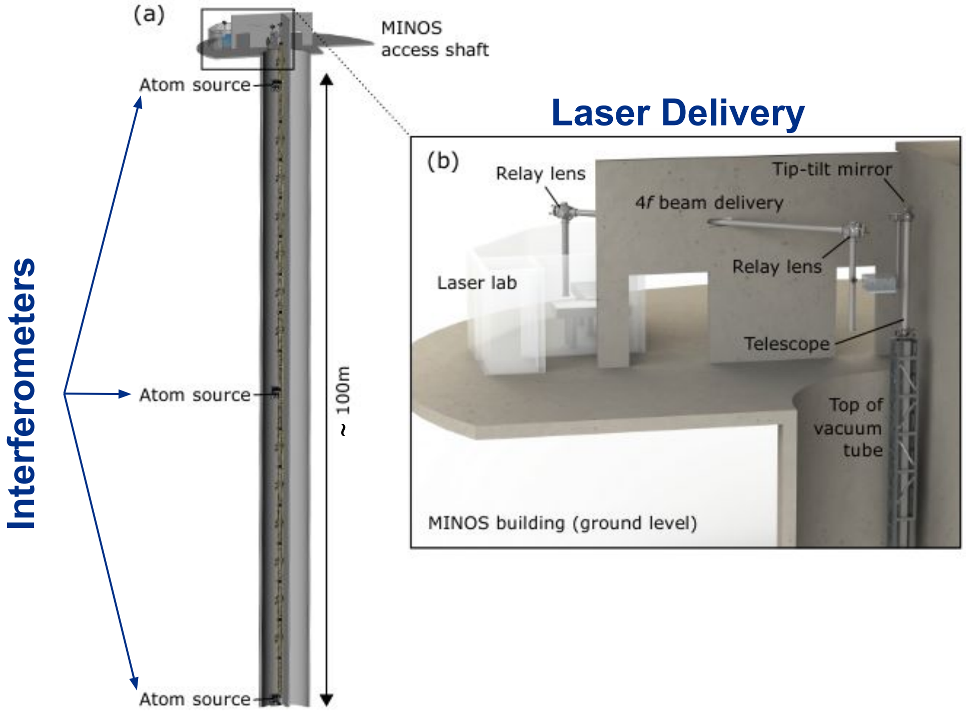

Quantum Sci. Technol. 6, 044003 (2021) [arxiv:2104.02835]

The MAGIS-100 Apparatus & Systems

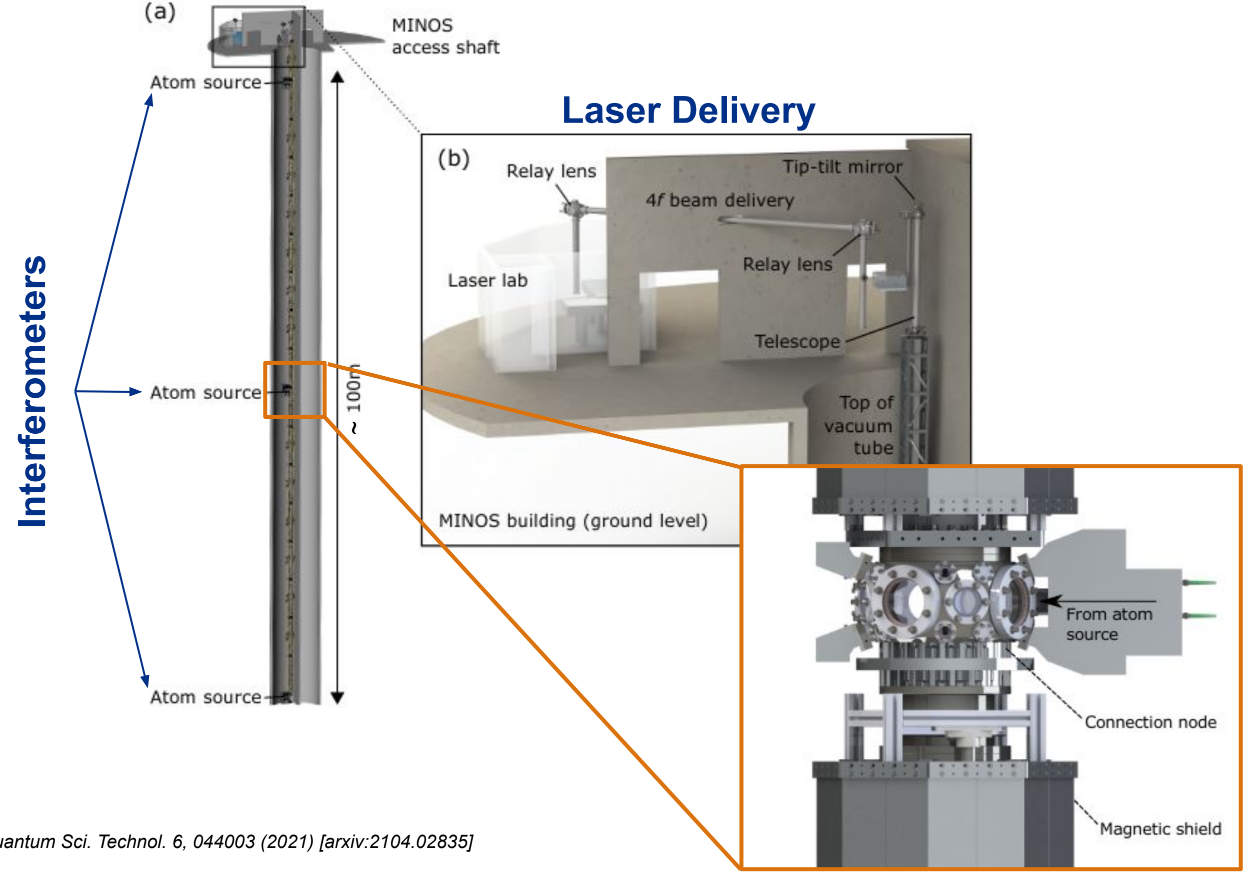

Quantum Sci. Technol. 6, 044003 (2021) [arxiv:2104.02835]

Fermilab MAGIS-100

The MAGIS-100 Apparatus & Systems

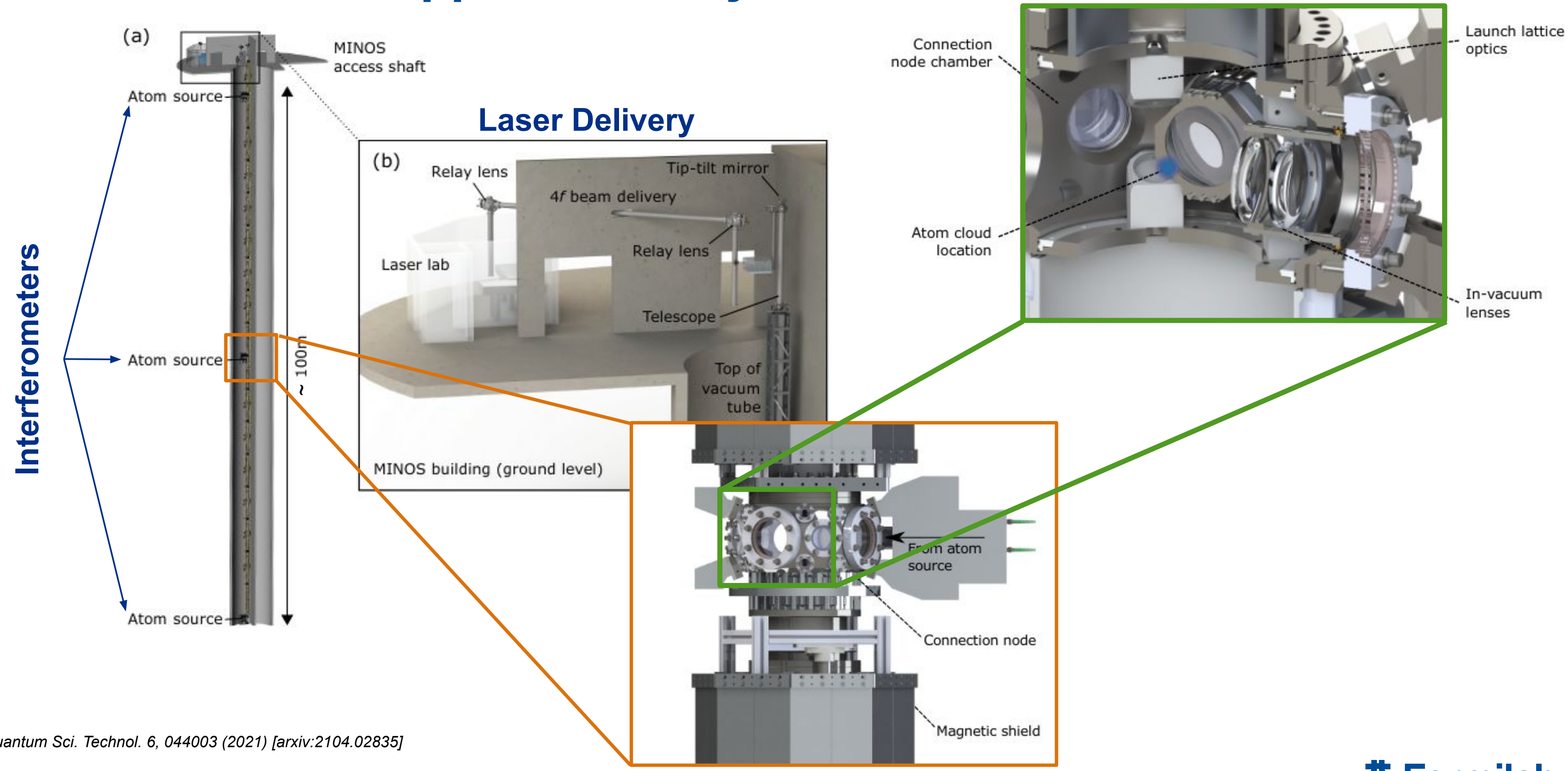

Quantum Sci. Technol. 6, 044003 (2021) [arxiv:2104.02835]

The MAGIS-100 Apparatus & Systems

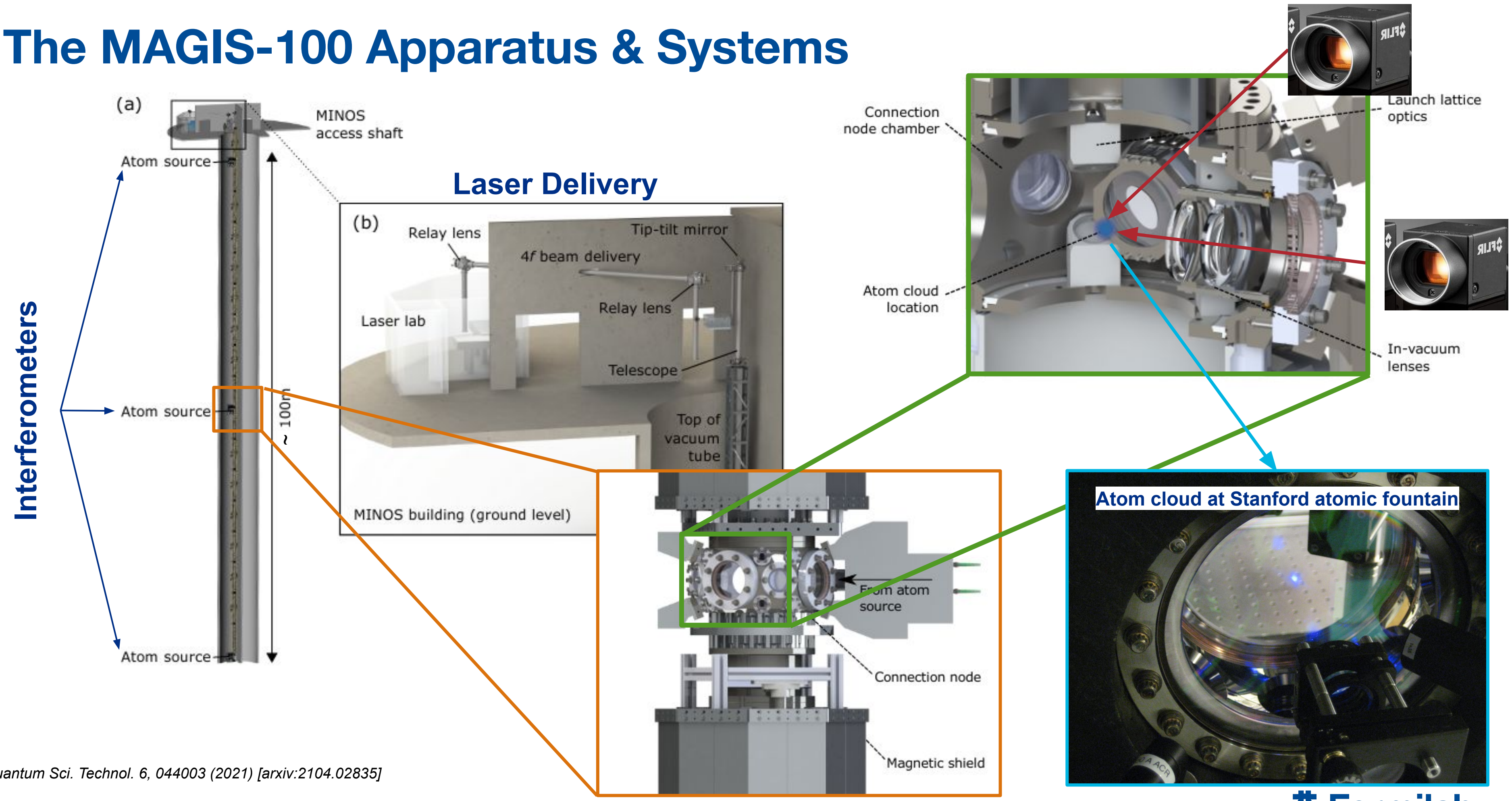

Quantum Sci. Technol. 6, 044003 (2021) [arxiv:2104.02835]

MAGIS-100 Laser Systems

Total: 22 beams in 8 wavelengths

- 679 nm - Raman / Repump
- 688 nm - Raman / Transparency
- 689 nm - Cooling
- **698 nm - Atom interferometry**
- 707 nm - Repump
- 922(461) nm - Blue MOT / Detection
- 1064 nm - Dipole trap
- 1542 nm - Optical reference system

Optical frequency comb enables <10 Hz frequency stability

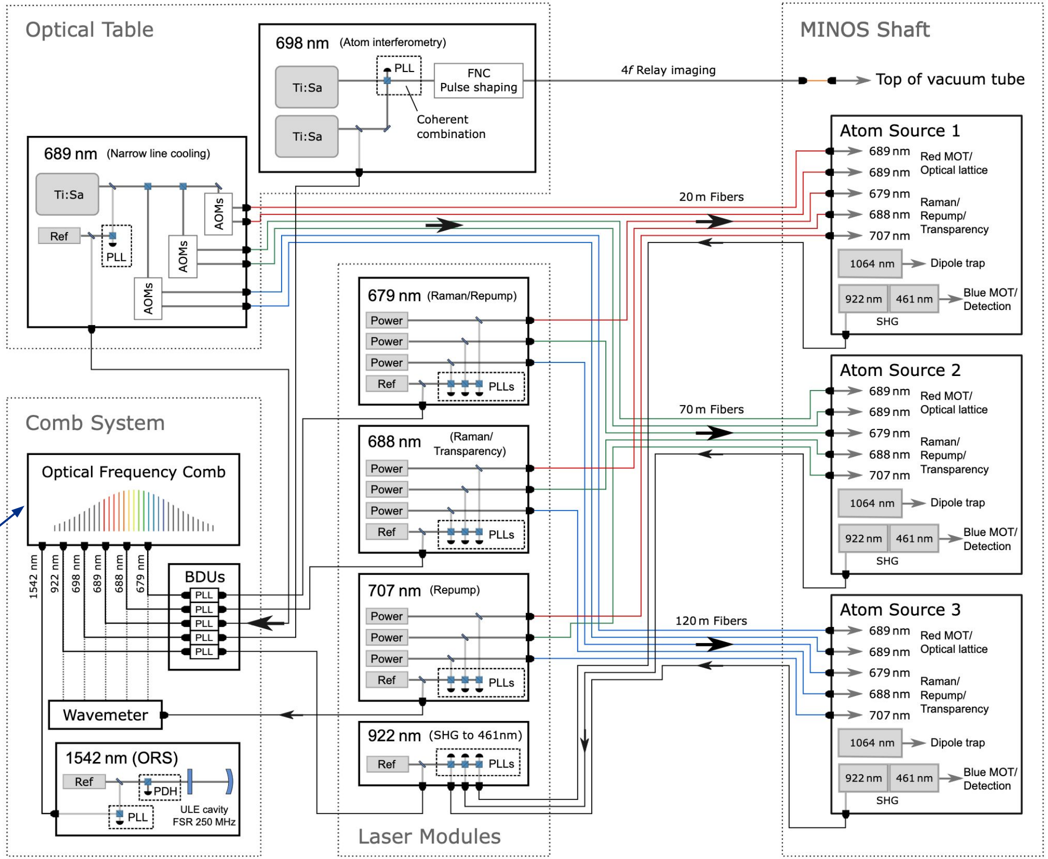

MAGIS-100 Laser Systems

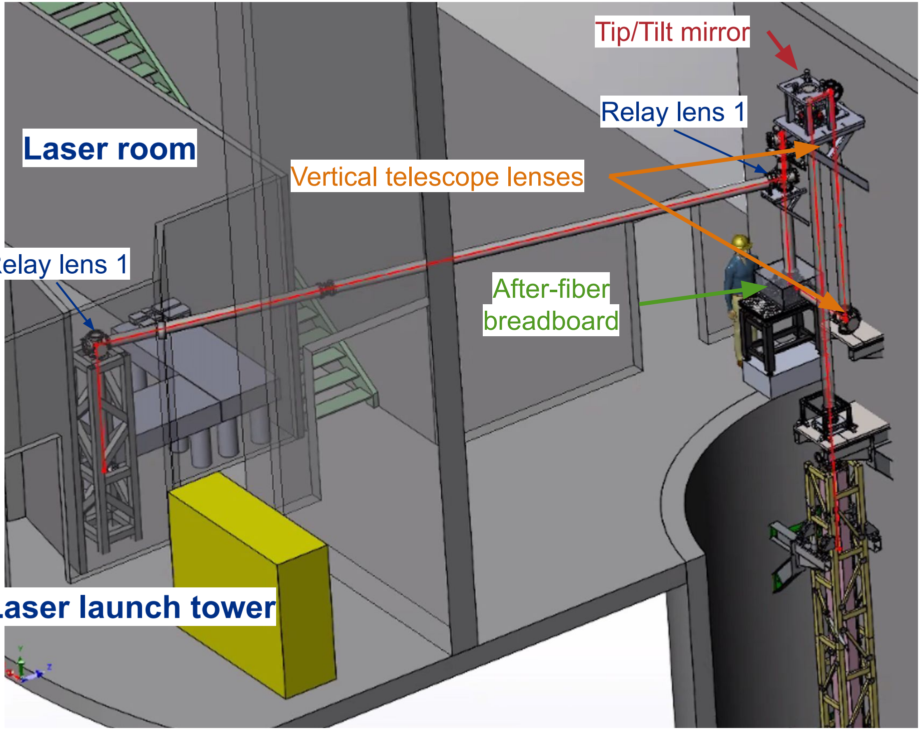

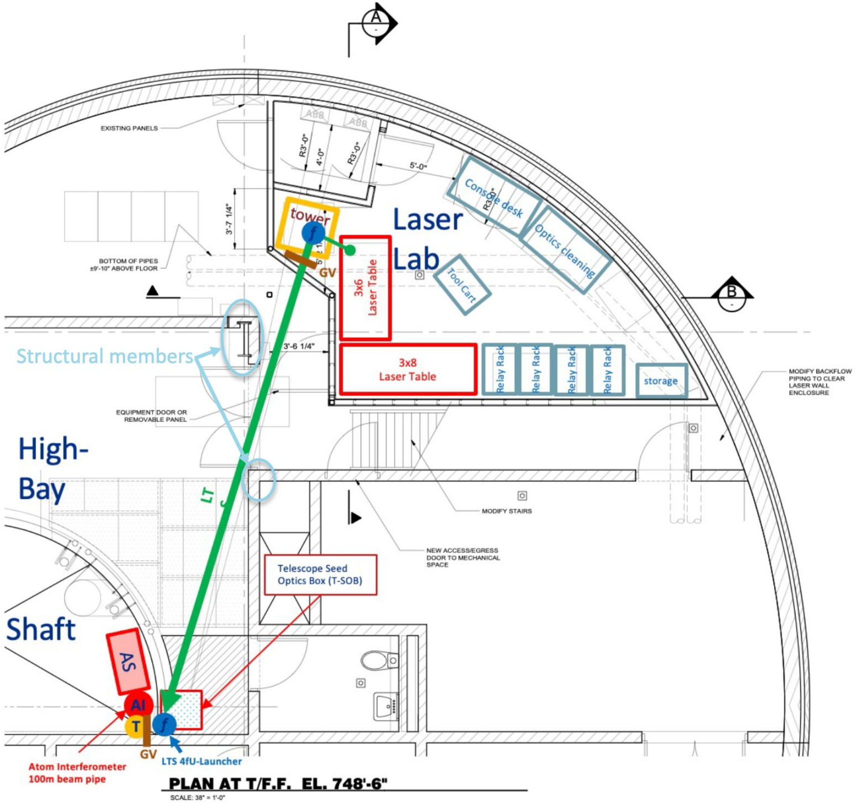

- The interferometer beam is relay-imaged over the 10m run between laser lab and top of shaft via two in-vacuum lenses (4f configuration)
- Relay-imaged beam coupled into optical fiber: pointing jitters → intensity fluctuations
- Laser power (post-fiber) actively stabilized with PID feedback loop

The MAGIS-100 Site: MINOS Service Building & Access Shaft

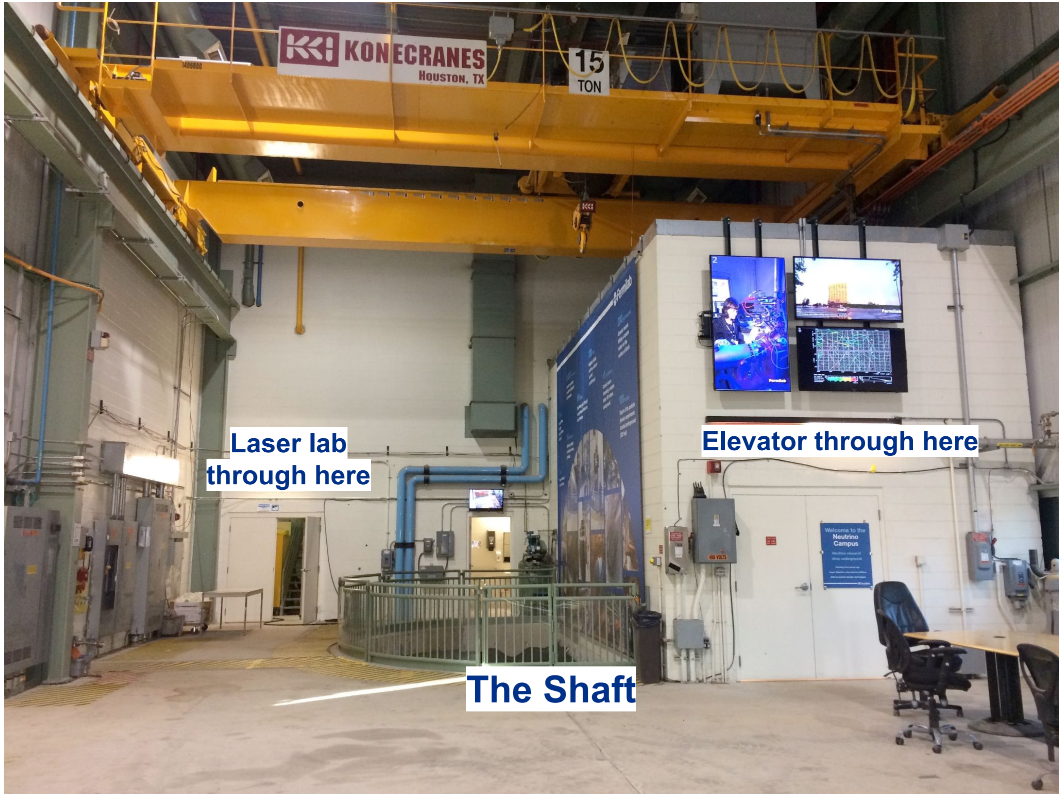

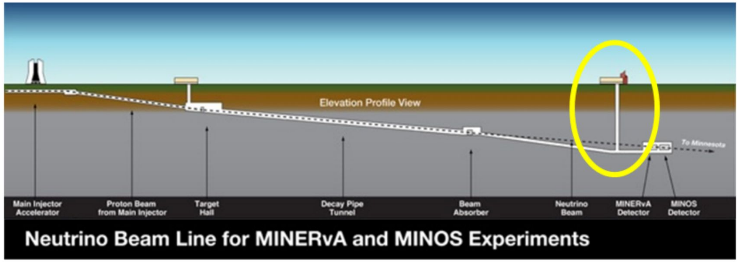

Fermilab
MAGIS-100

The MAGIS-100 Site: MINOS Service Building & Access Shaft

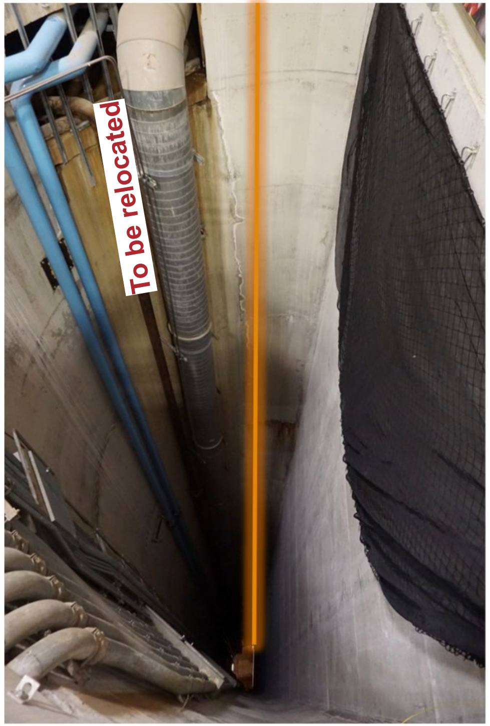

Top of shaft

Bottom of shaft

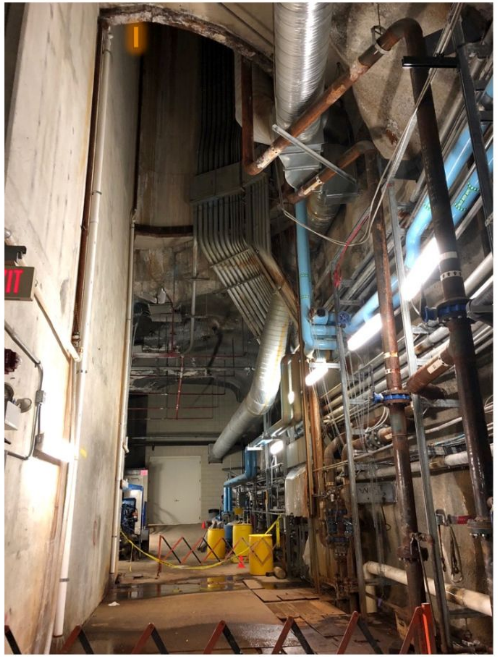

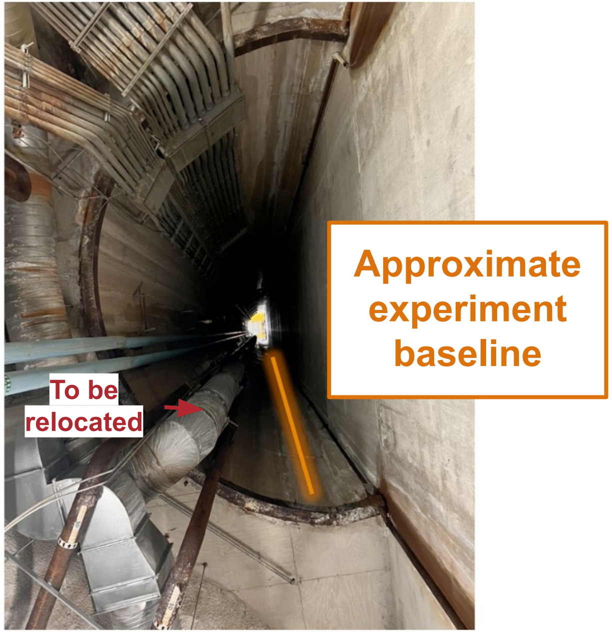

Bottom of shaft
Looking up

Slide from L. Valerio

Shaft Top View

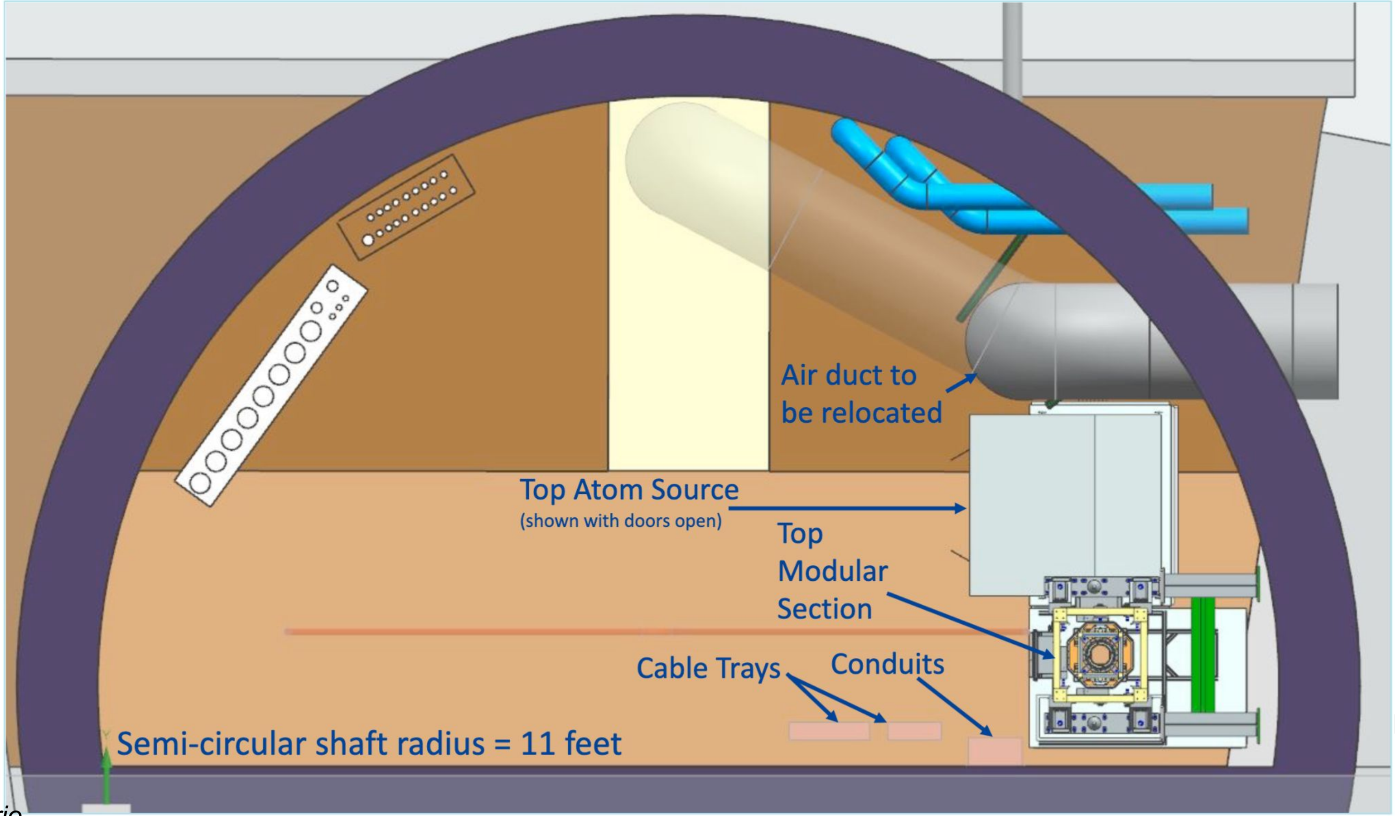

Laser telescope not shown

Slide from L. Valerio

Laser Lab Civil Construction Nearly Complete!

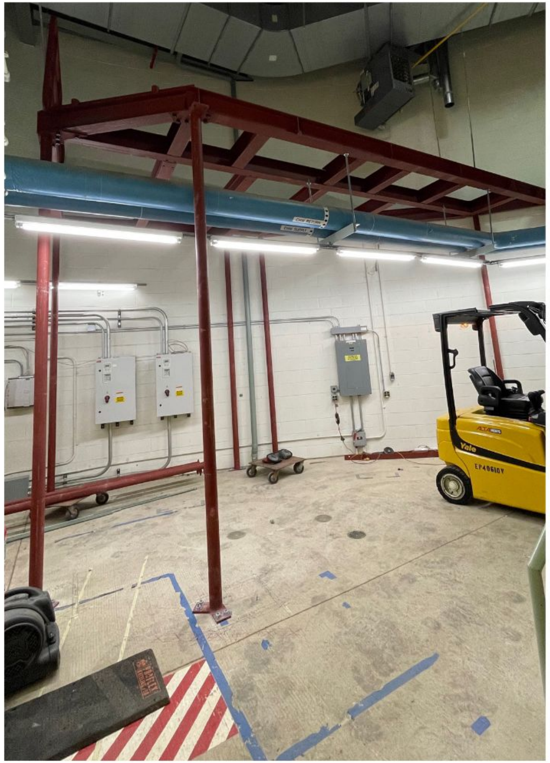

Construction started in 2023.

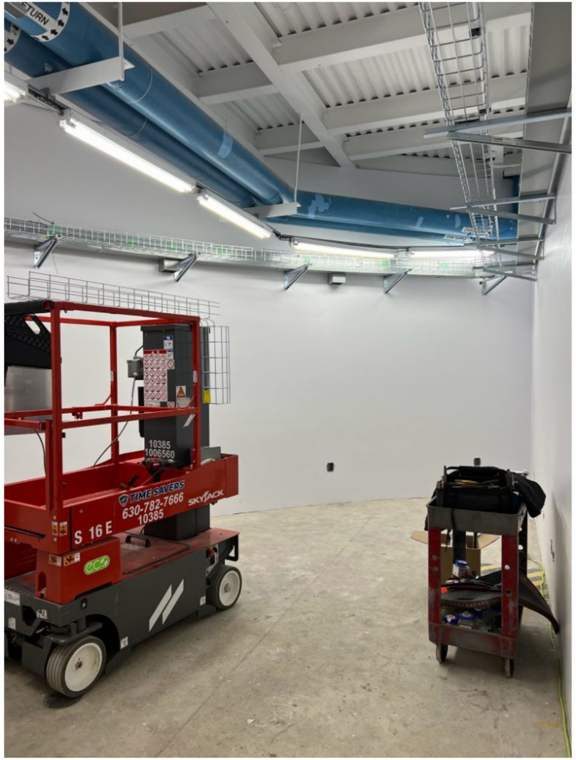

Status April 2024.

Current Status!

- Floor poured
- Electrical installed
- Cable trays in-place
- Overhead instrument racks installed
- Optics tables in-hand
- Laser launch tower installed

Current Status: Atom Sources

Two working prototype Sr atom sources at Stanford

- Still in progress:
  - Dipole traps
  - Shuttle lattice

Will be installed in Stanford 10m prototype atomic fountain first

Last components to be installed in-shaft at Fermilab

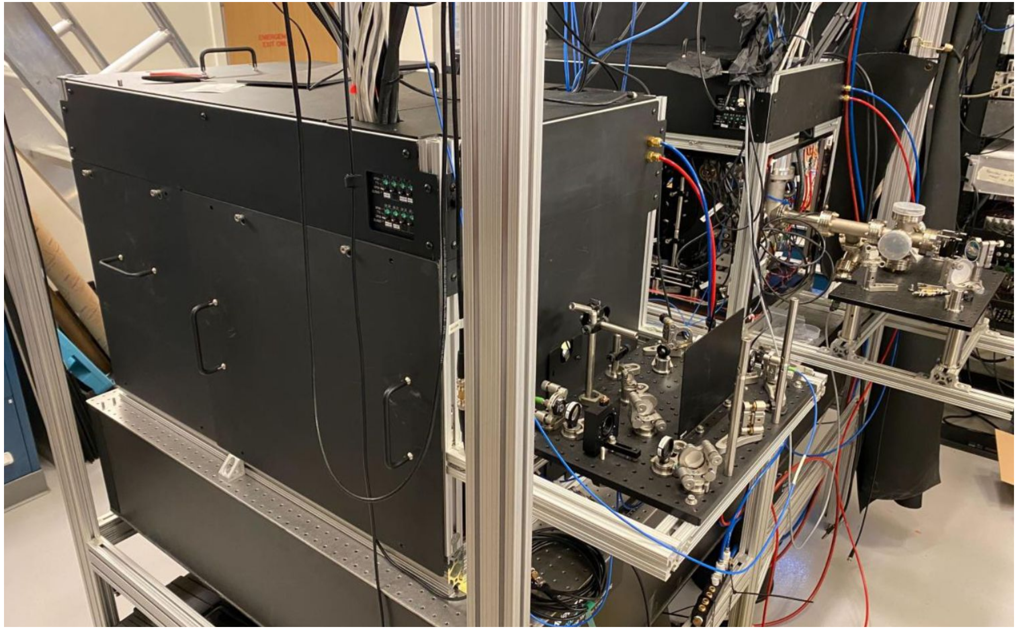

Current Status: Laser Systems

Ongoing development & testing of interferometry system & beam delivery

Interferometry system recent demonstrations:

- Coherent combination of 2x Ti:Sapph 698 nm lasers
- 4W pulsed beam delivery with mode-cleaning and active noise cancellation

Beam delivery status:

- Design complete
- Prototyping in progress
- Preparing to build system with optics recently received at FNAL

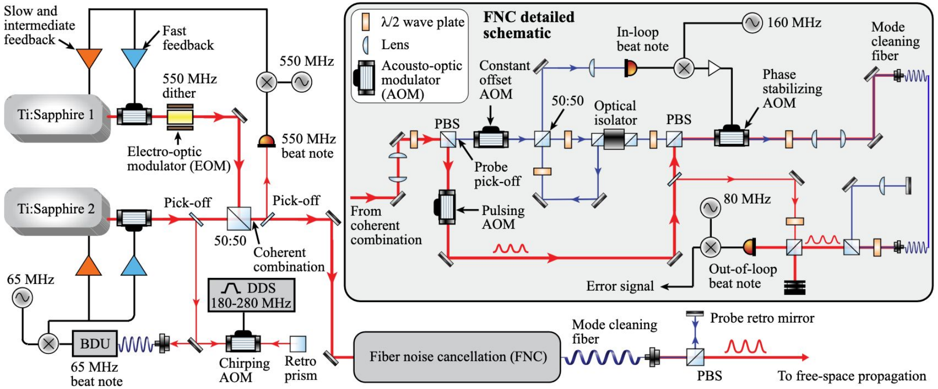

J. Glick, et al. AVS Quantum Sci. 6, 014402 (2024)
K. DeRose, et al. Opt. Lett. 48, 3893-3896 (2023)

Current Status: Primary Science Imaging System

3 cameras per atom source node

Lucid Vision Triton **Sony IMX541** CMOS **sensor:**

- 4.5k x 4.5k pixels, 2.74 μm square
- 5.5 FPS
- 12-bit ADC
- Global shutter
- Dark current 1.6e/s
- QE ~70% at 450nm
- ~2.1e read noise
- PoE

50mm fixed focal length lens:

- f/1.8 to f/16
- Mwd 200mm
- Max diameter ~50mm

Procured and under test @ Oxford

Camera & lens mount

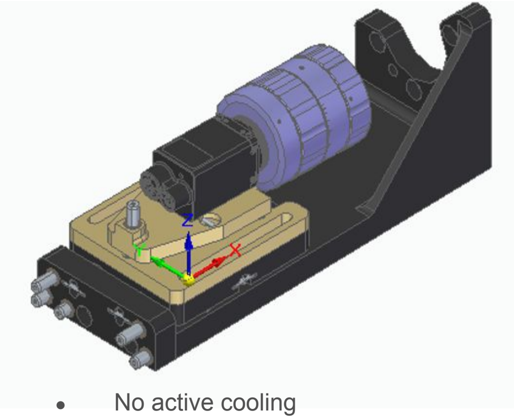

- No active cooling
- Three-axis fine position adjustment (~a few mm) accessible from exterior
- Cutaway view (fully enclosed)

Final design stages

Testbench @ Oxford

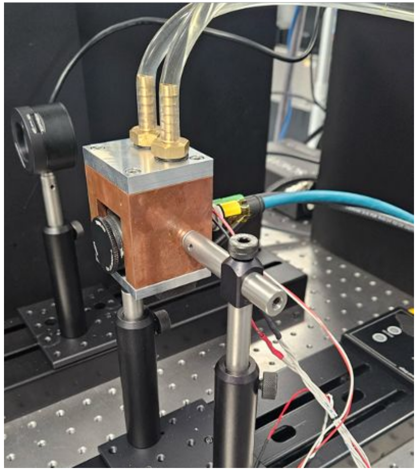

- Operational software, databasing, analysis finalised for real sensor data
- Initial shakedown data runs using a spare camera are underway
- First real calibration data in next few weeks.

Slide from D. Weatherill

Current Status: Distributed Imaging System

Distributed imaging system:

- 14 nodes with 3 cameras per node
- RPi + USB Hub at each node for control, DAQ, and temporary storage
- Hirose GPIO cables for trigger
- USB cables for DAQ

<u>Final design complete as of late 2023</u>

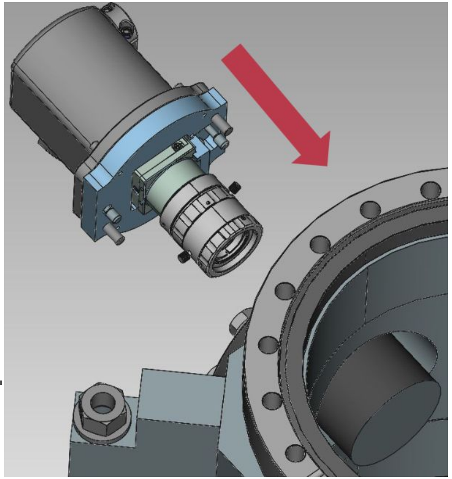

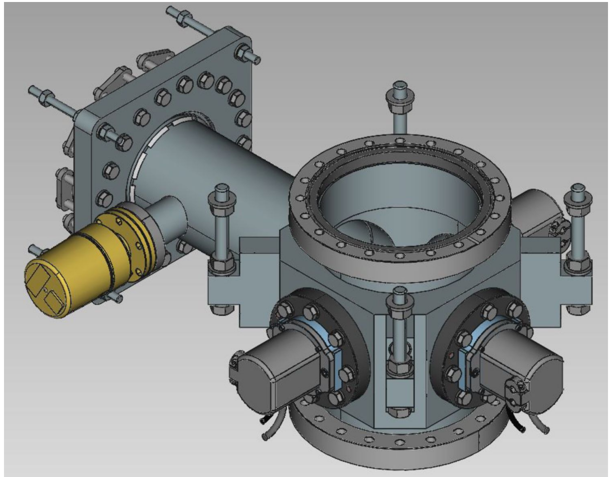

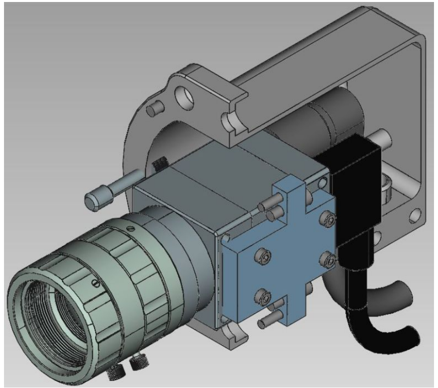

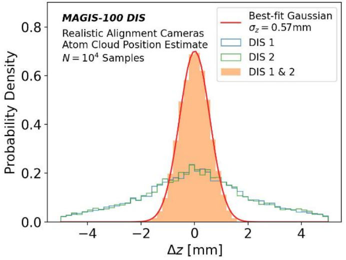

3D reconstruction of simulated atom cloud with chosen optics parameters

Cameras at each connection node:

- 2x Low-magnification -- 3D positioning (alignment)
- 1x High-magnification -- physics

Both lens types have been characterized at SLAC (magnification, depth of field, field of view, etc)

Current Status: Modular Sections

- Modular assembly uses 17 sections, each ~5.2m (17') long and ~2,000 lbs.
- Each section has a support frame containing a 6" diameter vacuum tube
  - Heating/insulation system with controls and temperature sensors
  - Bias field coils, octagonal mu metal shield & support frame + magnetometer
- Vacuum pumps and viewports with cameras will be placed between tube sections ("Connection Nodes").
- **Tubes procured and at FNAL ; Section design in final stages**

Sections for 10m prototype @ Stanford

Assembled prototype MAGIS module with horizontal bias coils and magnetic shield

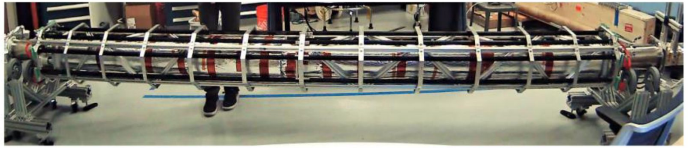
Before shield

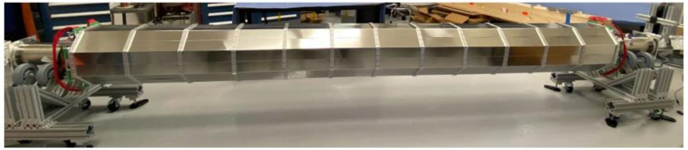
With shield

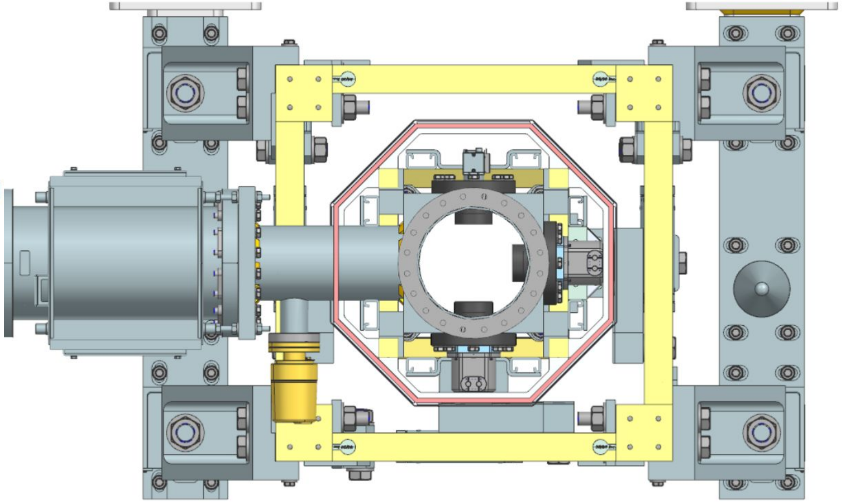

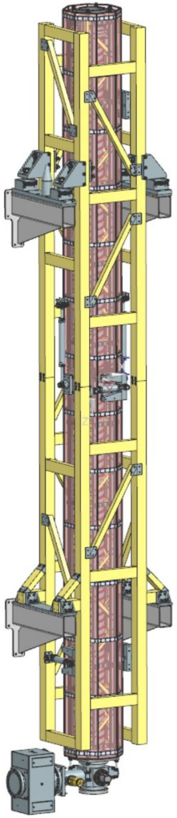
Single module with adjustable supports.

Slide from L. Valerio

Current Status: 10m prototype

Construction nearly complete!

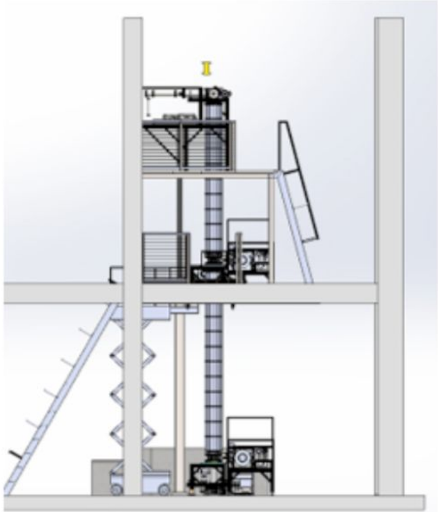

Identical atom sources & laser system ; shorter modular sections

Retro-chamber assembly underway at Stanford!

Connection nodes and laser optics are final steps in progress

Slide from G. Elertas

Current Status: Software & Computing

HEP Expertise: code management & deployment; handling of large data sets; remote detector operations

Ongoing simulation focus: detector optimization studies to inform final stages of design / operation modes

New efforts: detailed “end-to-end” simulation chain for physics signals in realistic data-taking scenarios & expanding analysis toolset

Upcoming collaboration simulation & analysis workshop!

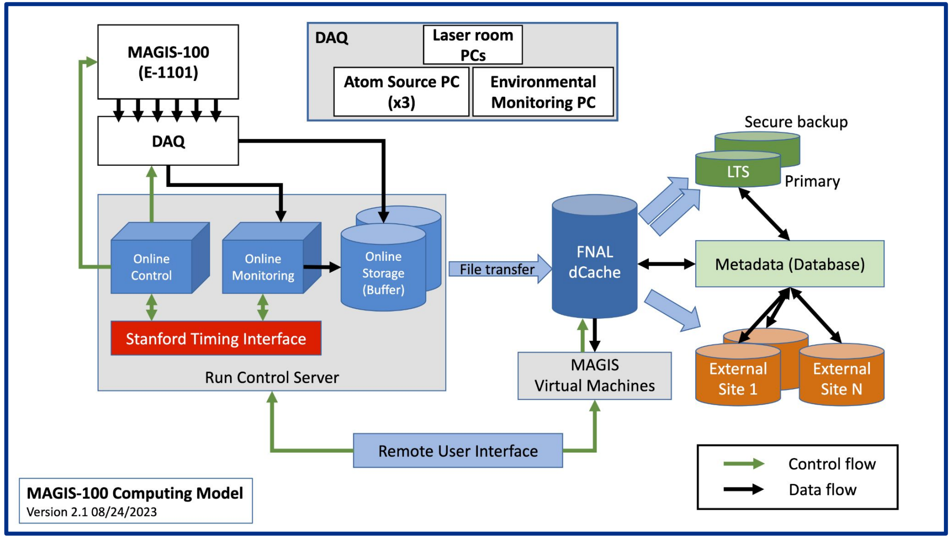

As the first AI experiment at this scale, MAGIS-100 has a great opportunity to spearhead development of simulation & analysis tools for the long-baseline AI community!

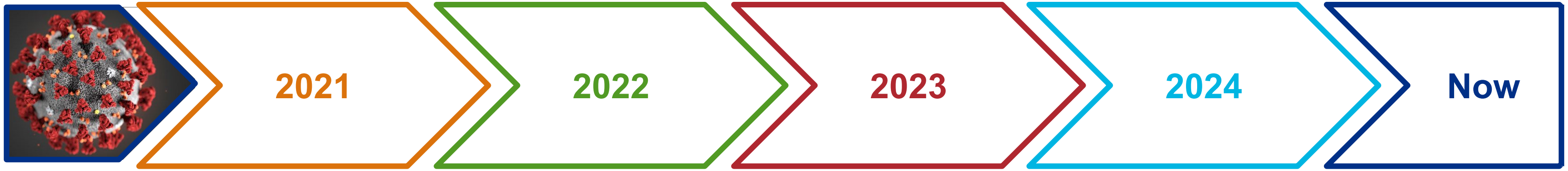
2021
2022
2023
2024
Now

Matter-wave Atomic Gradiometer Interferometric Sensor (MAGIS-100)

Mahiro Abe[1], Philip Adamson[2], Marcel Borcean[2], Daniela Bortoletto[8],
Kieran Bridges[5], Samuel P Carman[1], Swapan Chattopadhyay[2,7],
Jonathon Coleman[5], Noah M Curfman[2], Kenneth DeRose[3],
Tejas Deshpande[3], Savas Dimopoulos[1], Christopher J Foot[8],
Josef C Frisch[9], Benjamin E Garber[1], Steve Geer[2], Valerie Gibson[6],
Jonah Glick[3], Peter W Graham[1], Steve R Hahn[2], Roni Harnik[2],
Leonie Hawkins[5], Sam Hindley[5], Jason M Hogan[1], Yijun Jiang (姜一君)[1],
Mark A Kasevich[1], Ronald J Kellett[2], Mandy Kiburg[2], Tim Kovachy[3],
Joseph D Lykken[2], John March-Russell[8], Jeremiah Mitchell[6,7],
Martin Murphy[2], Megan Nantel[1], Lucy E Nobrega[2],
Robert K Plunkett[2], Surjeet Rajendran[4], Jan Rudolph[1],
Natasha Sachdeva[3], Murtaza Safdari[9], James K Santucci[2],
Ariel G Schwartzman[9], Ian Shipsey[8], Hunter Swan[1], Linda R Valerio[2],
Arvydas Vasonis[2], Yiping Wang[3], and Thomas Wilkason[1]
(The MAGIS-100 Collaboration)

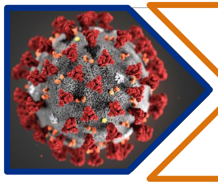

2021 → 2022 → 2023 → 2024 → Now

- Subsystem preliminary designs underway
- Laser lab design complete
- Site vibration studies

Matter-wave Atomic Gradiometer Interferometric Sensor (MAGIS-100)

Mahiro Abe[1], Philip Adamson[2], Marcel Borcean[2], Daniela Bortoletto[8], Kieran Bridges[5], Samuel P Carman[1], Swapan Chattopadhyay[2,7], Jonathon Coleman[5], Noah M Curfman[2], Kenneth DeRose[3], Tejas Deshpande[3], Savas Dimopoulos[1], Christopher J Foot[8], Josef C Frisch[9], Benjamin E Garber[1], Steve Geer[2], Valerie Gibson[6], Jonah Glick[3], Peter W Graham[1], Steve R Hahn[2], Roni Harnik[2], Leonie Hawkins[5], Sam Hindley[5], Jason M Hogan[1], Yijun Jiang (姜一君)[1], Mark A Kasevich[1], Ronald J Kellett[2], Mandy Kiburg[2], Tim Kovachy[3], Joseph D Lykken[2], John March-Russell[8], Jeremiah Mitchell[6,7], Martin Murphy[2], Megan Nantel[1], Lucy E Nobrega[2], Robert K Plunkett[2], Surjeet Rajendran[4], Jan Rudolph[1], Natasha Sachdeva[3], Murtaza Safdari[9], James K Santucci[2], Ariel G Schwartzman[9], Ian Shipsey[8], Hunter Swan[1], Linda R Valerio[2], Arvydas Vasonis[2], Yiping Wang[3], and Thomas Wilkason[1]
(The MAGIS-100 Collaboration)

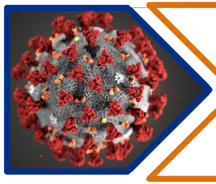

2021

2022

2023

2024

Now

First collaboration simulation & analysis workshop

Subsystem preliminary designs underway

Laser lab design complete

Site vibration studies

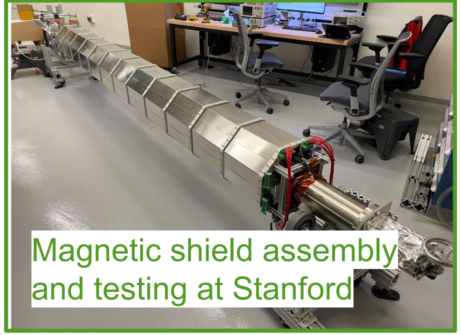

Magnetic shield assembly and testing at Stanford

Fermilab MAGIS-100

Matter-wave Atomic Gradiometer Interferometric Sensor (MAGIS-100)

Mahiro Abe[1], Philip Adamson[2], Marcel Borcean[2], Daniela Bortoletto[8], Kieran Bridges[5], Samuel P Carman[1], Swapan Chattopadhyay[2,7], Jonathon Coleman[5], Noah M Curfman[2], Kenneth DeRose[3], Tejas Deshpande[3], Savas Dimopoulos[1], Christopher J Foot[8], Josef C Frisch[9], Benjamin E Garber[1], Steve Geer[2], Valerie Gibson[6], Jonah Glick[3], Peter W Graham[1], Steve R Hahn[2], Roni Harnik[2], Leonie Hawkins[5], Sam Hindley[5], Jason M Hogan[1], Yijun Jiang (姜一君)[1], Mark A Kasevich[1], Ronald J Kellett[2], Mandy Kiburg[2], Tim Kovachy[3], Joseph D Lykken[2], John March-Russell[8], Jeremiah Mitchell[6,7], Martin Murphy[2], Megan Nantel[1], Lucy E Nobrega[2], Robert K Plunkett[2], Surjeet Rajendran[4], Jan Rudolph[1], Natasha Sachdeva[3], Murtaza Safdari[9], James K Santucci[2], Ariel G Schwartzman[9], Ian Shipsey[8], Hunter Swan[1], Linda R Valerio[2], Arvydas Vasonis[2], Yiping Wang[3], and Thomas Wilkason[1]

(The MAGIS-100 Collaboration)

First collaboration simulation & analysis workshop

Laser lab construction begins

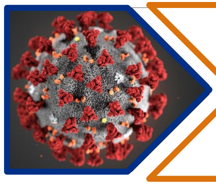

2021 → 2022 → 2023 → 2024 → Now

Subsystem preliminary designs underway

Laser lab design complete

Site vibration studies

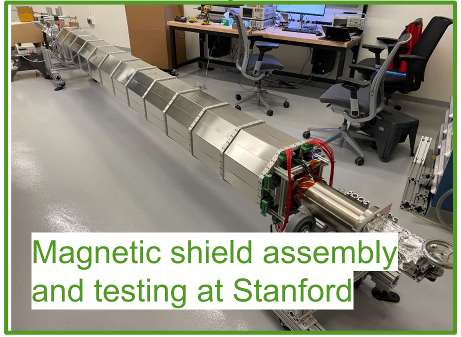

Matter-wave Atomic Gradiometer Interferometric Sensor (MAGIS-100)

Mahiro Abe[1], Philip Adamson[2], Marcel Borcean[2], Daniela Bortoletto[8], Kieran Bridges[5], Samuel P Carman[1], Swapan Chattopadhyay[2,7], Jonathon Coleman[5], Noah M Curfman[2], Kenneth DeRose[3], Tejas Deshpande[3], Savas Dimopoulos[1], Christopher J Foot[8], Josef C Frisch[9], Benjamin E Garber[1], Steve Geer[2], Valerie Gibson[6], Jonah Glick[3], Peter W Graham[1], Steve R Hahn[2], Roni Harnik[2], Leonie Hawkins[5], Sam Hindley[5], Jason M Hogan[1], Yijun Jiang (姜一君)[1], Mark A Kasevich[1], Ronald J Kellett[2], Mandy Kiburg[2], Tim Kovachy[3], Joseph D Lykken[2], John March-Russell[8], Jeremiah Mitchell[6,7], Martin Murphy[2], Megan Nantel[1], Lucy E Nobrega[2], Robert K Plunkett[2], Surjeet Rajendran[4], Jan Rudolph[1], Natasha Sachdeva[3], Murtaza Safdari[9], James K Santucci[2], Ariel G Schwartzman[9], Ian Shipsey[8], Hunter Swan[1], Linda R Valerio[2], Arvydas Vasonis[2], Yiping Wang[3], and Thomas Wilkason[1]

(The MAGIS-100 Collaboration)

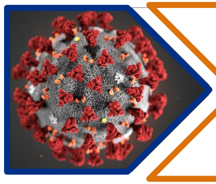

2021

- Subsystem preliminary designs underway
- Laser lab design complete
- Site vibration studies

2022

First post-covid collaboration meeting at Northwestern

First collaboration simulation & analysis workshop

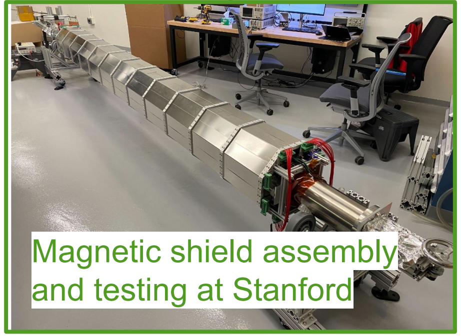

Magnetic shield assembly and testing at Stanford

2023

Bake out control system successfully tested at FNAL

Laser lab construction begins

Laser launch tower arrives at FNAL

2024

DOE/OHEP project begins!

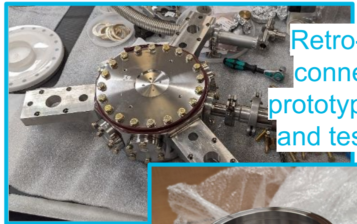

Retro-chamber & connection node prototype assembled and tested at FNAL

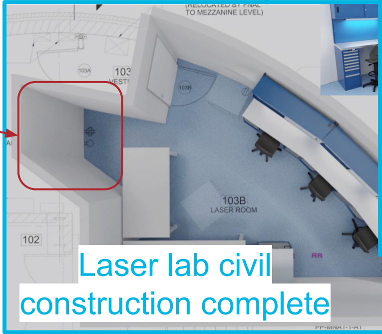

Laser lab civil construction complete

Now

Laser tower installed

Fermilab MAGIS-100

Project Timeline

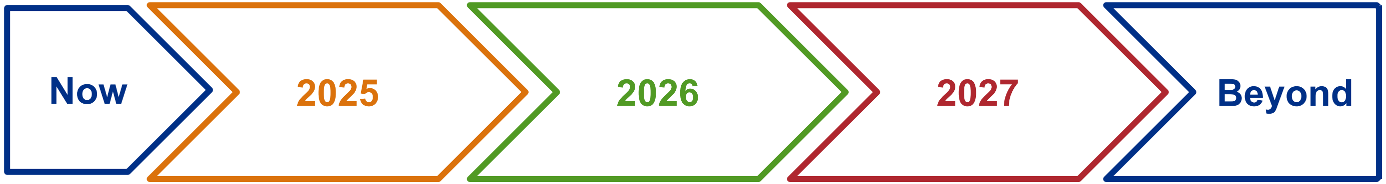

Finalizing designs of apparatus
Building of science equipment
Installation planning
Civil construction in shaft begins

Project Timeline

Completing design & civil construction
Constructing modular sections
Exercising software & computing tools

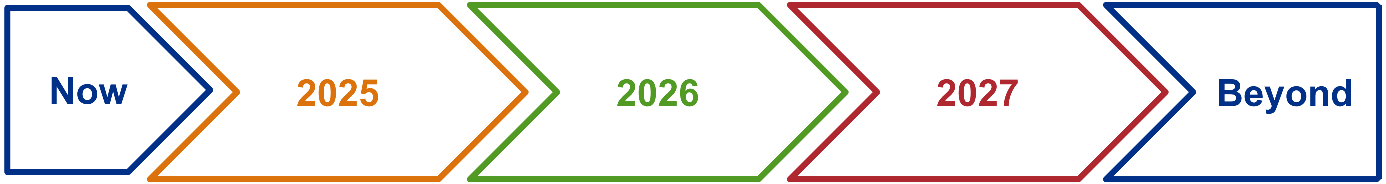

Finalizing designs of apparatus
Building of science equipment
Installation planning
Civil construction in shaft begins

Project Timeline

Completing design & civil construction
Constructing modular sections
Exercising software & computing tools

Now → **2025** → **2026** → **2027** → **Beyond**

Finalizing designs of apparatus
Building of science equipment
Installation planning
Civil construction in shaft begins

Final Installation
Initial system bake out
Alignment

Project Timeline

Completing design & civil construction
Constructing modular sections
Exercising software & computing tools

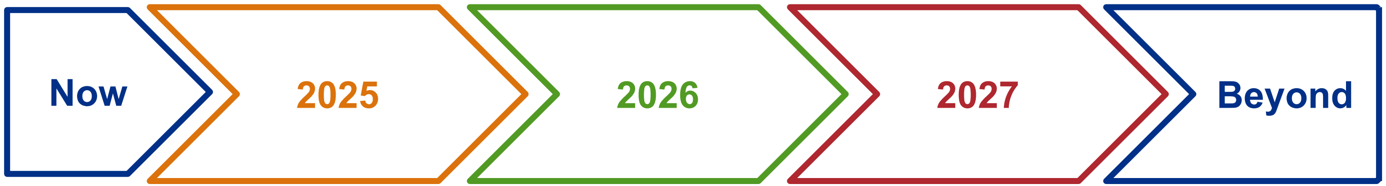

Commissioning
Science Run 1

Finalizing designs of apparatus
Building of science equipment
Installation planning
Civil construction in shaft begins

Final Installation
Initial system bake out
Alignment

The Next Year (FY25) of MAGIS @ FNAL

- Final design reviews for all outstanding subsystems
- Finalizing installation plan -- it's complicated!
  - Vertical installation in shaft
  - Heavy equipment: 1000+ lb components
  - Tight tolerances on alignment over 100 m
- Outfitting laser lab
  - Install optical tables and equipment
  - Start commissioning laser & computing systems
- Software & computing infrastructure development
- Establishing an imaging platform with Northwestern

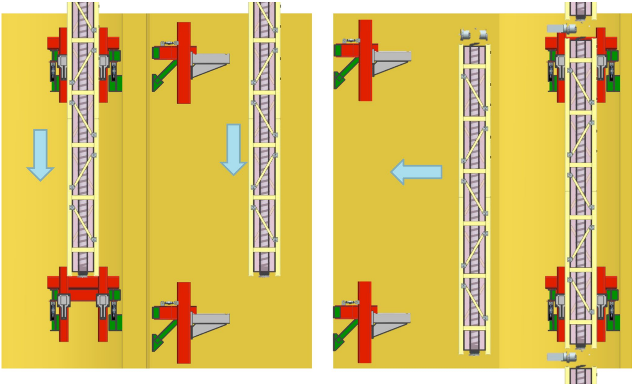

Installation Planning: Working in the Shaft

Vertical installation: the most obvious challenge.

Added complexity: overhead crane does not reach experiment region.

Tight tolerances:

- Wall supports: ±1” , ±2°
- Beam tube - vertical: ±5 mm
- Beam tube - transverse: ±1 mm

Other technical difficulties:

- Small space
- Must accommodate other uses of shaft
- Curved wall for load bearing
- Environmental (water, thermal gradients)

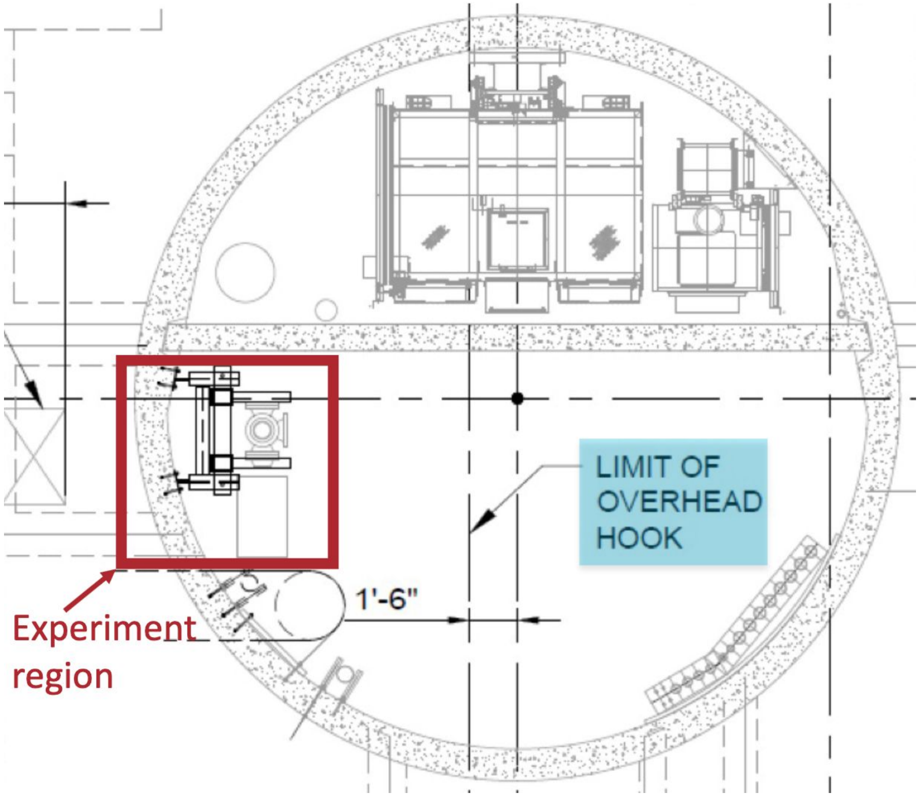

Slide from L. Valerio

Some Recent Results

[Northwestern] “Coriolis Force Compensation and Laser Beam Delivery for 100-Meter Baseline Atom Interferometry”
arxiv:2311.05714 (2023)

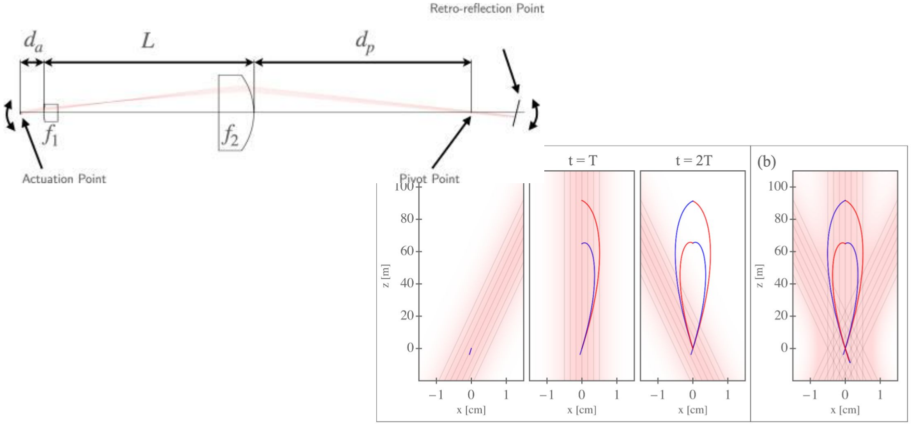

[Stanford] “Atom Interferometry with Floquet Atom Optics”
Phys. Rev. Lett. 129, 183202 (2022) arxiv:2205.06965

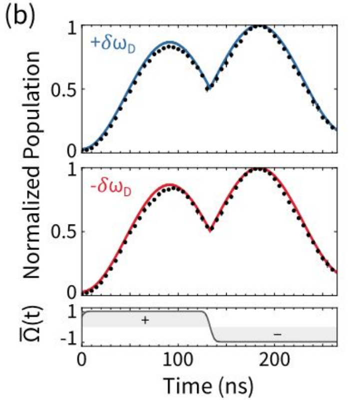

Efficiency: 99.4%
LMT: 400$\hbar k$

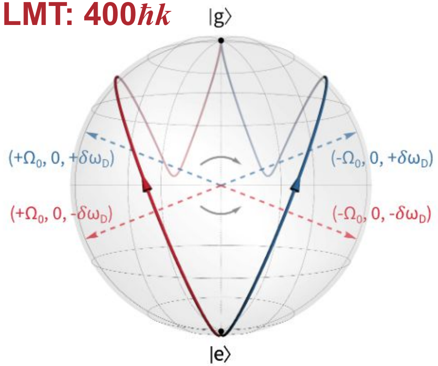

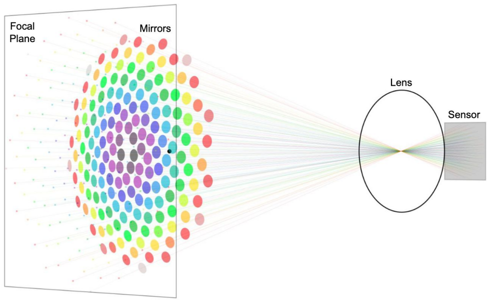

[SLAC] “Novel Light Field Imaging Device with Enhanced Light Collection for Cold Atom Clouds”
JINST 17 P08021 (2022)
arxiv:2205.11480

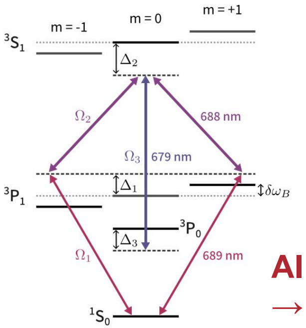

[Stanford] “Collinear three-photon excitation of a strongly forbidden optical clock transition”
arxiv:2406.07902 (2024)

AI with forbidden clock transition in ^{88}Sr → reduced sensitivity to B field

Near-Term R&D with MAGIS and Supporting Systems

Near-term R&D concurrent with first deployment of detector apparatus

- Develop advanced LMT technology ($100\hbar k \rightarrow 40{,}000\hbar k$)
- Increase steady-state source flux ($10^4 \rightarrow 10^6$ atoms/sec)
- Spin-squeezed sources to further increase intensity (statistics!)
- Resonant interferometry modes

Will be critical input for scaling this technology up to > 1 km!

- Modular construction
- Large scale integration and operation
- Identify any design problems early
- Increased laser power

- Additional mitigation of systematics:
  - Wavefront transverse phase variation
  - Laser pointing
  - Coriolis compensation
  - Gravity gradient noise

MAGIS Beyond 100 Meters

Experiment	(Proposed) Site	Baseline L (m)	LMT Atom Optics n	Atom Sources	Phase Noise $\delta\phi$ (rad/$\sqrt{\text{Hz}}$)
Sr prototype tower	Stanford	10	10^2	2	10^{-3}
MAGIS-100 (initial)	Fermilab (MINOS shaft)	100	10^2	3	10^{-3}
MAGIS-100 (final)	Fermilab (MINOS shaft)	100	4×10^4	3	10^{-5}
MAGIS-km	Homestake mine (SURF)	2000	4×10^4	40	10^{-5}
MAGIS-Space	Medium Earth orbit (MEO)	4×10^7	10^3	2	10^{-4}

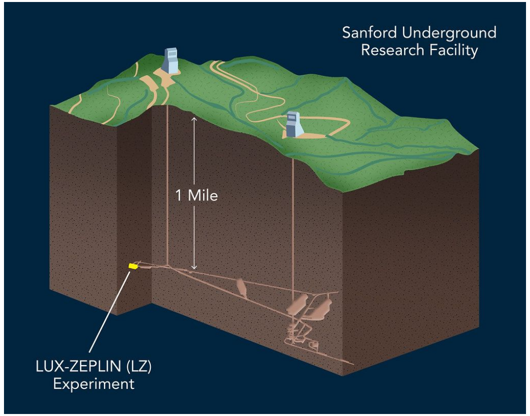

MAGIS Beyond 100 Meters

Experiment	(Proposed) Site	Baseline L (m)	LMT Atom Optics n	Atom Sources	Phase Noise $\delta\phi$ (rad/$\sqrt{\text{Hz}}$)
Sr prototype tower	Stanford	10	10^2	2	10^{-3}
MAGIS-100 (initial)	Fermilab (MINOS shaft)	100	10^2	3	10^{-3}
MAGIS-100 (final)	Fermilab (MINOS shaft)	100	4×10^4	3	10^{-5}
MAGIS-km	Homestake mine (SURF)	2000	4×10^4	40	10^{-5}
MAGIS-Space	Medium Earth orbit (MEO)	4×10^7	10^3	2	10^{-4}

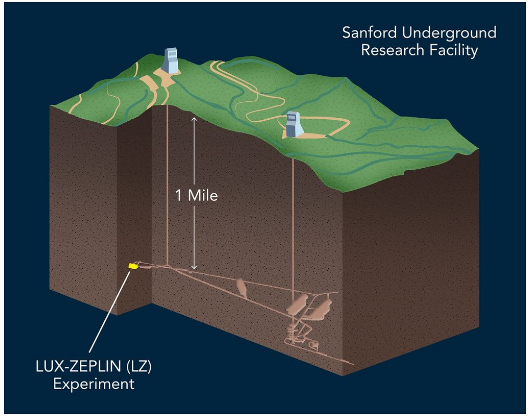

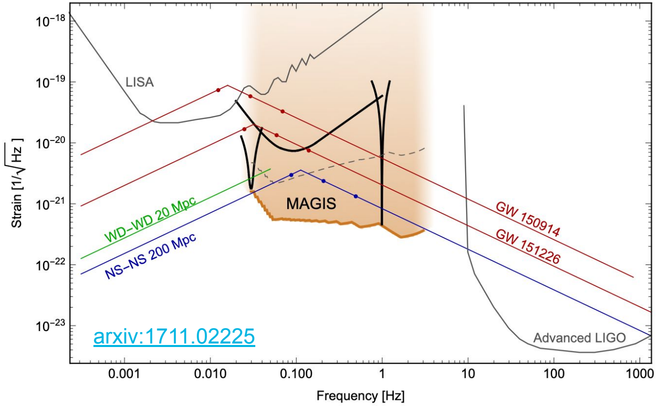

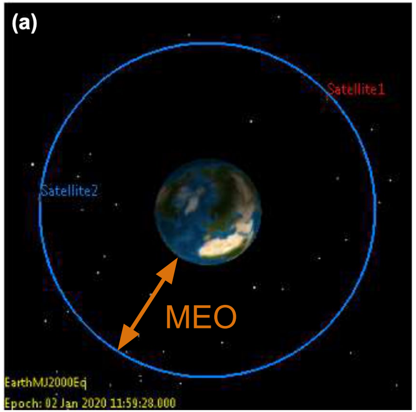

MAGIS + AION Consortium

Establish an AI network to enable new and exciting physics opportunities inaccessible to either AI alone

- Improved sky localization (GW)
- Unequivocal proof of any observation
- Will require precise time synchronization

Proof of principle for future global AI network

<u>**A**tomic **I**nterferometric **O**bservatory and **N**etwork (UK)</u>

- Stage I: 10 meter baseline @ Oxford (funded)
- Stage II: 100 meter baseline @ Boulby (proposed)

CRADA with the UK institutions signed this year
Formal collaboration underway!

Terrestrial Very-Long-Baseline Atom Interferometry arxiv:2310.08183

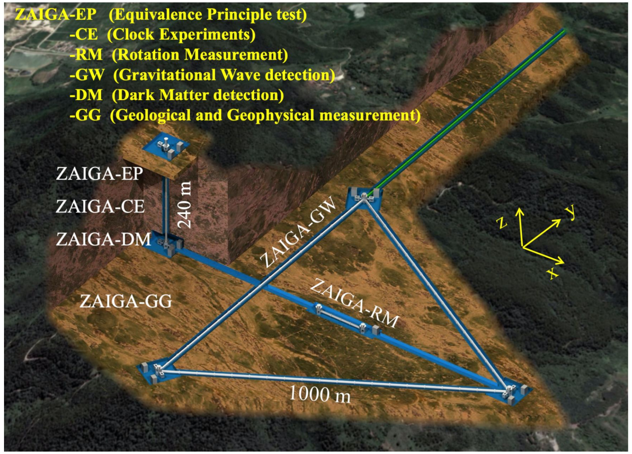

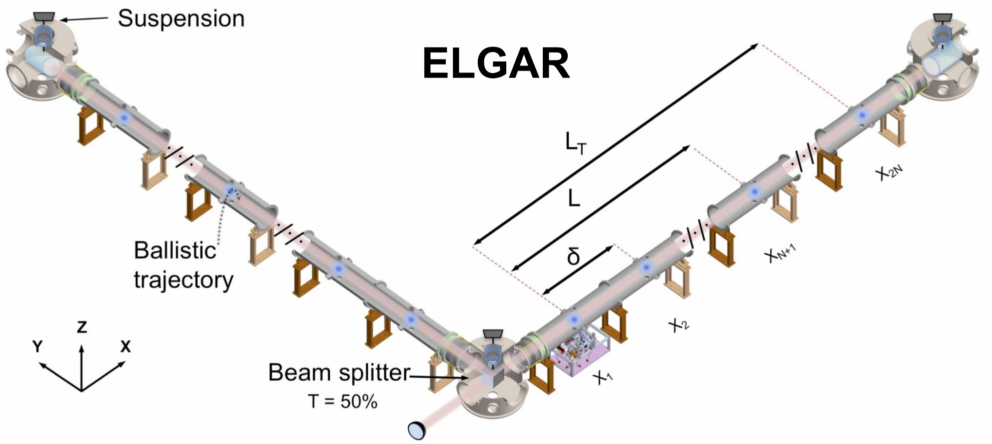

Funded Platforms		
• Sr Prototype	10m	Stanford, USA
• **MAGIS-100**	**100m**	**Chicago, USA**
• MIGA	200m	Rustrel, France
• VLBAI	10m	Hanover, Germany
• AION-10	10m	Oxford, UK
• Prototype	10m	Zhaoshan, China
• ZAIGA	300m(+)	Zhaoshan, China

Proposed Platforms		
• *AION-100*	*100m*	*Boulby, UK*
• *AION-km*	*1000m*	*Boulby, UK*
• ***MAGIS-km***	***2000m***	***Lead, SD, USA***
• *ELGAR*	*3200m*	*France/Italy*
• *Advanced ZAIGA*	*1000m*	*Zhaoshan, China*

Caveat: these platforms at varying stages of "proposed"

Northwestern University
August 2023

Conclusions

MAGIS-100

U.S. DEPARTMENT OF ENERGY | Office of Science

- MAGIS-100 is a first-of-its-scale atom interferometry experiment (& collaboration) that will advance the state of the art in the field.
- Multipurpose physics platform -- beyond just null results!
  Novel sensitivity to ultralight dark matter and "mid-band" gravitational waves
- Subsystems in (or beyond) final stages of design & procurement while civil construction is underway at Fermilab.
- The next year at Fermilab will be focused on finalizing the installation plan, outfitting the laser lab, software & computing infrastructure development, and civil construction.
- Exciting science coming soon!

Thank You!

This manuscript has been authored by Fermi Research Alliance, LLC under Contract No. DE-AC02-07CH11359 with the U.S. Department of Energy, Office of Science, Office of High Energy Physics. This work is funded in part by the U.S. Department of Energy, Office of Science, High-Energy Physics Program Office as well as the QuantiSED program, the Gordon and Betty Moore Foundation (GBMF7945), and the UK Science and Technology Facilities Council.

Backup

In partnership with:

Ultralight Dark Matter

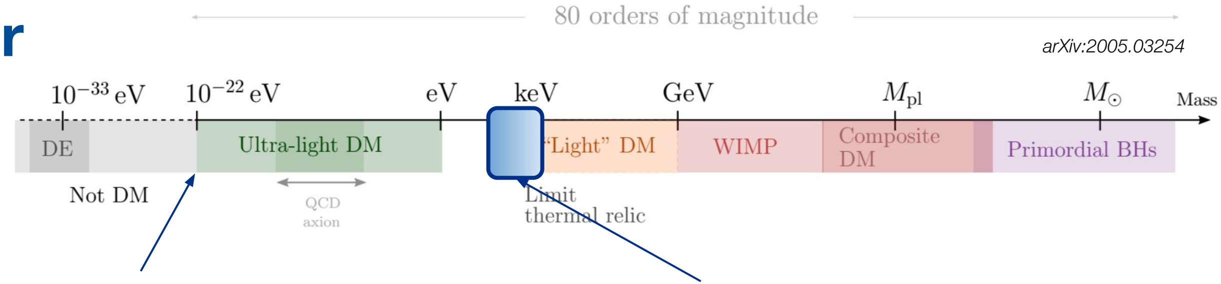

arXiv:2005.03254

Compton wavelength larger than dwarf spheroidal galaxy

Lower limit for fermionic DM
Tremaine-Gunn Bound

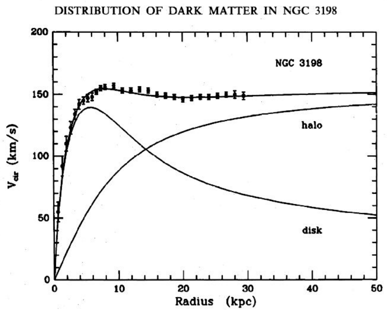

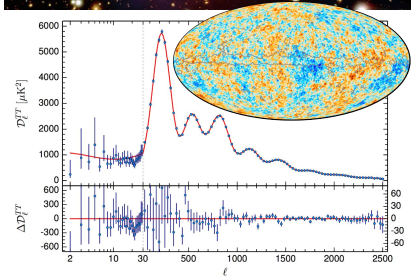

GeV+ scale (WIMP-like) - Extensive searches, decades of null results, 10^7x increase in sensitivity

Sub-GeV (LDM) - "Early" days, many experiments underway

Ultralight DM (m << eV) - want to explore down to 10^{-22} eV

- Axions - Current exploration focused in 10^{-5} -- 10^{-7} eV range
- Other candidates: hidden photons, dilaton, relaxion
- Landscape <10^{-10} eV wide open - current constraints from EP-violation and 5th force searches

Ultralight Dark Matter Properties

- Bosonic: scalar, pseudoscalar, and vector couplings
- DM density in galaxies → high occupation number in each coherence volume
- Classical oscillating field

$$\phi(t) \approx \phi_0 \cos(m_\phi t) \qquad \text{where} \qquad \phi_0 = \sqrt{2\rho_{\mathrm{DM}}}/m_\phi$$

  – Characteristic coherence time & length

$$\tau_{\mathrm{coh}} \sim 2\pi/\Delta E_\phi \quad \lambda_{\mathrm{coh}} \sim 2\pi/\Delta p_\phi$$

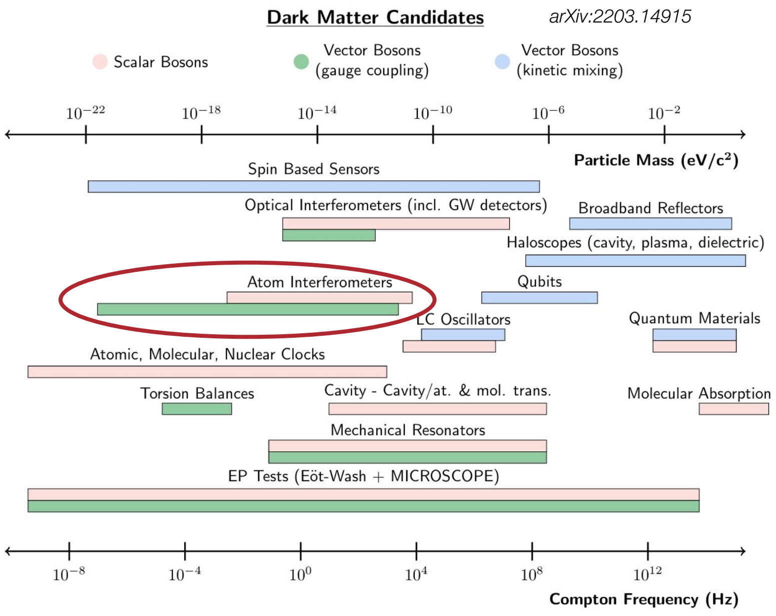

Interactions with matter:

- *Cause precession of nuclear* or electron *spins*
- Generate currents in electromagnetic systems
- Produce photons
- *Induce equivalence-principle-violating accelerations*
- *Modulate the values of the fundamental "constants" of nature*

→ Use precision atomic clocks and inertial references to measure these effects

Ultralight Scalar Bosons

Linear couplings to photons and electrons

$$\mathcal{L} \supset \sqrt{4\pi G_N}\phi\left(\frac{d_e}{4e^2}F_{\mu\nu}F^{\mu\nu} - d_{m_e}m_e\bar{\psi}\psi\right)$$

Generates time-dependent terms in electron mass and fine-structure constant

$$m_e(t,x) = m_{e0}\left(1 + d_{m_e}\sqrt{4\pi G_N}\phi(t,x)\right)$$

$$\alpha(t,x) = \alpha_0\left(1 + d_e\sqrt{4\pi G_N}\phi(t,x)\right)$$

Leading to oscillating energy splittings in atomic states with amplitude

$$\Delta\omega_A = \omega_A\sqrt{4\pi G_N}\phi_0\left(d_{m_e} + \xi d_e\right)$$

$$\text{where} \quad \phi_0 = \sqrt{2\rho_{\mathrm{DM}}}/m_\phi$$

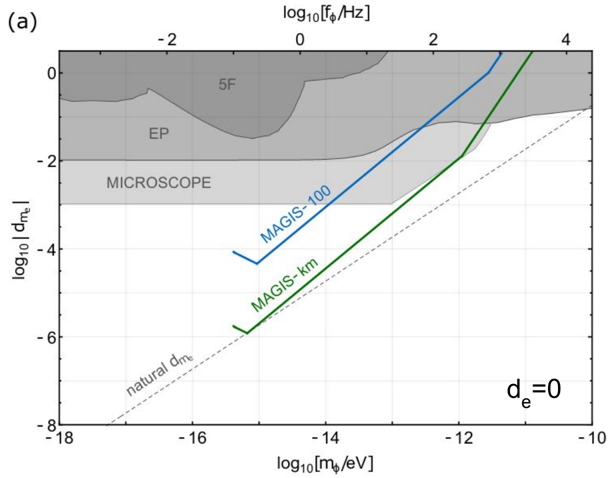

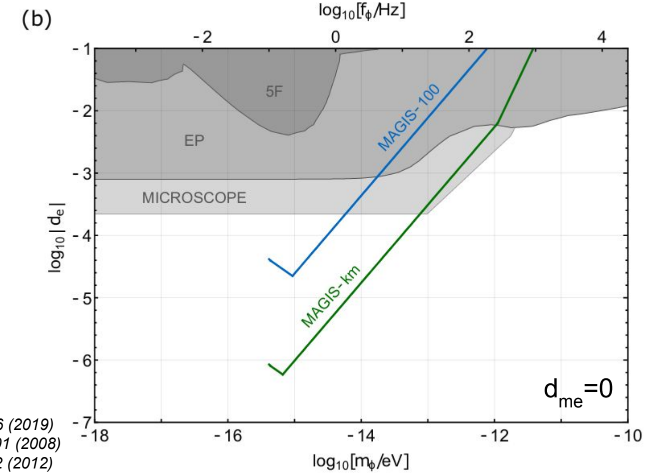

Current bounds:
Touboul et al, Class. Quantum Grav. ***36*** *225006 (2019)*
Schlamminge et al, Phys. Rev. Lett. 100, 041101 (2008)
Wagner et al, Class. Quantum Grav. 29 184002 (2012)
Adelberger et al, Annu. Rev.Nucl. Part. Sci. 53, 77 (2003)

Arvanitaki et al, Phys. Rev. D 97, 075020 (2018)
Abe et al, Quantum Sci. Technol. 6, 044003 (2021)

Fermilab MAGIS-100

Ultralight Scalar Bosons

Ultralight dilaton DM acts as a background field (e.g., mass ~10^{-15} eV)

$$\mathcal{L} = +\frac{1}{2}\partial_\mu\phi\partial^\mu\phi - \frac{1}{2}m_\phi^2\phi^2 - \sqrt{4\pi G_N}\phi\left[d_{m_e}m_e\bar{e}e - \frac{d_e}{4}F_{\mu\nu}F^{\mu\nu}\right] + \ldots$$

- $\frac{1}{2}\partial_\mu\phi\partial^\mu\phi - \frac{1}{2}m_\phi^2\phi^2$: DM scalar field
- $d_{m_e}m_e\bar{e}e$: Electron coupling
- $\frac{d_e}{4}F_{\mu\nu}F^{\mu\nu}$: Photon coupling
- $\ldots$: e.g., QCD

$$\phi(t, \mathbf{x}) = \phi_0 \cos\left[m_\phi(t - \mathbf{v}\cdot\mathbf{x}) + \beta\right] + \mathcal{O}\left(|\mathbf{v}|^2\right)$$

$$\phi_0 \propto \sqrt{\rho_{\mathrm{DM}}}$$ DM mass density

DM coupling causes time-varying atomic energy levels:

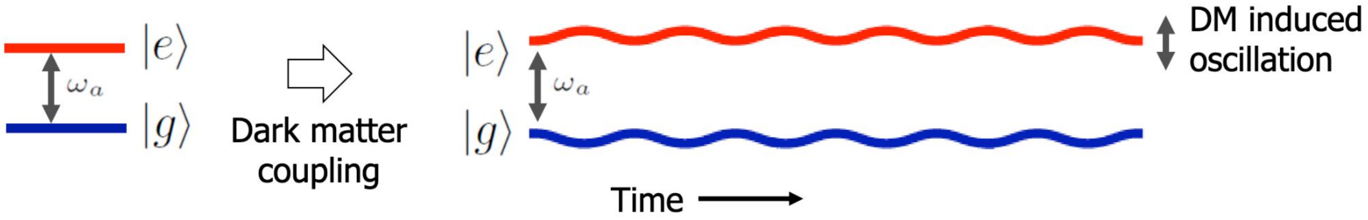

Slide from J. Hogan

Ultralight Vector Bosons

Consider a massive vector A^μ coupled to a $U(1)_{B\text{-}L}$ charge (neutron content)

$$\mathcal{L} \supset -\frac{1}{4}F^{\mu\nu}F_{\mu\nu} + \frac{1}{2}m_A^2 A^\mu A_\mu - g_{B-L} J^\mu A_\mu$$

This exerts a differential force on isotopes of the same element

$$\mathbf{F} = m_A g_{B-L} Q_{U(1)_{B-L}} \sum_i A_i \mathbf{e}_i \sin\left(m_A t - m_A v_{\mathrm{DM}} \hat{\mathbf{k}}_i \cdot \mathbf{x} + \phi_i\right)$$

→ Equivalence principle violating force

Leading to a time-varying differential acceleration (if it's DM, static otherwise)

Requires operation of dual-species colocated interferometer ($^{87/88}$Sr)

Abe et al, Quantum Sci. Technol. 6, 044003 (2021)

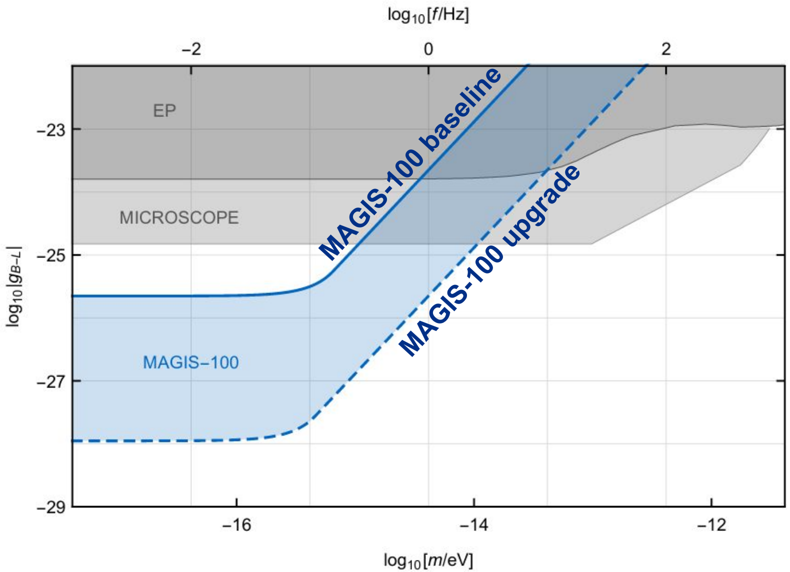

Theoretical calculations from *Graham et al, Phys. Rev. D 93, 075029 (2016)*

Detailed signal & readout simulation with target MAGIS parameters underway

Axion Like Particles

Work by **Sam Hindley** (Liverpool)

Axion field couples to atoms via interaction with spins
→ time-oscillating "dark magnetic fiel $\mathcal{L} \supset g_{aNN}\partial_\mu a\bar{\psi}\gamma^5\gamma^\mu$

MAGIS sensitivity scales linearly in g_{aNN}

- Axion telescopes & resonant cavities ~ $g_{a\gamma\gamma}^{2}$
- Light shining through walls ~ $g_{a\gamma\gamma}^{4}$

Induces time-varying effects on nuclear spins

- Larmor precession, modifications to Hamiltonian under which the spins evolve in time.
- Frequency, direction set by properties of the axion field.
- Measured by interference of atom cloud that has evolved in a superposition of different spin-states.

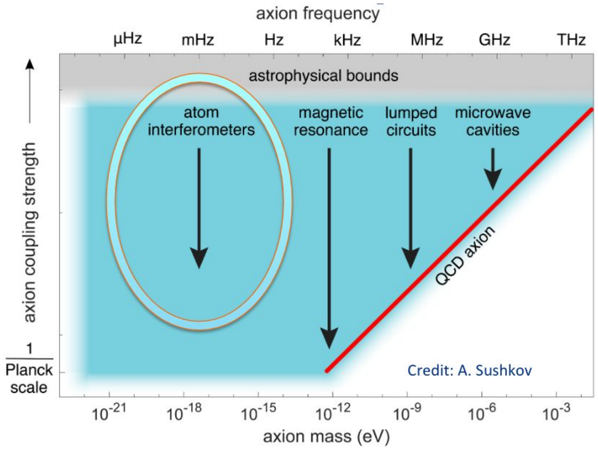

2018 DOE Dark Matter Research Needs report

Spin interferometry never before realized in laboratory!

Axion Like Particles

Work by **Sam Hindley** (Liverpool)

Must prepare ensembles of the same isotope in differing spin states: Sr $^1S_0$-$^3P_0$ optical clock transition

- **Background:** stray magnetic fields
- No benefit from free-fall over long distances

Need to “bounce” atoms in a region of enhanced magnetic shielding (x$10^{3.5}$ over planned) to achieve necessary interrogation times

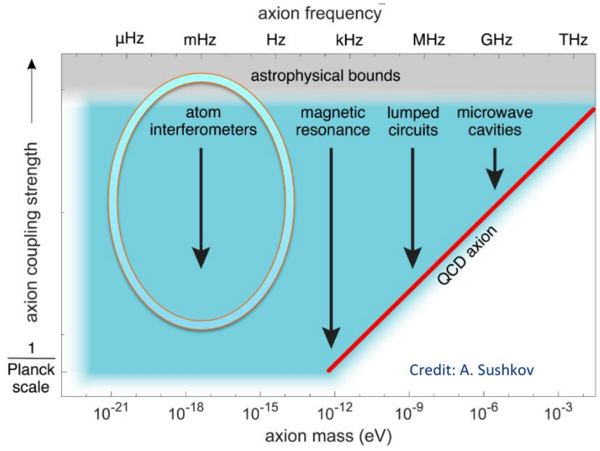

2018 DOE Dark Matter Research Needs report

Other MAGIS Science

"Mid-Band" Gravitational Waves

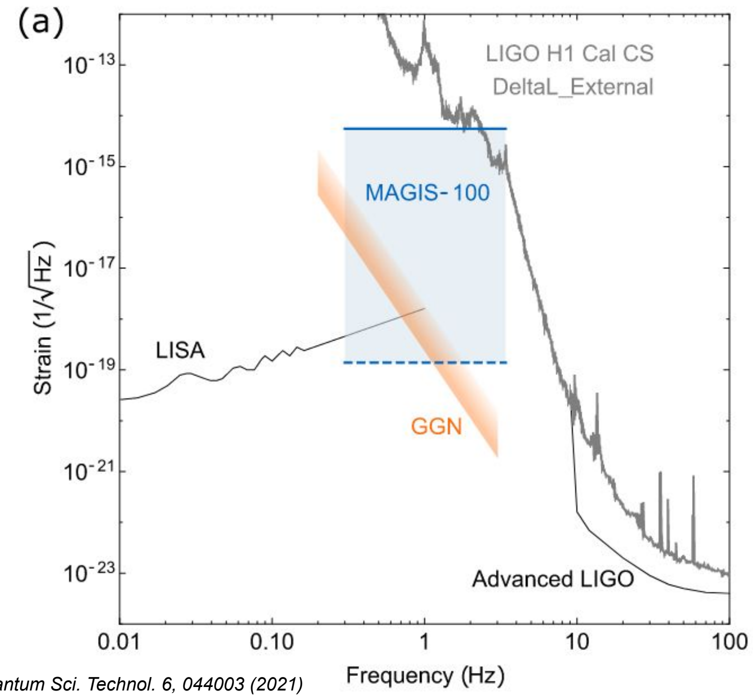

Quantum Sci. Technol. 6, 044003 (2021)

Precision Tests of Quantum Mechanics

- Demonstrate superposition across unprecedented length scales
  - Wavepacket separation (~10 m)
  - Coherence time (~9 sec)
- Investigate optimal quantum control sequences (QIS)
- Probe non-linear corrections to Schrödinger's Equation
- Utilize spin-squeezed atom ensembles to surpass the standard quantum limit

Science-Driven Requirements

Atom interferometry state-of-the-art

Sensor Technology	State-of-the-art
LMT atom optics	$10^2\ \hbar k$
Matter-wave lensing	50 pK
Laser Power	10 W
Spin squeezing	20 dB (Rb), 0 dB (Sr)
Atom flux	10^5 atoms/s (Rb)
Baseline length	10 m

arxiv:2310.08183

MAGIS-100 Requirements & Goals

arxiv:2310.08183

Experiment	(Proposed) Site	Baseline L (m)	LMT Atom Optics n
Sr prototype tower	Stanford	10	10^2
MAGIS-100 (initial)	Fermilab (MINOS shaft)	100	10^2
MAGIS-100 (final)	Fermilab (MINOS shaft)	100	4×10^4

Noise & systematics mitigation

Parameter	Target Value	Primary Driving Factors
LMT atom optics	$n = 100$	Increase sensitivity to science signals
Phase resolution	10^{-3} rad/$\sqrt{\text{Hz}}$	Increase sensitivity to science signals
Frequency noise/drift	< 10 Hz	Increase pulse transfer efficiency (Section 4.3)
Per shot position uncertainty	10 μm/$\sqrt{\text{Hz}}$	Coupling to wavefront aberrations (Section 5.2)
Per shot velocity uncertainty	10 μm/s/$\sqrt{\text{Hz}}$	
Laser wavefront variation	5 mrad*	Coupling to cloud kinematic and laser pointing jitter (Section 5.2 and Section 5.4)
Laser intensity stabilization	0.1%/$\sqrt{\text{Hz}}$	AC Stark shifts (Section 5.5)
Laser pointing stability	30 nrad/$\sqrt{\text{Hz}}$	Coupling to wavefront aberrations (Section 5.4)
Magnetic field uniformity	1 mG (rms)	Clock frequency shifts

*at transverse length scales $\lesssim 3$ mm

Parameter	Target Value	Primary Driving Factors
Laser power	8 W	Reduce pulse inefficiencies (enabling high LMT)
Atom flux	10^6 atoms/s (Sr)	Sensitivity to science signals

Fermilab MAGIS-100

Systematics & Backgrounds

Source	Magnitude of phase noise	*Spectral densities in 0.1 -- 3 Hz range
Magnetic fields	10^{-3} rad $Hz^{-1/2}$	*Dickerson, et al. Rev. Sci. Instrum. 83, 065108 (2012)*
Laser wavefront aberrations	10^{-4} rad $Hz^{-1/2}$	*Schkolnik, et al. Appl. Phys. B 120, 311–316 (2015)*
Laser pointing jitter	10^{-4} rad $Hz^{-1/2}$	*Hogan et al. Gen. Relativ. Gravit. 43, 1953–2009 (2011)*
AC Stark shifts	10^{-4} rad $Hz^{-1/2}$	*Kovachy, et al. Nature 528, 530–533 (2015)*

Sub-dominant sources: laser phase noise, seismic vibrations, Coriolis & Earth effects, mean field shifts, blackbody radiation shifts.

All sources are well understood and can be controlled within the requirements of MAGIS-100.

For complete discussion, see *Quantum Sci. Technol. 6, 044003 (2021) 2104.02835*

Rabi Oscillations

Sinusoidally driven system will oscillate between two states |1⟩and |2⟩

The Rabi Frequency provides a measure of the strength of the interaction

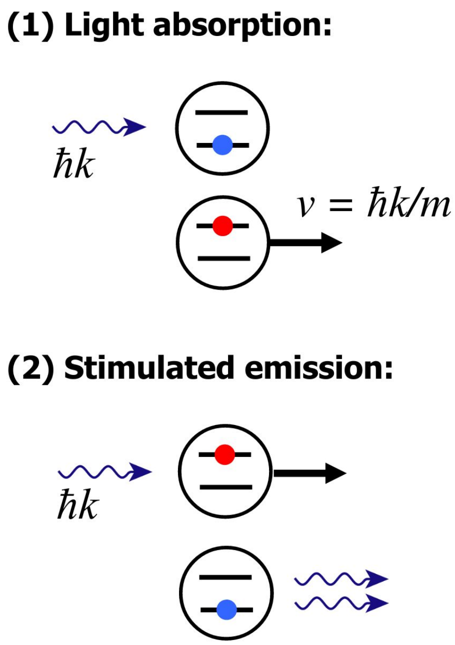

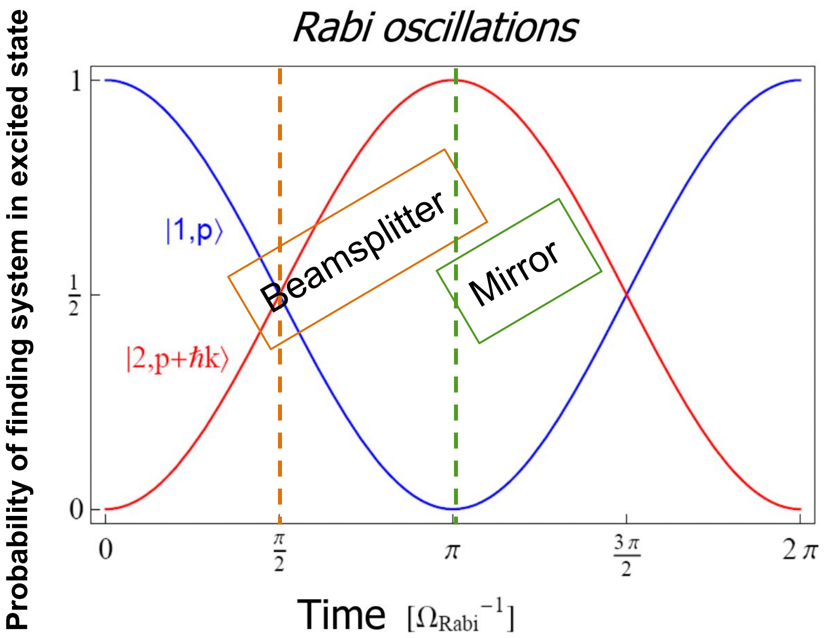

Fermilab
MAGIS-100

Strontium Clock States

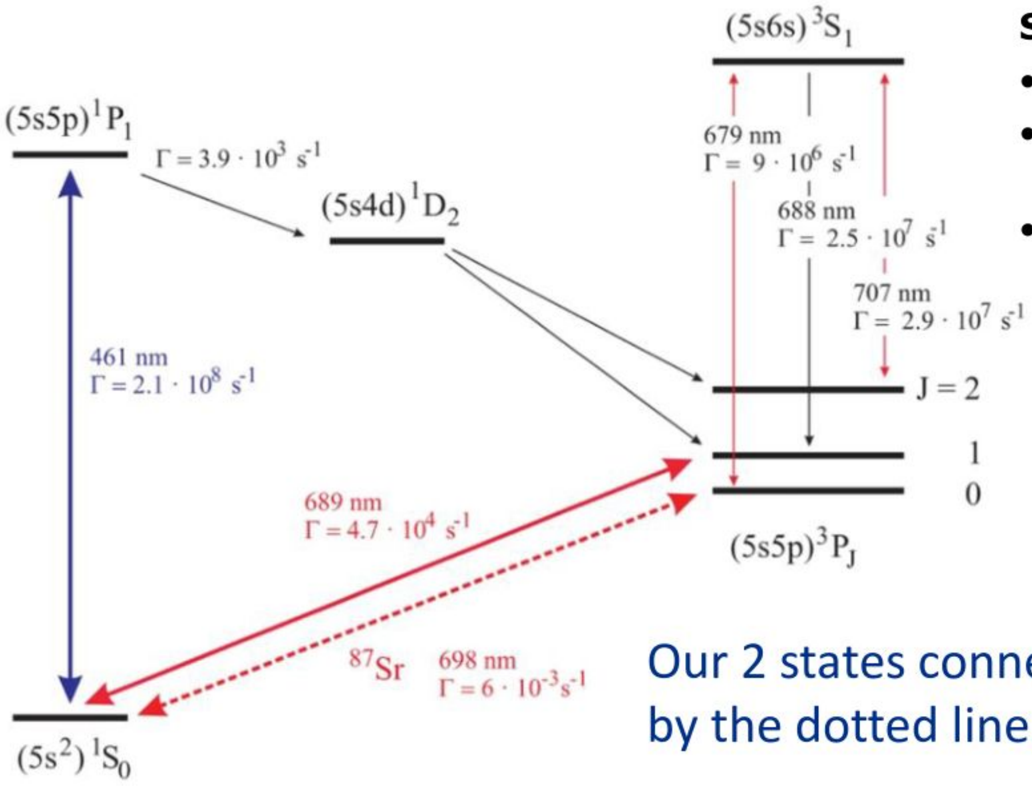

Our 2 states connected by the dotted line.

Single photon clock transitions

- Requires long-lived excited state
- Reduced spontaneous emission (other levels far detuned)
- Possibility to support > 10^6 pulses

Use **689 nm transition** for initial demonstration of LMT clock atom interferometry

689 transition features:

- 1-photon AI possible
- 22 μs lifetime
- High Rabi frequency possible

Advantages of Strontium

- Narrow excited state has long lifetime (~ 150 s).
- Resonant single laser beam excitations can be used while avoiding spontaneous emission, which would cause particle loss.
- The long-lived metastable state could in principle allow interrogation times up to 100 seconds.
- Achieving a long-lived state with one laser photon (and one laser) reduces laser phase noise – good for gradiometer measurements.
- Sr has greatly reduced sensitivity to external magnetic fields (factor of 1000).

Note: Significant laser power needed to rapidly populate 689 nm state

Single-Photon vs Double-Photon Transitions

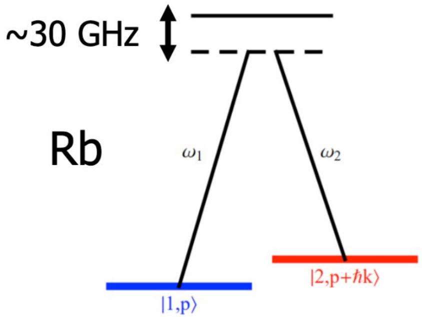

Two-photon transitions

- Conventional atom interferometers use two-photon Raman or Bragg transitions
- Requires large detuning, high power to suppress spontaneous emission
- Current state of the art: ~100 pulses

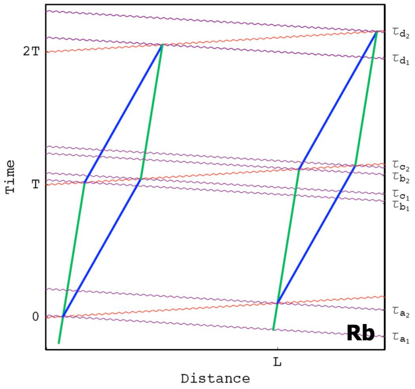

Laser phase **not** common

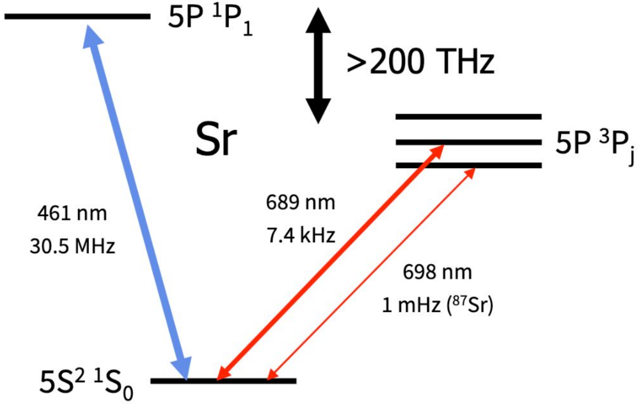

Single photon clock transitions

- Requires long-lived excited state
- Reduced spontaneous emission (other levels far detuned)
- Possibility to support > 10^6 pulses

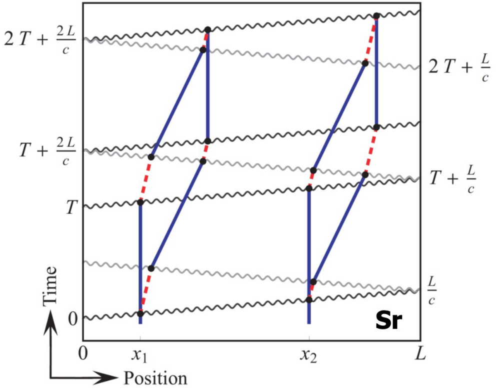

Laser noise suppressed

Slide from J. Hogan

Light-Pulse Atomic Clock

$$|\text{atom}\rangle = |1\rangle$$

π/2 beamsplitter

$$\frac{1}{\sqrt{2}}(|1\rangle + |2\rangle)$$

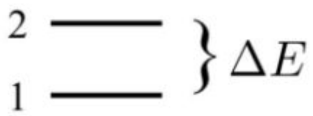

wait time t

$$\frac{1}{\sqrt{2}}\left(|1\rangle + e^{i(\Delta E)t}|2\rangle\right)$$

π/2 beamsplitter

$$\frac{1}{2}\left[\left(1 - e^{i(\Delta E)t}\right)|1\rangle + \left(1 + e^{i(\Delta E)t}\right)|2\rangle\right]$$

output ports N_1 N_2

can measure times $t \sim \frac{1}{\Delta E} \sim 10^{-10}$ s

Fermilab MAGIS-100

Coupled Atomic Clocks

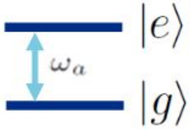

Time

1. Laser pulses creates superposition of clock states, "starts clock ticking"
2. Second pulse represents end of measurement, phase reflects amount clock ticked during measurement time

Phase evolved by atom after time T (second clock starts slightly later, by amount L/c for baseline length L, than first because of light travel time, but also ends time L/c later)

$$\frac{1}{\sqrt{2}}|g\rangle + \frac{1}{\sqrt{2}}|e\rangle\, e^{-i\omega_a T}$$

$$\frac{1}{\sqrt{2}}|g\rangle + \frac{1}{\sqrt{2}}|e\rangle\, e^{-i\omega_a T}$$

GW changes baseline, and therefore light travel time, between pulses (signal maximized when GW period on scale of time between pulses)
$T \rightarrow T + \Delta T$
with $\Delta T \sim Lh/c$

Coupled Atomic Clocks

1. Light propagates across the baseline at a constant speed
2. Clocks read transit time signal over baseline
3. Something changed the number of clock ticks associated with light transit
    a. DM modifies clock ticking rate
    b. GW modifies light travel time across baseline
4. Many pulses sent across baseline (large momentum transfer) to coherently enhance signal
5. Differential phase shift between two or more interferometers separated in space

Atom Interferometry

Laser pulses act as beam splitters and mirrors for atomic wavefunction

Highly sensitive to accelerations (or to time-variations of atomic energy levels)

$$|\text{atom}\rangle = |p\rangle$$

π/2 pulse "beamsplitter"

$$\frac{1}{\sqrt{2}}(|p\rangle + e^{i\Delta\phi}|p + \hbar k\rangle)$$

π pulse "mirror"

$$\frac{1}{\sqrt{2}}(|p + \hbar k\rangle + e^{i\Delta\phi}|p\rangle)$$

π/2 pulse "beamsplitter"

$$\frac{1}{2}((1 + e^{i\Delta\phi})|p\rangle + ((1 - e^{i\Delta\phi}))|p + \hbar k\rangle)$$

$$\text{Probability in State } |p\rangle = \cos^2\left(\frac{\Delta\phi}{2}\right)$$

$$\text{Probability in State } |p + \hbar k\rangle = \sin^2\left(\frac{\Delta\phi}{2}\right)$$

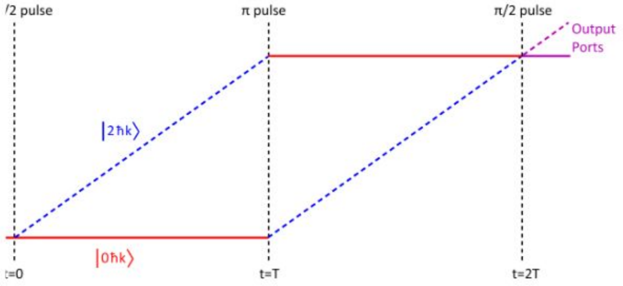

Effects scale like AREA, so

Long T good

High Momentum Good

Light-Pulse Atom Interferometry

Abe et al. Quantum Sci. Technol. 6, 044003 (2021) [arxiv:2104.02835]
Rudolph et al. Phys. Rev. Lett. 124, 083604 (2020) [arxiv:1910.05459]
Kovachy et al. Nature volume 528, pages 530–533 (2015)

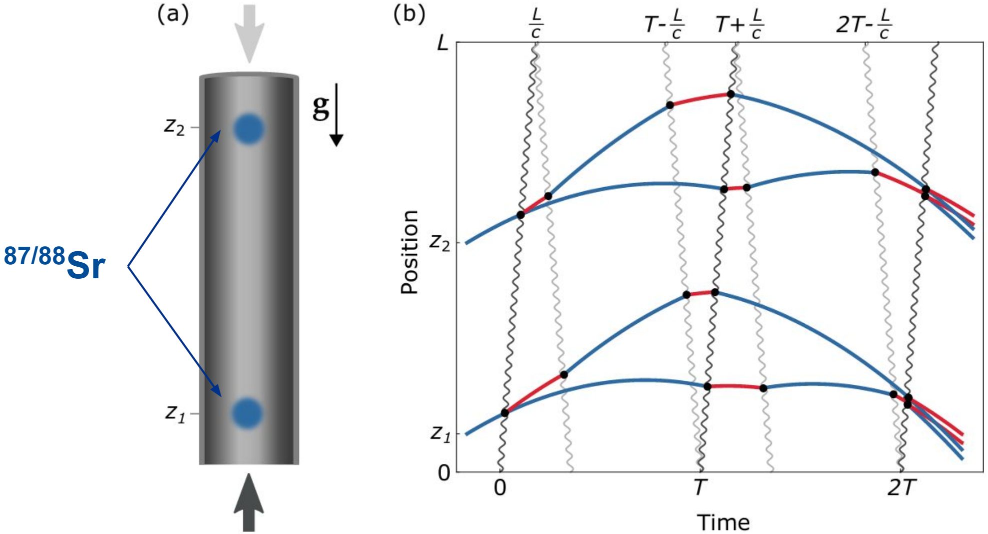

Large momentum transfer laser pulses applied to further separate wave packets' momenta → sensitivity scales linearly with momentum separation

LMT atom optics of order *n* refers to an $n\hbar k$ momentum splitting between the two arms of the atom interferometer (corresponding to *n* photon recoil kicks)

Can tune the light to interact with only one arm due to Doppler shift

Fermilab MAGIS-100

Light-Pulse Atom Interferometry

Probability of observing in port 1 vs port 2 depends on relative accumulated phase

Do this for an ensemble of 10^6 atoms

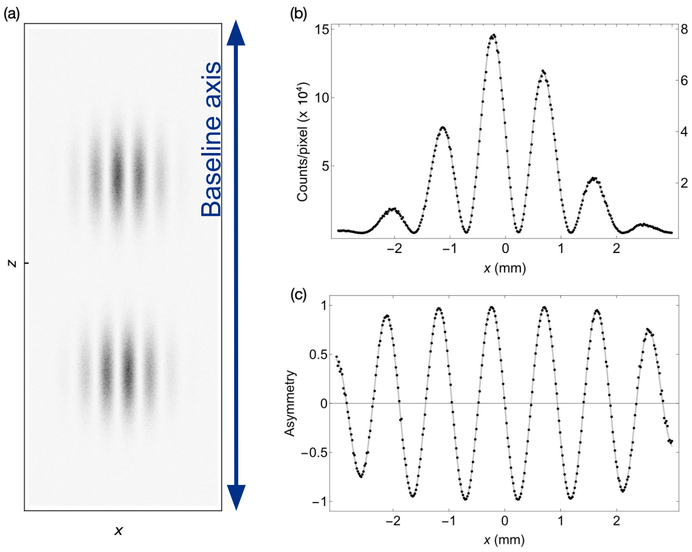

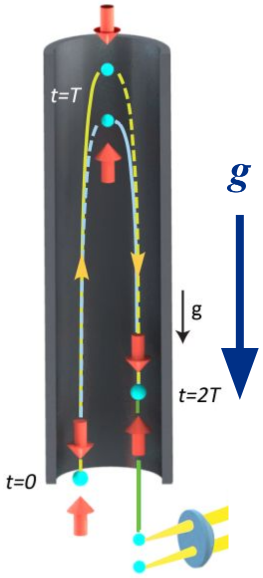

Fit fringe pattern to extract interferometer phase $\delta\varphi$

Mach-Zehnder Matter-Wave Interferometer

Abe et al, Quantum Sci. Technol. 6, 044003 (2021) [arxiv:2104.02835]

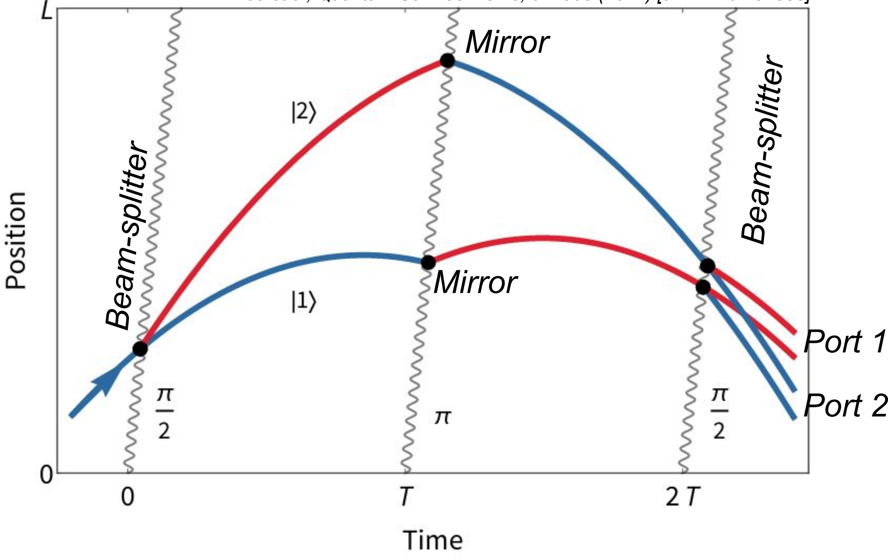

Phase shift from gravitational potential:

- *For n=100, 461 nm light (for Sr), T = 1 s*
- *$\delta\varphi$ from g is 10^{10} radians*

Fermilab
MAGIS-100

Large Momentum Transfer (LMT) Pulse Sequences

- Perform LMT atom optics using π pulses from **alternating directions**
- Each π pulse interacts with **both arms** due to high Rabi Frequency (+2 ħk)

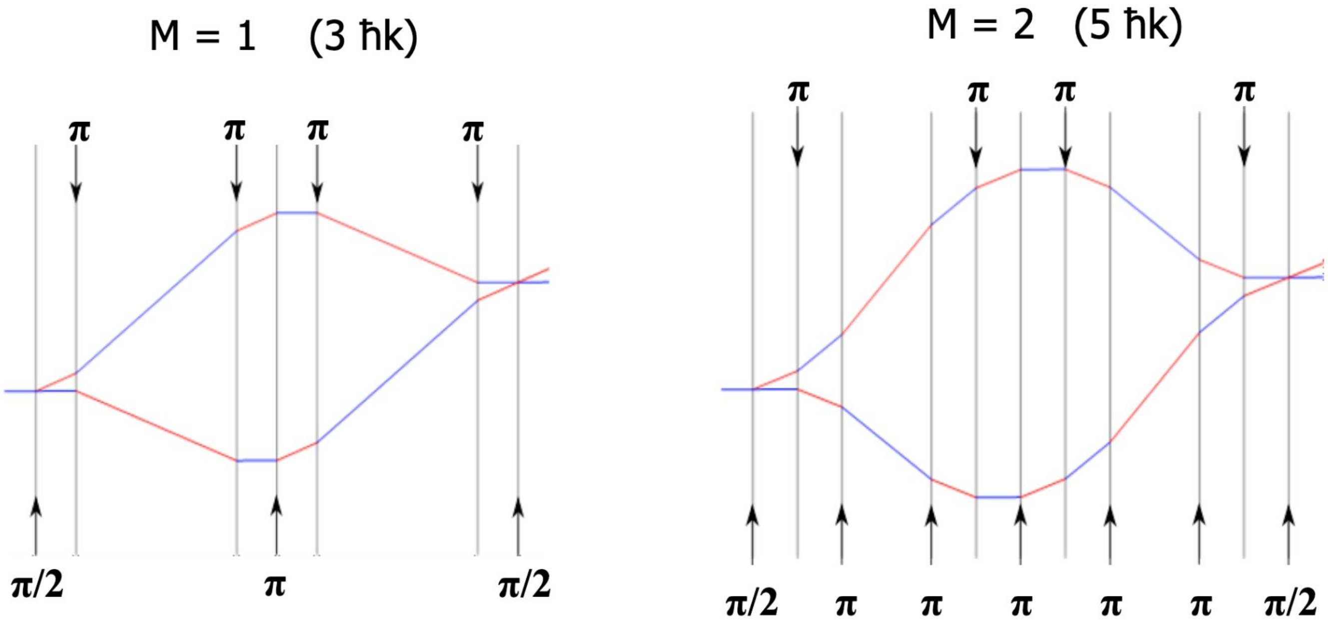

Slide from J. Hogan

Fermilab
MAGIS-100

Large Spacetime Area Interferometry

$$\Delta\phi = -\frac{m}{\hbar} g \Delta z_{\mathrm{max}} T \qquad \Delta z_{\mathrm{max}} = \frac{n\hbar k}{m} T \qquad \Delta\phi = -nkgT^2$$

Inertial sensitivity proportional to enclosed spacetime area

1. Increase momentum splitting nħk between the two interferometer arms.
2. Make a tall atomic fountain to increase the free fall distance ~gT2.
3. Do both at the same time. Typical operating conditions: arm splitting >10 cm, T ~ 1 s

T. Kovachy, et al. Nature 2015
P. Asenbaum, et al. PRL 2017

Fermilab MAGIS-100

Gradiometer DM/GW Signal

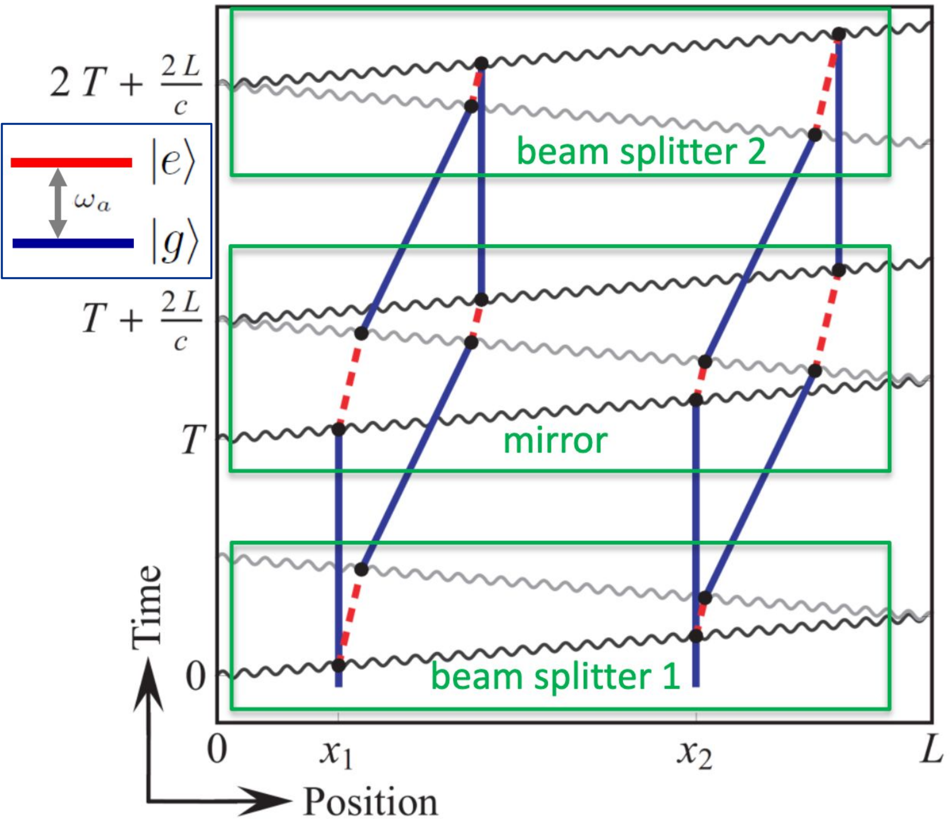

Phase shift of an interferometer determined by **difference in time spent in excited clock state** for arm 1 vs arm 2

Look at difference in **phase shifts for two interferometers** separated by baseline ~L (gradiometer phase shift)

Magnitude of contribution to gradiometer phase shift from each interferometer zone: $\Delta\phi = \omega_A(2L/c)$

For constant (or linearly drifting) L and transition frequency, **gradiometer phase shift cancels** between all three zones

To have a nonzero gradiometer phase shift, need **transition frequency or L to vary on the time scale of T between each zone**

Fermilab MAGIS-100

Laser Lab Civil Construction Complete!

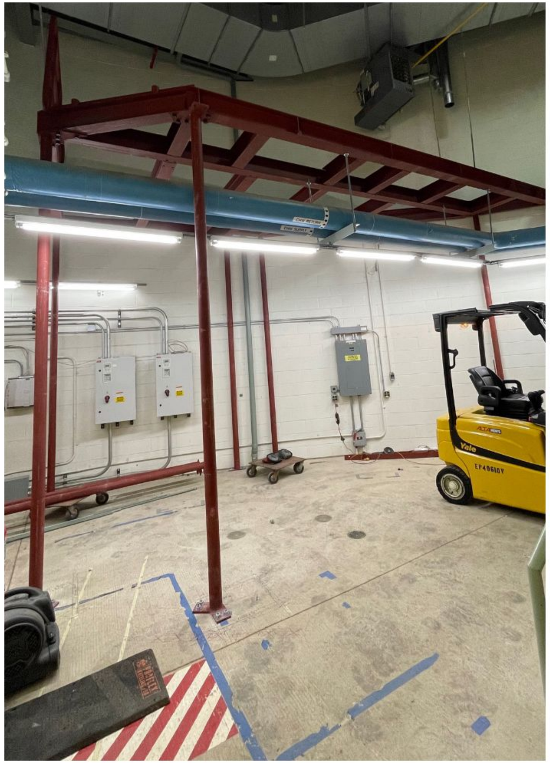

Construction started in 2023.

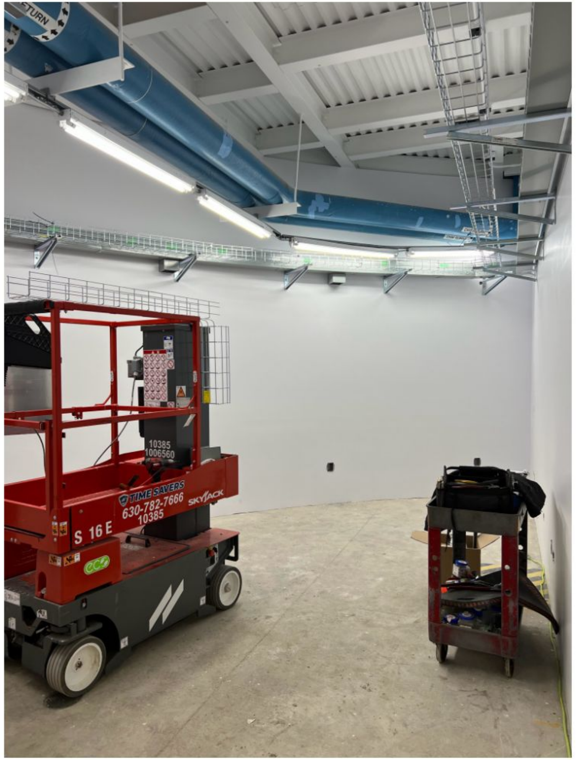

Status April 2024.

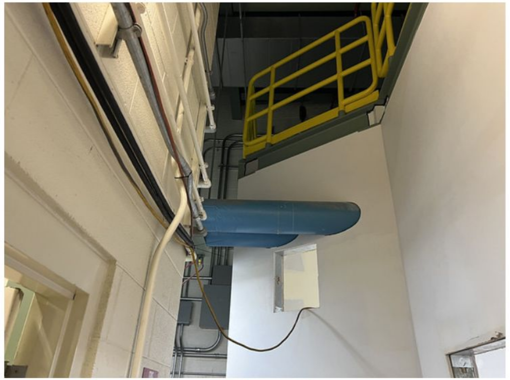

Cutout for LTS to exit laser lab.

Slide from L. Valerio

Fermilab

MAGIS-100

MAGIS UHV System

- Required pressure 10^{-11} Torr or better for interferometry region.
- Dual pumps (ion pump + titanium sublimation pump OR non-evaporable getter pump + small ion pump) will be on each modular section.
- Vacuum bake required to reach this pressure.
- Minimally magnetic 316L stainless steel tubes and non-magnetic heaters required.
- Tubes have been electropolished and will be hydrogen degassed.*

* Preparing magnetic measurements to determine if annealing necessary.

Conclusion: no unexpected behavior, test is a success!

Temperature ramps SSR0-SSR7 Temperature ramps SSR8-SSR15

16-channel bake test setup.

6” OD beam tube

Slide from L. Valerio

Fermilab MAGIS-100

MAGIS-100 Magnetic Field Systems

- Magnetic field is controlled with mu metal shielding and optimally placed magnet coils.
- Mu metal cannot have mechanical stresses – creates magnetic “holes”
- Sections are longer than typical mu metal annealing furnaces.
- Adapted from an existing design, octagonal shield chosen with four layers of staggered seams using flat and angled pieces.
- Fixtures required for successful tight-fitting assembly.

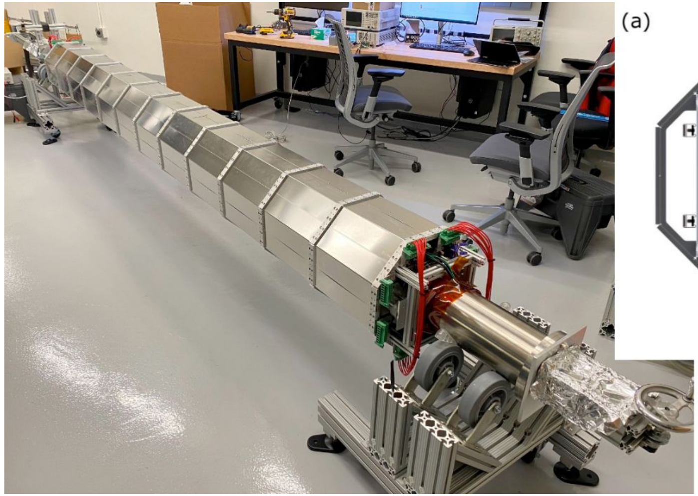

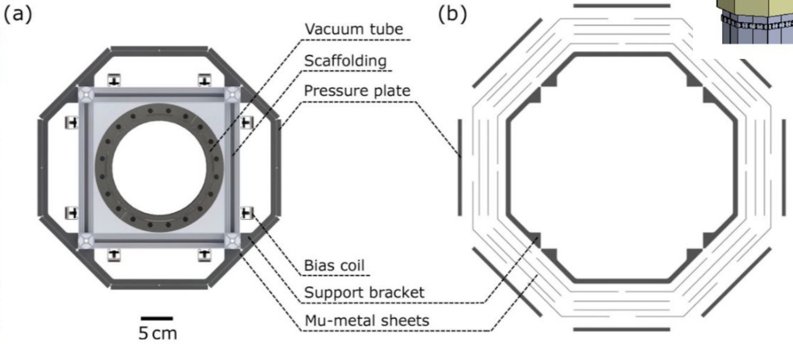

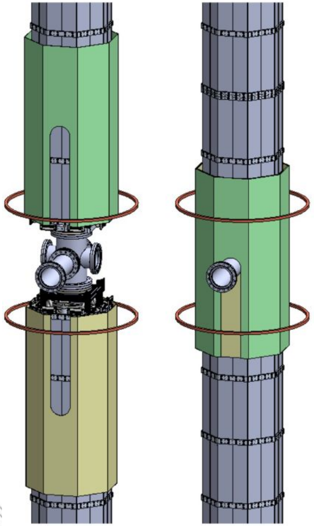

Left: Prototype section assembly at Stanford University 2022.
Above: Cross-section view of magnetic shield and bias coils.
Above right: Magnetic coupler and additional coils will be placed around modular connection nodes.

Modular Connection Node Design

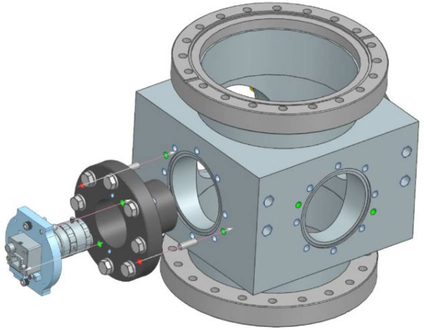

Cameras mount inside re-entrant viewports with light tight covers.

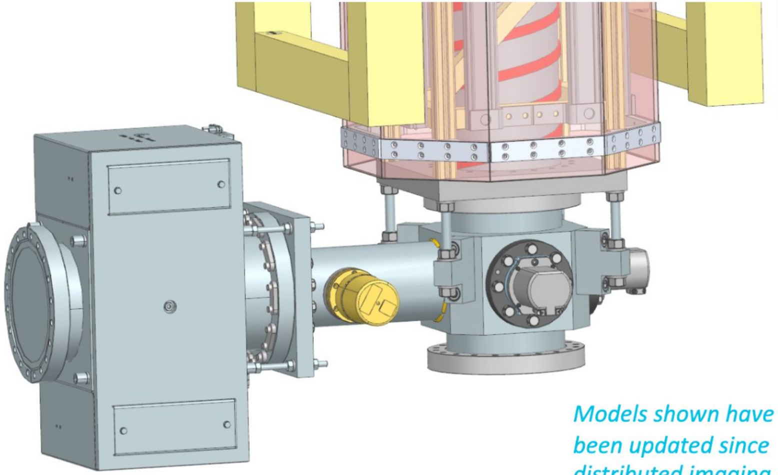

Slide from L. Valerio Detail of modular connection node.

Models shown have NOT been updated since distributed imaging system (DIS) design review 8/1/23.

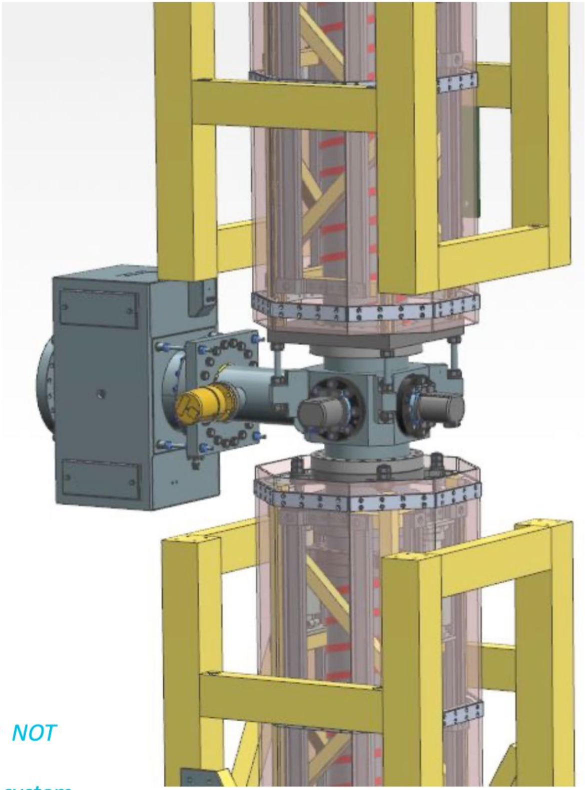

Two modules connected.

Modular Connection Node Mockup

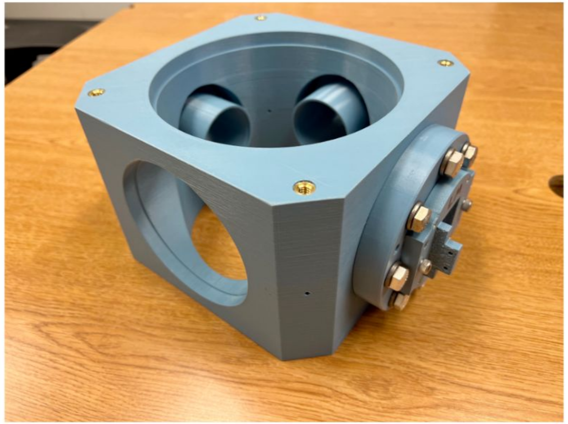

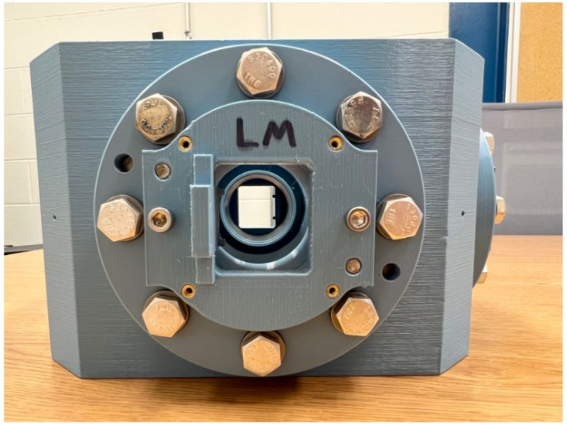

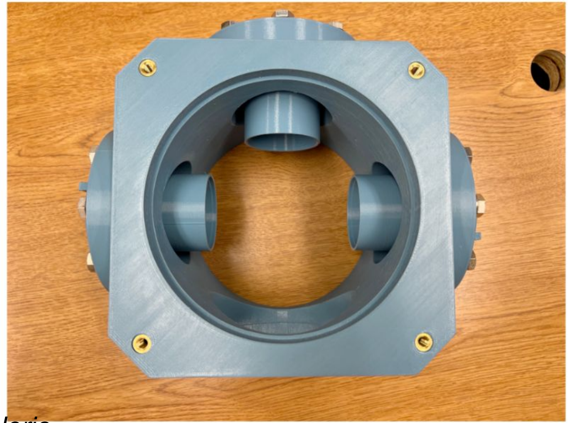

- 3D prototype printed and assembled; sent to SLAC.
- Prototype connection node ordered at Fermilab.
- Viewport quotes collected. Preparing for prototype purchases.

Slide from L. Valerio

Fermilab
MAGIS-100

Atom Source Design

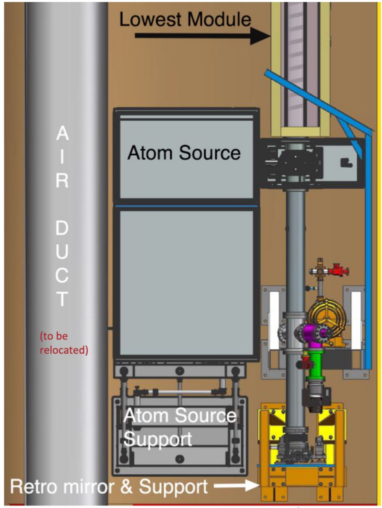

Bottom atom source, atom source connection node, vacuum rough pumping station, and retroreflective mirror shown.

- Up to 1,000 lbs weight.
- Top, middle, and bottom of shaft.
- Last components installed.
- Approximate cost $1M each.
- Designed and built at Stanford University with access challenges considered.
- Transportation will be planned and tested.

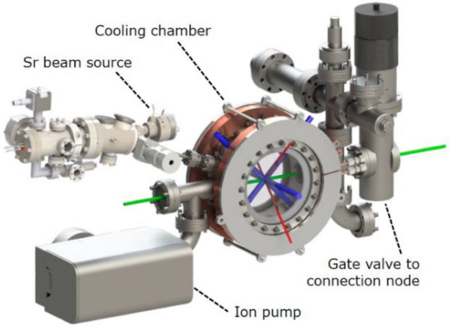

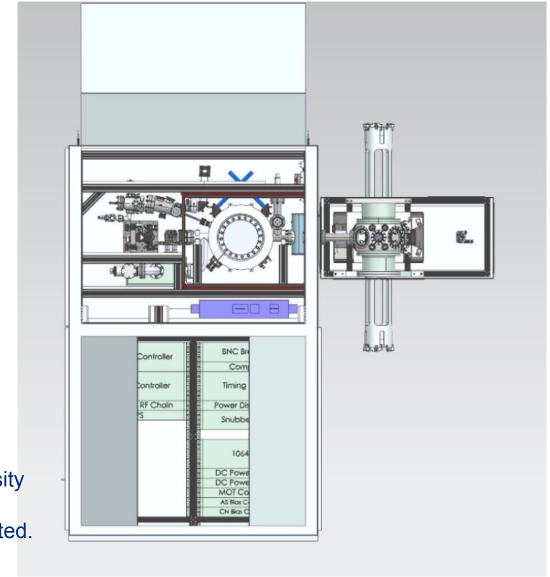

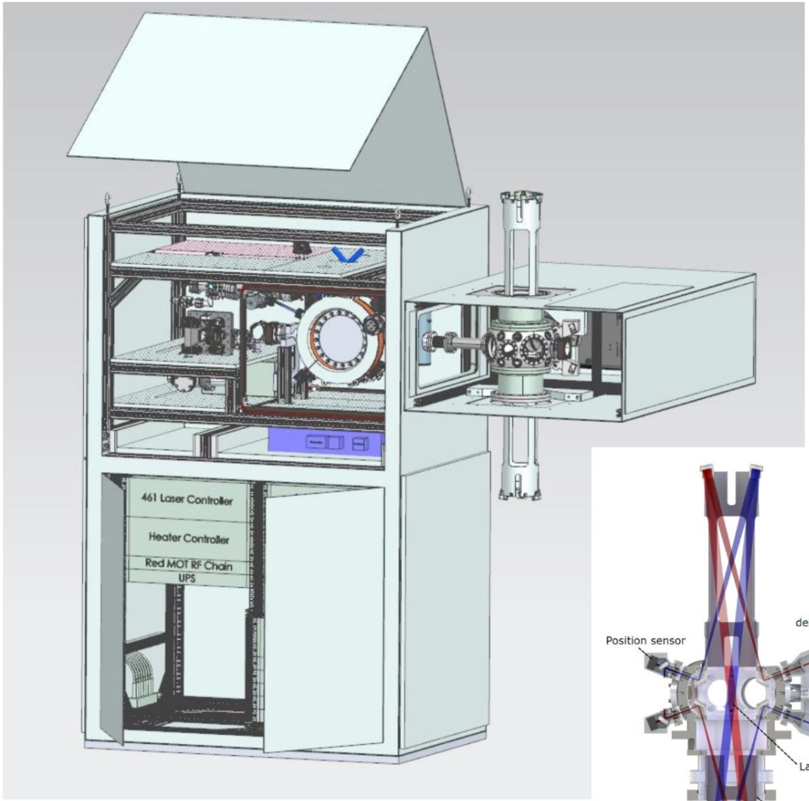

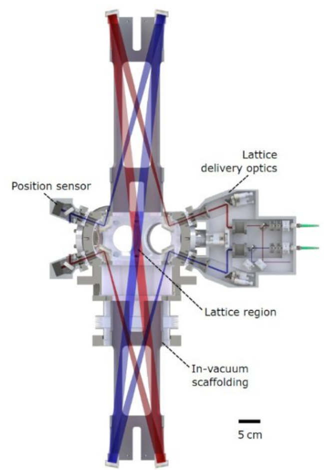

Views inside the atom source enclosure and adjacent atom source connection node.

In-vacuum scaffolding extends into modular section vacuum tubes.

Slide from L. Valerio

Interferometry Laser System

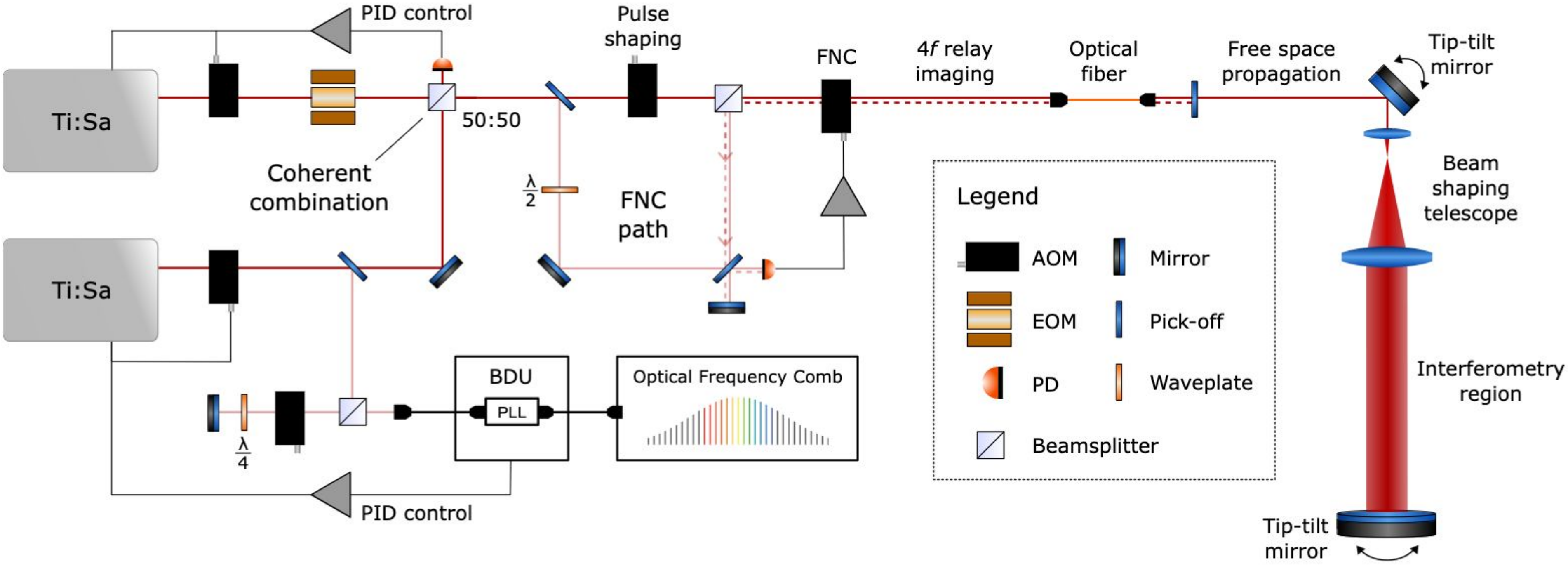

Fermilab MAGIS-100

Interferometry Telescope

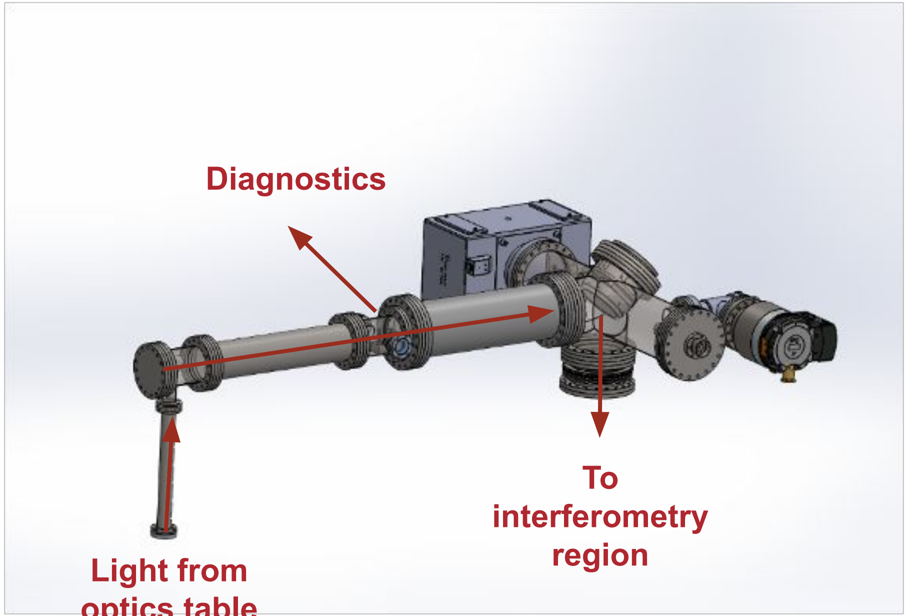

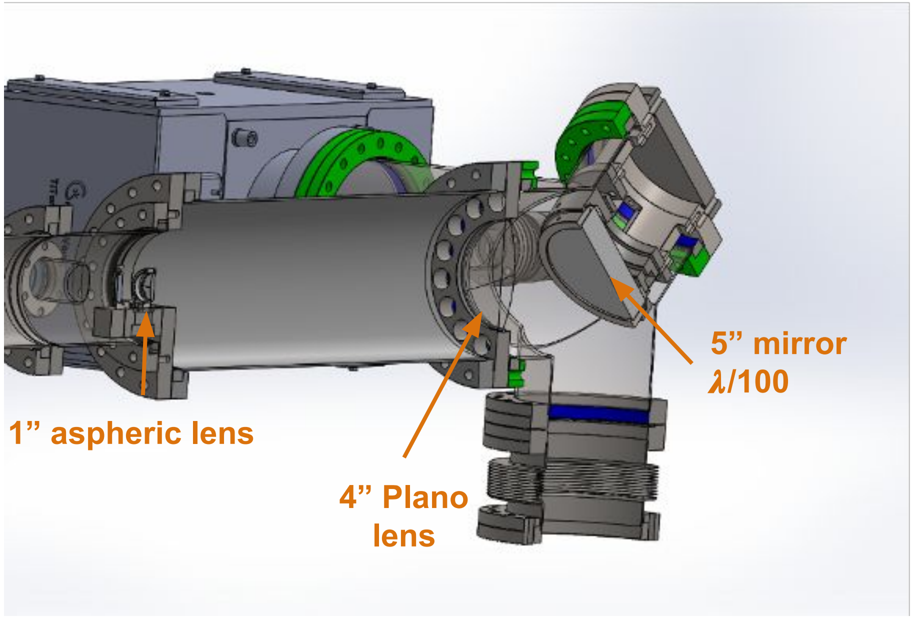

- An in-vacuum beam-expanding telescope
- Uniform beam to minimise laser divergence
- High-quality optics to reduce beam aberrations

Slide from G. Elertas

Laser Injection System for Broadband Interferometry

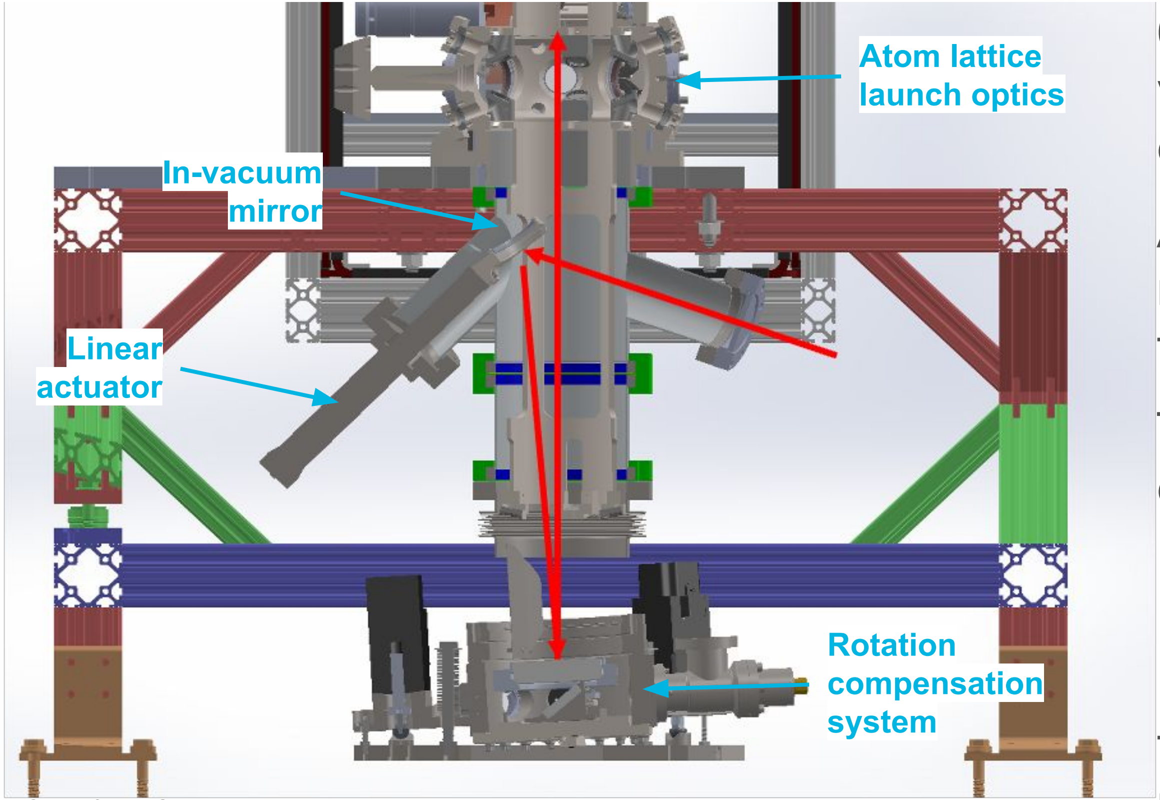

Slide from G. Elertas

689 nm laser enters the tower via this angled tee vacuum chamber

A retractable in-vacuum mirror reflects light down onto the tip tilt mirror

The lower retro reflection chamber is tilted at 3^0 to reflect light upwards into the interferometry region

Extended UHV bellows allow for flexible tilting of the retro reflection platform

Fermilab MAGIS-100

Apparatus Bake Out Control System

Each modular section in the shaft:

- PWM-driven AC heaters
- 16x thermocouples w/ Raspberry Pi readout for PID control

Heater control systems in surface-level racks

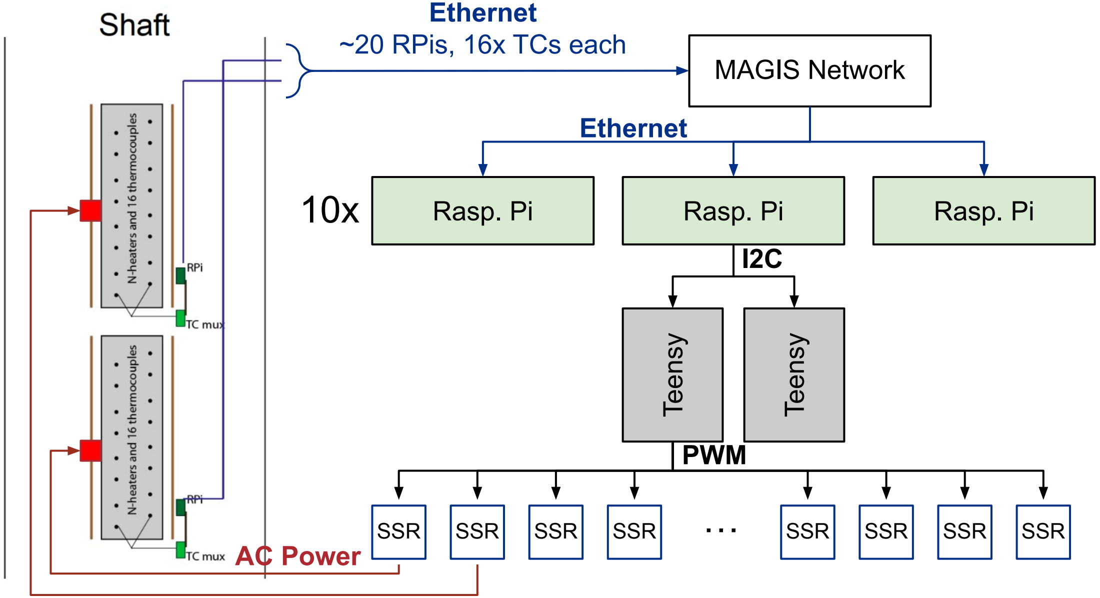

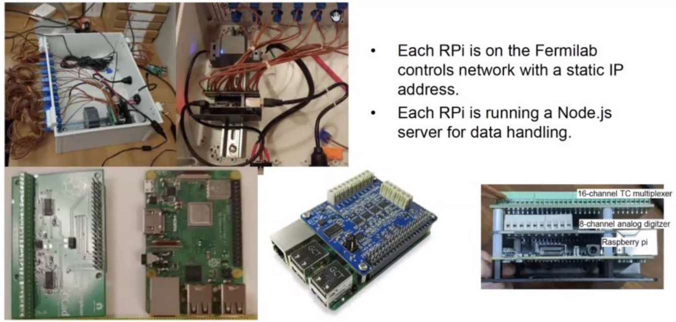

- Each RPi is on the Fermilab controls network with a static IP address.
- Each RPi is running a Node.js server for data handling.

TC-MUX Board
- SPI + GPIO
- 16 inputs

RPi

MCC-118 ADC
- 8 analog inputs
- Stackable: expand to 64 channels

25 TC-MUX boards delivered from UChicago

↑ *In-shaft*

Surface ↓

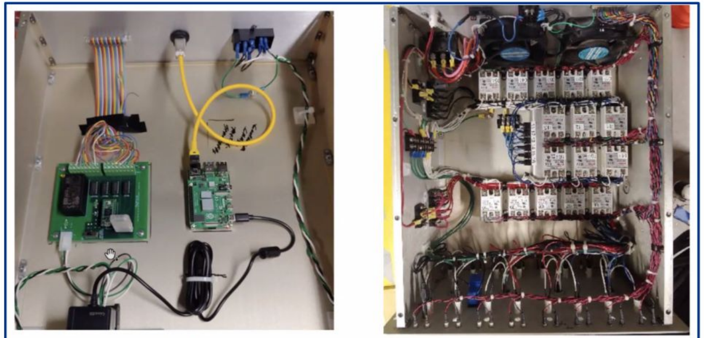

16-channel PWM

16-channel SSR

Fermilab MAGIS-100

Current Status: Civil Engineering & Construction

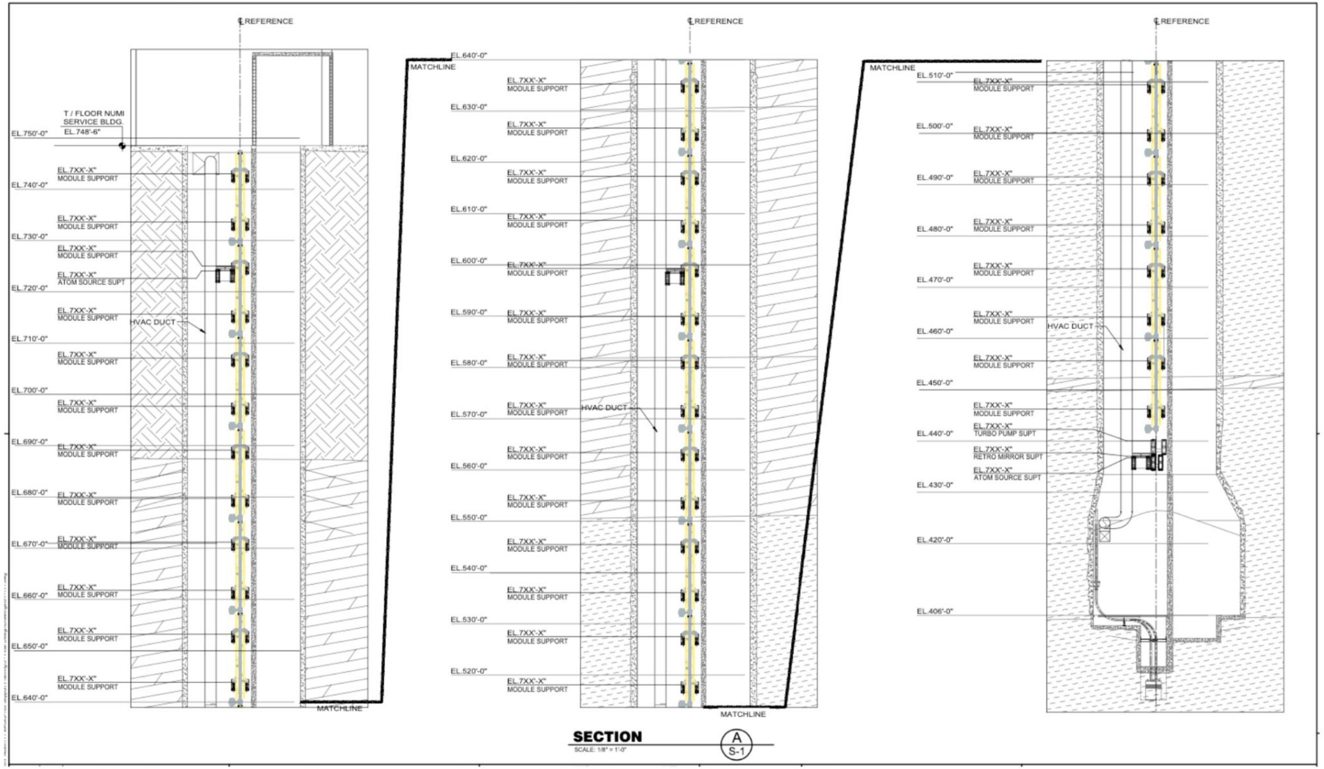

- **Preliminary drawings developed for installing shaft components.**
- **Compressed air and cooling water designs started, requirements to be set.**
- **Air duct relocation investigation started.**

Slide from L. Valerio

Fermilab
MAGIS-100

Current Status: Retroreflection Chamber

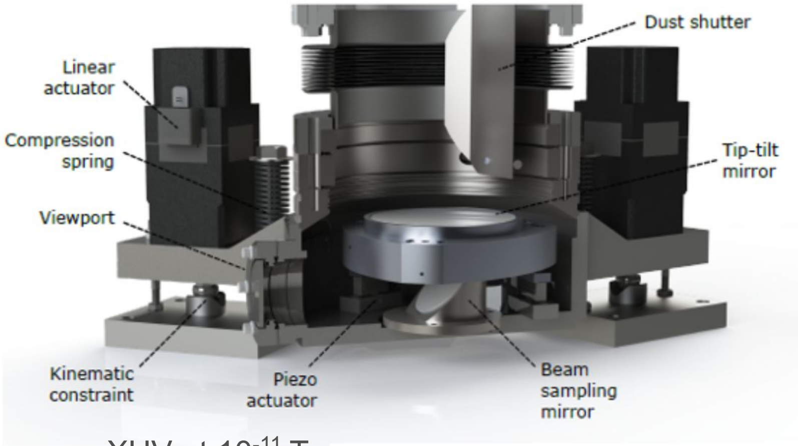

- XHV at 10^{-11} Torr
- Fast actuation: 1.3 mrad, <100 ms settling time (piezo actuators)
- 50 nrad precision with optical feedback loop
- Slow actuation for alignment of interferometry beam: ±1 degree range (linear stepper motors)

Control systems:

- ✓ Stepper motors & controllers @ FNAL
- ✓ Piezo actuator controllers @ FNAL
- ● Piezos - in manufacturing
- ● 4” Retroreflection mirror - shipping
- ✓ Remaining optics @ FNAL
- ✓ NEG pump

Two chambers machined, electropolished, leak tested, and UHV ready (@ FNAL + Stanford).

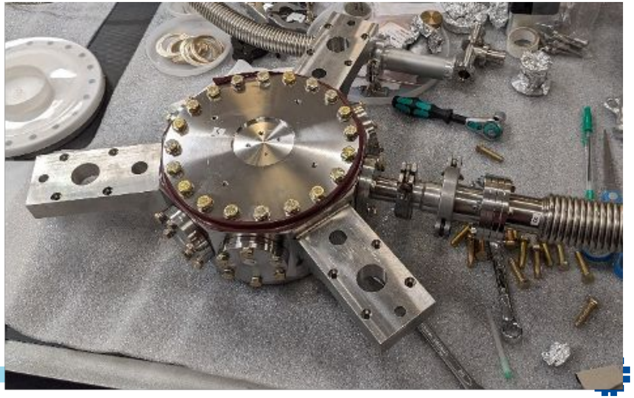

Slide from G. Elertas

Current Status: Primary Science Imaging System

3 cameras per atom source node

Lucid Vision Triton
Sony IMX541 CMOS sensor:

- 4.5k x 4.5k pixels, 2.74 μm square
- 5.5 FPS
- 12-bit ADC
- Global shutter
- Dark current 1.6e/s
- QE ~70% at 450nm
- ~2.1e read noise
- PoE

50mm fixed focal length lens:

- f/1.8 to f/16
- Mwd 200mm
- Max diameter ~50mm

Procured and under test @ Oxford

Camera & lens mount

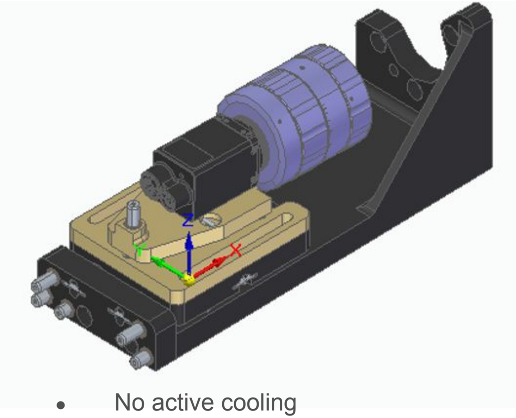

- No active cooling
- Three-axis fine position adjustment (~a few mm) accessible from exterior
- Cutaway view (fully enclosed)

Final design stages

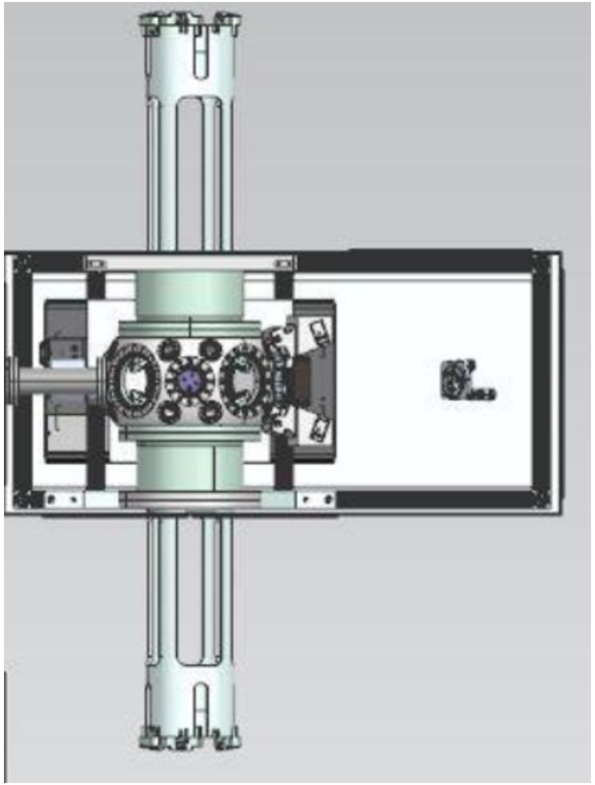

Slide from D. Weatherill

Current Status: Primary Science Imaging System

MAGIS characterisation testbench at Oxford:

- accurate radiometry
- flat fielding
- tunable light source + monochromator

Each camera and lens will be characterised across a range of temperatures: bias frames, fark frames, flat-field images, QE.

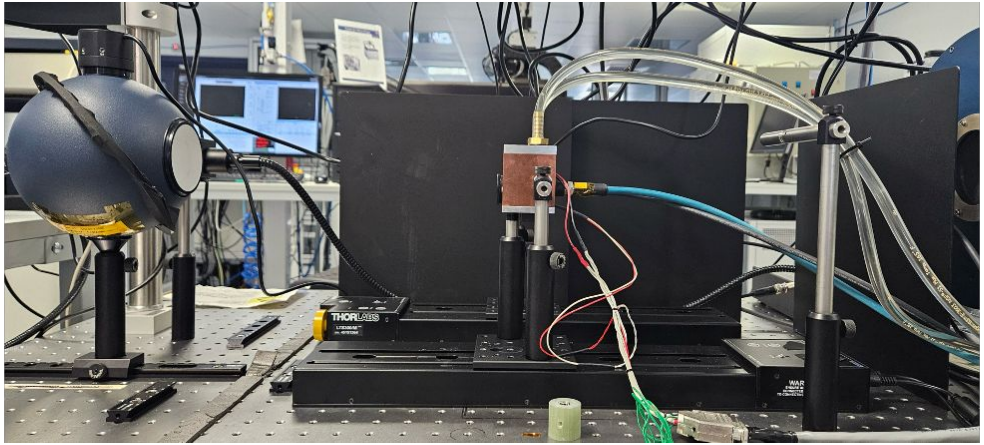

Slide from D. Weatherill

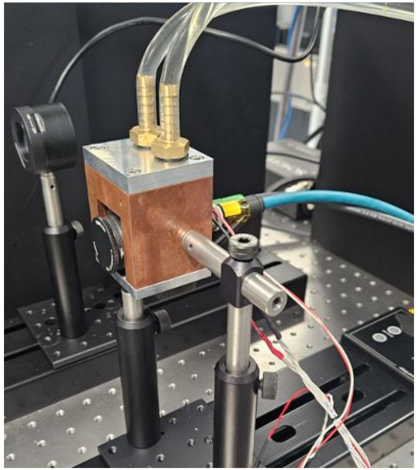

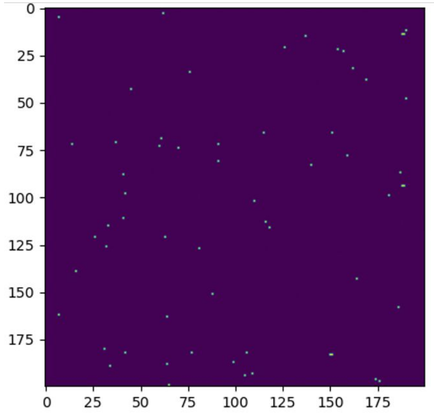

Example dark map. 200 x 200 pixels ROI - 0.17% pixels outside 5 sigma of mean value

Current status

- Operational software, databasing, analysis finalised for real sensor data
- Initial shakedown data runs using a spare camera are underway
- First real calibration data in next few weeks.

Current Status: Magnetic Shielding

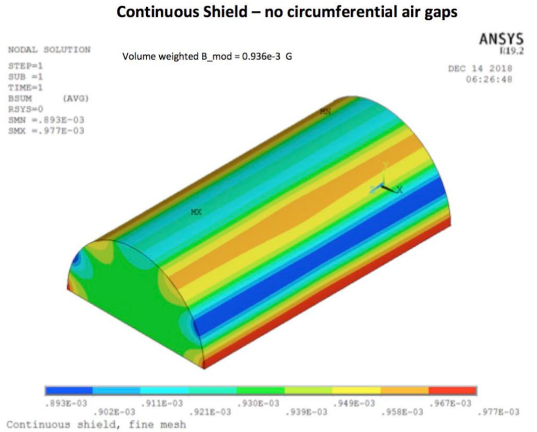

3D simulations have been done at Fermilab with ANSYS.

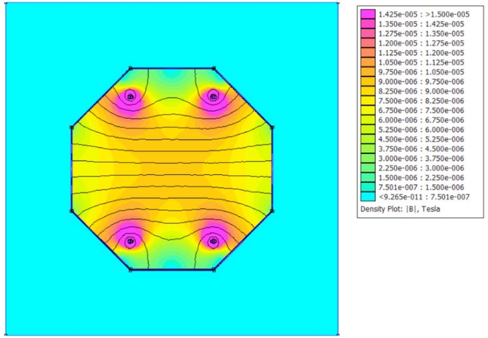

Stanford has done 2D simulation (cross-sectional view) of bias magnetic field inside an octagonal shield

Magnetometry testbed under development @ FNAL

- Assay UHV tubing pre-construction
- Quantify flux reduction from shield
- Platform to evaluate control systems and interface with FNAL computing

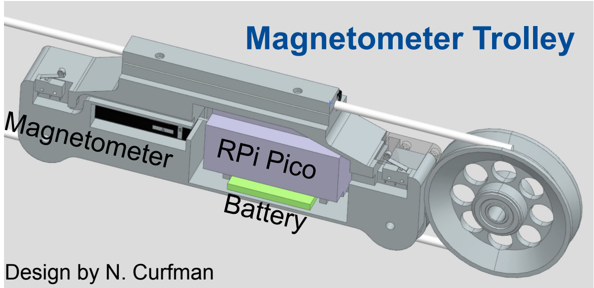

After degauss, magnetic shield meets specifications:

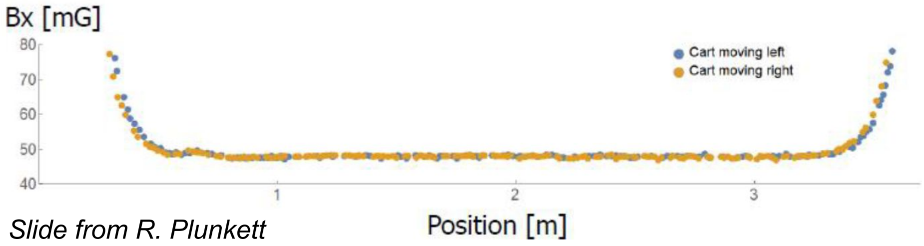

Slide from R. Plunkett

Testing magnetic field reduction inside prototype shield @ Stanford

Installation Planning: Wall Supports

Wall supports will be installed through a civil construction contract.

- Conceptual plan to land components on wall supports with dagger system and cameras.
- Investigating rail systems, rolling carts, and other engineered methods for moving components accurately into place.
- Mock-up will be tested in advance of actual installation.

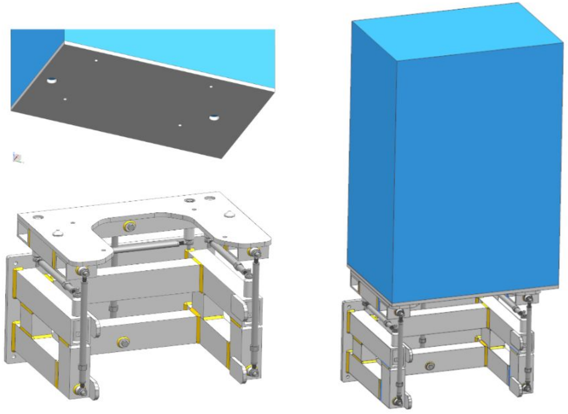

Atom source and adjustable wall support.

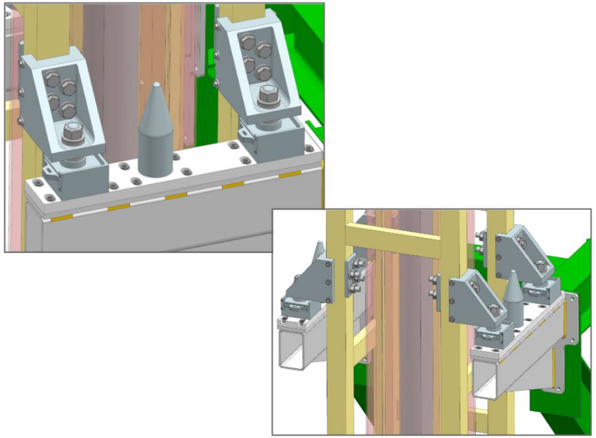

Modular section adjustable wall support.

Slide from L. Valerio

Installation Planning: Structural Challenges

Adjustable supports required for alignment:

- Must minimize penetrations in magnetic shield.
- Six-strut system will be used for positioning modular sections inside frames, also for atom sources.
- Custom rod ends were ordered July 2022 because long lead time anticipated. Delivery expected May 2024.

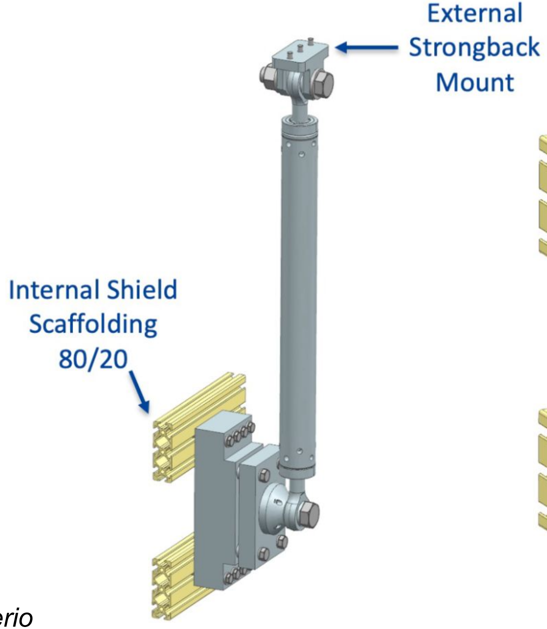

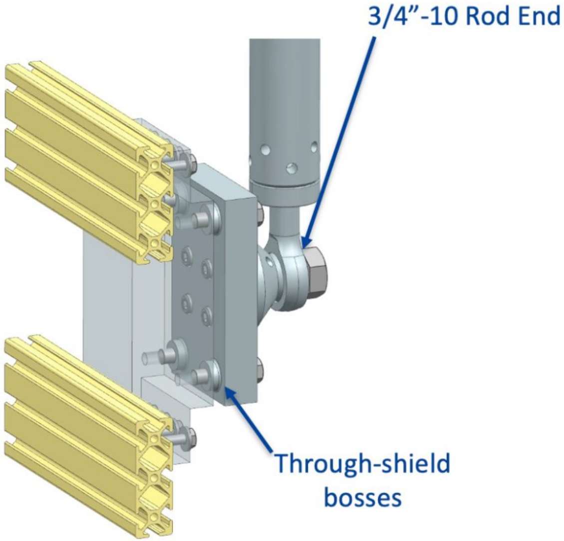

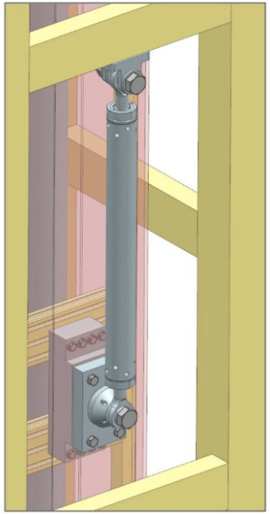

Slide from L. Valerio

Installation Planning: Alignment

Optical plummets will be mounted at the bottom of the shaft to achieve required alignment.

- **Mounting base must be sturdy.**
- **Bottom of shaft has metal plates which will flex and is also a "stay clear" zone. Original plan was to use concrete block.**
- **Consider if mounting base to elevator wall would work better.**

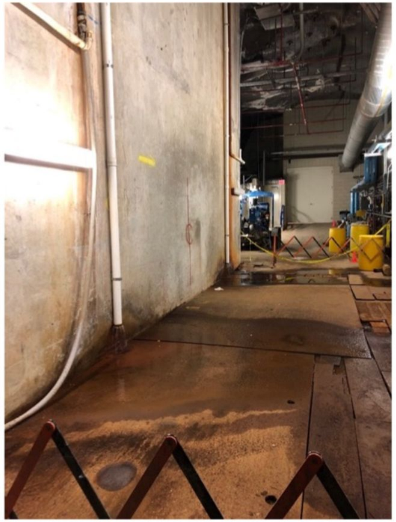

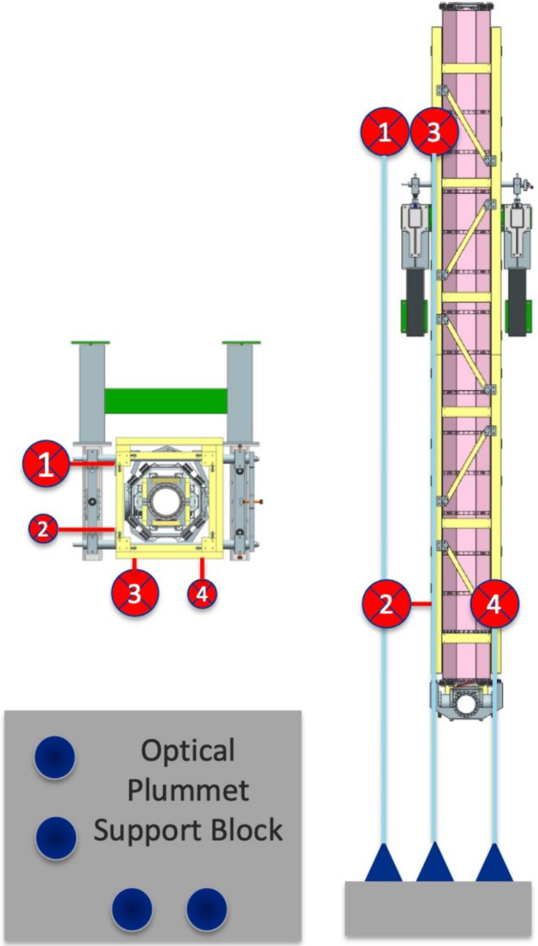

Slide from L. Valerio

Installation Planning: Personnel Access

- Component installation
- Alignment
- Setup of vacuum, camera, magnetic, and controls systems
- Maintenance, particularly at atom source locations
- Accommodate other uses of the shaft

Existing personnel basket in use.

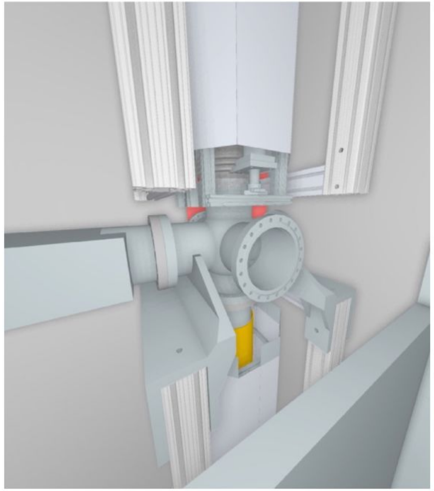
VR model image.

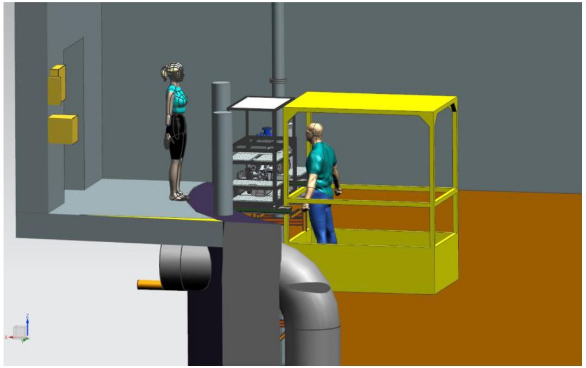
Atom source access from personnel basket.

- Confirming shaft space required by other users.
- Investigating concepts such as crane personnel basket, platforms, and motorized scaffolding systems.
- Virtual Reality (VR) model can confirm if components are able to be reached from access system or if special tooling must be designed.

Slide from L. Valerio

Magnetic Fields

The clock energy levels of Sr shift in response to magnetic fields.

→ Time varying magnetic fields can mimic DM or GW signals

→ Largest effect on phase response - most important to minimize & track

Detector enclosed in mu-metal magnetic shielding along entire baseline

Bias field applied to compensate for (transverse) residual static component

Problematic frequencies: DC - 10 Hz

Sensor requirements:

- < 0.1 mG resolution
- > ±1 G dynamic range
- > 10 Hz sampling rate

$$\delta\phi_{\mathrm{mag}} \sim \left(1 \times 10^{-3}\ \mathrm{rad}/\sqrt{\mathrm{Hz}}\right)\left(\frac{B_0}{1\ \mathrm{G}}\right)\left(\frac{\delta B}{1\ \mathrm{mG}/\sqrt{\mathrm{Hz}}}\right)\left(\frac{T}{1\ \mathrm{s}}\right)$$

Applied bias field (B_0); Time-varying component (δB); Time from BS to M pulse (T)

Vibrations

Ground vibrations imprint phase noise on the interferometry laser pulses due to vibrations of the critical beam delivery and steering optics.

$$\delta\phi_{\text{vibration}} \sim \left(10^{-8}\ \text{rad}/\sqrt{\text{Hz}}\right)\left(\frac{n}{100}\right)\left(\frac{\Delta v}{100\ \mu\text{m/s}}\right)\left(\frac{T}{1\ \text{s}}\right)\left(\frac{\delta a}{10^{-4}\text{m/s}^2/\sqrt{\text{Hz}}}\right)$$

- n: # LMT pulses
- Δv: Velocity difference between atom clouds
- T: Time from BS to M pulse
- δa: Amplitude spectral density

Track vibrations with:

- 2x Seismometer: **Trimble 151B**
  - Located on surface
- Accelerometers: Nanometrics Titan (DC – 430 Hz)
  - Variable range: ±0.25 g to ±4 g
  - One at each atom source

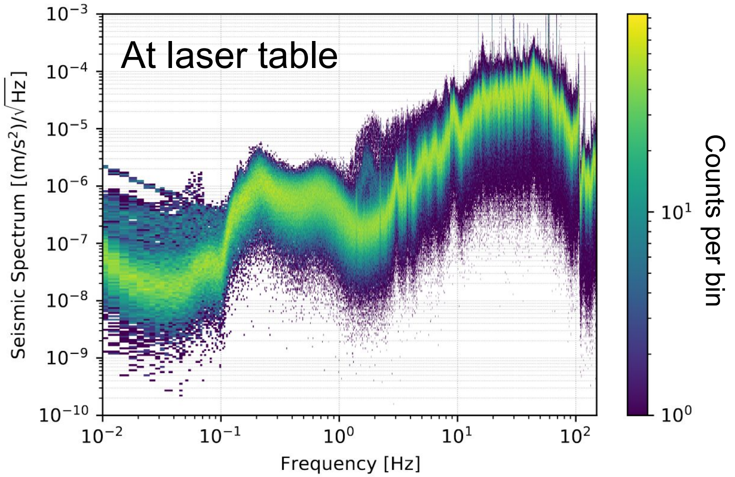

*J. Mitchell et al 2022 JINST **17** P01007 [arxiv:2202.04763]*

Gravitational Disturbances: Gravity Gradient Noise

Fluctuation of the local gravitational potential sourced by mass density fluctuations of the ground

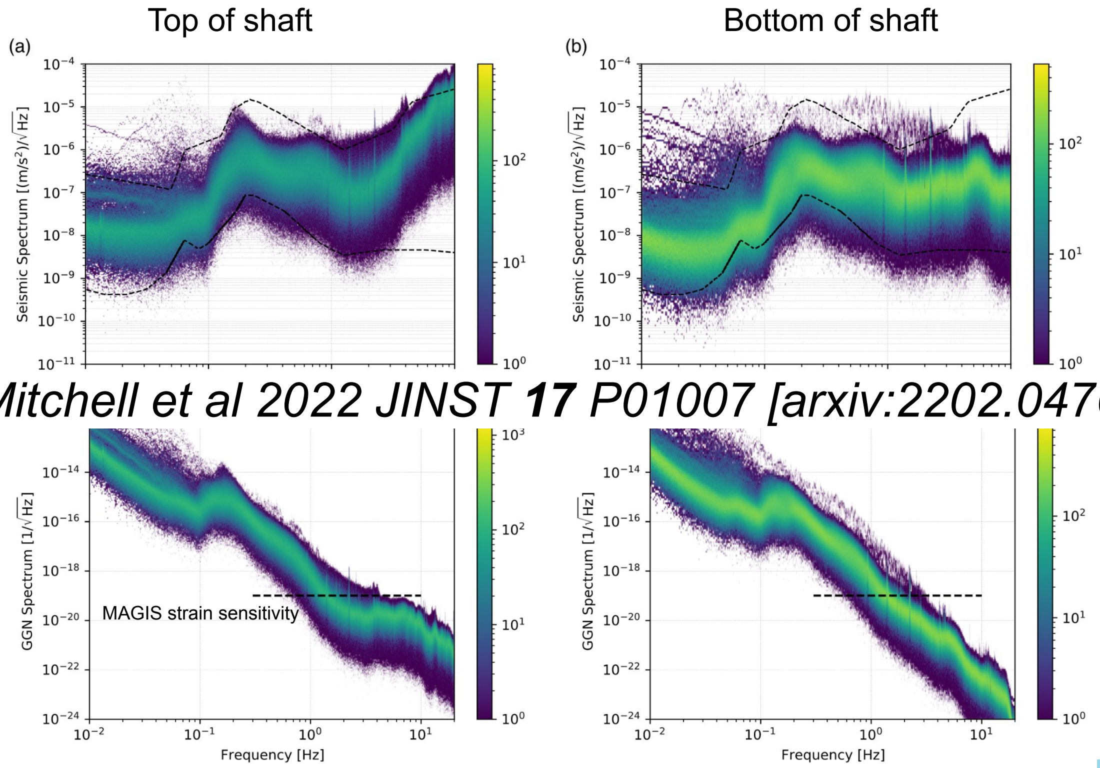

J. Mitchell et al 2022 JINST **17** P01007 [arxiv:2202.04763]